Department of Chemical Engineering

Distillation of Mallee Biomass for Eucalyptus Oil Extraction and Thermochemical Behaviour of the Spent Biomass

Syamsuddin Yani

This thesis is presented for the Degree of

Doctor of Philosophy

of

Curtin University

February 2015

DECLARATION

To the best of my knowledge and belief this thesis contains no material previously published by any other person except where due acknowledgment has been made.

This thesis contains no material which has been accepted for the award of any other degree or diploma in any university.

Signature: .....

Date: 12/02/2015

To my beloved family

ABSTRACT

Due to the rising energy demand, high cost of fossil fuels, decreasing fossil fuel reserves and contribution of fossil fuel usage to greenhouse effect, biomass is becoming increasingly important globally as a clean alternative source of energy to fossil fuels. In Western Australia (WA), mallee eucalyptus is an important biomass in the Wheatbelt agricultural area. Its plantation is a key strategy in managing the serious dryland salinity problem and erosion in Australia's premium agricultural area, as well as improving biodiversity protection and carbon sequestration. Mallee leaves have a potential as a renewable energy source due to a short harvesting period. In addition, the leaves also contain eucalyptus essential oil, which is widely used in various fragrance and pharmaceutical industries. The assimilation of mallee leaves as feedstock for production of eucalyptus essential oil and as a renewable energy source offers a promising solution for providing sustainable renewable chemicals and energy.

Despite several studies that have been done related to this research area, an integrated study of the extraction of essential oil and its fuel properties of the spent leaves after steam distillation as well as characteristics of their biochars during pyrolysis and the formation of particulate matter (PM) during the combustion are limited. Therefore, it is important to study and get a better understanding of those subjects so that the information for the integrated utilisation of mallee biomass as chemical and fuel feedstock can be provided.

The main aim of this study is to accomplish a comprehensive understanding of utilisation characteristics of mallee leaves during steam distillation as well as the application of the spent leaves (after steam distillation) as feedstock for pyrolysis and combustion. The specific objectives of this study are to: (1) investigate the effects of the conditions of steam distillation (for eucalyptus oil extraction from mallee leaves) on the distillation performances and kinetics, as well as the properties of spent leaves, particularly the evolution of biomass structure, fuel properties and inherent inorganic species; (2) examine the properties of biochars produced from the pyrolysis of spent leaves under various conditions, particularly the transformation of inherent

inorganic species during pyrolysis; (3) evaluate the combustion characteristics of spent leaves with particular interest on inorganic PM; and (4) characterise the fuel properties of torrefied leaf after torrefaction and the emission of inorganic PM from its combustion. These objectives have been well accomplished in this PhD study, a brief summary on the key results of which is given as follows.

Firstly, steam distillation of mallee leaves was performed and extracted~90% of 1,8-cineole rapidly in the first 15 min. The extraction followed zero-order kinetics, regulated by the latent heat (provided by steam) for 1,8-cineole evaporation. After 15 min, the extraction was slow and followed first-order kinetics, controlled by the slow internal diffusion of the residual 1,8-cineole. Overall, 1,8-cineole extraction was virtually completed after steam distillation for 60 min. Steam distillation led to little changes in the proximate and ultimate analyses as well as mass energy density of the spent leaves. However, the distillation removed some of total organic carbon and significant amount of Mg, Ca, and Cl in the raw leaves via interactions between the leaves and the steam (and/or reflux). Furthermore, the distillation changed the chemical association of Mg and Ca with the chemical structure of organic matter in the spent leaves.

Secondly, slow and fast pyrolysis of mallee leaves and two spent leaves collected after distilling the raw leaves in steam for 30 and 60 min were performed at temperatures of 400−700°C to produce a set of 24 biochars. Under the same experimental conditions, the pyrolysis of the raw and spent leaves produced biochars of similar yields and properties in terms of proximate and elemental analyses. However, the biochars from the raw leaves generally have higher contents of Na, K, Mg, Ca and Cl than those from the spent leaves. The biochars were then leached via water to evaluate the recycling of inherent inorganic nutrients (i.e., Na, K, Mg, Ca, and Cl) and the leaching of organic carbon (C). In both slow and fast pyrolysis, the quantities of Na, K, and Cl leached out by water from the biochars of the raw leaves were considerably higher than those from the biochars of the spent leaves. However, the leaching of Mg in the slow pyrolysis biochars followed an opposite trend. In the fast pyrolysis at temperatures higher than 400 °C, there were considerable decreases in the quantities of Na and Mg as well as K and C leached out from all the biochars.

Thirdly, a study on the characteristics and behaviour of PM_{10} emission during the combustion of raw mallee leaves and spent leaves after steam distillation was performed. The spent leaves used in the study were prepared via distilling the raw leaves in steam for 60 min. The combustion experiments were conducted at 1400 ºC in air, using a laboratory-scale drop tube furnace (DTF). Steam distillation has affected the structure and contents of inorganic species in the spent leaves. The spent leaves have lower retention of alkali and alkaline earth metallic (AAEM) species and Cl. Therefore, during the spent leaves combustion, the emission of PM_{10} was lower than that of the raw leaf. The yields of PM_1 were dominated by particles containing Na, K, Cl and S. Approximately 32% of SO_4^{3-} is distributed in PM_1 with the remaining distributed in PM_{1-10}. The less volatile Ca and Mg were dominant in PM_{1-10}, with only ~18% of Ca and~3-7% of Mg being distributed in PM_1. In term of PM emission, spent leaves from steam distillation is a promising feedstock for energy conversion technology due to its ability to lower the emission of PM_{10}.

Finally, a study on the emission behaviour of inorganic PM_{10} from torrefied leaves combustion was performed. Raw mallee leaves and their derived torrefied leaves (at 220−280 ^{o}C) were combusted at 1400 °C in air, using the DTF employed in the third task. Compared to that of the raw biomass, the combustion of the torrefied biomass led to considerable reductions in the ash-based (i.e., normalized to equivalent ash input) yields of PM with an aerodynamic diameter <0.1 μm ($PM_{0.1}$). The yields of Na, K, and Cl in $PM_{0.1}$ were also lower in torrefied biomass than that of raw biomass. The lower yields of these elements in $PM_{0.1}$ are predominantly due to the removal of ~54−77% of Cl in the raw biomass during torrefaction. In contrast, the ash-based yields of PM with an aerodynamic diameter of 1−10 μm (PM_{1-10}) as well as Mg and Ca in PM_{1-10} from the torrefied biomass are substantially higher than those from the raw biomass. On an equivalent energy input basis, which is of more practical relevance, the combustion of the torrefied biomass leads to similar yields of $PM_{2.5}$ but considerably higher yields of PM_{10} than the direct combustion of the raw biomass.

ACKNOWLEDGEMENTS

In the name of God almighty, the most merciful, the most beneficent.

I would like to express my great gratitude to my PhD supervisor, Professor Hongwei Wu, for providing me the opportunity to join his research group, for his utmost guidance, advice, inspiration, dedication, support and patience throughout the course of my PhD study.

My gratefulness also goes to Dr Xiangpeng Gao for his patience, dedication and support. I would also like to acknowledge Professor Ming Ang for assistance and help as thesis committee member.

I would like to express my deepest gratitude to my parents and family, for their moral support, encouragement and understanding during my life in overseas. Most importantly, I would like to express my greatest appreciation to wife, Setyawati Yani for his love, support and understanding. Her invaluable sacrifice, patience and help are things that I hold dearly in my heart. I thank God for giving me a son Adam and a beautiful daughter Rayya. You are my inspirations.

I would like to express my appreciation to the Chemical Engineering laboratory staff including Ms. Karen Haynes, Mr. Jason Wright, Ms. Ann Carroll, Mr Jimmy and Mr Andrew for their laboratory assistance. Thanks also go to the administrative staff in the Department of Chemical Engineering for their help and the staff in the Department of Applied Physics Department for assistance in SEM analysis.

I also want to thank our research team members, including Dr Yun Yu, Dr Yi Li, Dr Yanwu Yang, Ms. Zhaoying Kong, Mr. Alan Burton, Mr Sui Boon Liau, Mr Muhammad Usman Rahim, Mr Da Wei Liu, Mrs Mingming Zhang, Mr Matthew Witham, Mrs Zainun Mohd Safie, Mr Mansoor Hassani Ghezelchi, Mrs Xixia Cheng, Mr Chao Feng, Mr Bing Song and Mr Yu Long, my friends as well as all my other colleagues in Department of Chemical Engineering are thanked for their help in various ways.

I deeply acknowledge Directorate General of Higher Education (DIKTI), the Ministry of Education of the Republic of Indonesia for providing DIKTI International Scholarship for my PhD study.

I also greatly acknowledge the financial support for my PhD research received from the Western Australia Energy Research Alliance (WA:ERA) and the Centre for Research into Energy for Sustainable Transport (CREST) through the Western Australian Government Centre of Excellence Program. I'm also grateful to other research funds in Australia for supporting my PhD study.

Last but not least, I would like to sincerely thank my home university, the Muslim University of Indonesia (UMI) Makassar, for providing the opportunity for me to undertake this PhD study. I hope all the knowledge and invaluable experiences which I gain during my PhD study will be beneficial for UMI and Indonesia.

LIST OF PUBLICATIONS

Papers published in refereed international journals:

1. **Syamsuddin Yani**, Xiangpeng Gao, Peter Grayling and Hongwei Wu. Steam Distillation of Mallee Leaf: Extraction of 1,8-cineole and Changes in the Fuel Properties of Spent Biomass, *Fuel* **2014**, 133: 341–349.

2. Xiangpeng Gao, **Syamsuddin Yani** and Hongwei Wu. Pyrolysis of Spent Biomass from Mallee leaf Steam Distillation: Biochar Properties and Recycling of Inherent Inorganic Nutrients, *Energy & Fuels* **2014**, 28: 4642−4649.

3. **Syamsuddin Yani**, Xiangpeng Gao and Hongwei Wu. Emission of Inorganic PM_{10} from The Combustion of Torrefied Biomass under Pulverized-Fuel Conditions, *Energy & Fuels* **2015**, 29: 800-807.

4. Xiangpeng Gao, **Syamsuddin Yani** and Hongwei Wu. Emission of Inorganic PM_{10} during the Combustion of Spent Biomass from Mallee Leaf Steam Distillation, *Energy & Fuels* **2015**, 29: 5171-5175.

TABLE OF CONTENTS

LIST OF FIGURES

LIST OF TABLES

CHAPTER 1 INTRODUCTION

1.1 Background and Motive

The present world's energy consumption is dominantly dependent on fossil fuel. However, increasing global energy demand and fossil fuel price as well as reducing fossil fuel reserves and contribution of the use of fossil fuel to greenhouse effect have made biomass as promising-clean alternative energy source to fossil fuel. Biomass is the only direct renewable source of carbon-based materials. Therefore, biomass will play an important role in the future sustainable development of the world[1].

Mallee eucalyptus biomass is an important biomass resource in the wheatbelt agricultural area of Western Australia (WA)[2]. Its plantation is considered to be a key strategy in managing the serious dryland salinity problem and erosion in Australia's premium agricultural area, and also improving biodiversity protection and carbon sequestration[1, 3]. Mallee leaves contain eucalypts essential oil, which is widely used in various fragrance and pharmaceutical industries [4], as well as being envisaged as feedstock for industrial solvents and bioplastics in the future[5, 6].

The large-scale production of mallee biomass requires large-scale utilisation of the biomass and its spent biomass after essential oil extraction processes. Application of these biomass materials as feedstock for bioenergy is an important strategy[7]. There are various options available in processing mallee biomass and/or its spent biomass for energy conversion, such as direct utilisation of solid mallee biomass through combustion and mallee biomass pyrolysis to produce bio-oil, gas and biochar. To improve fuel properties, the biomass/spent biomasss can also be pretreated via torrefaction. During the combustion of mallee raw leaves/spent leaves/biochar, particulate matter (PM) emission is another important topic for a comprehensive study on thermochemical processing of mallee biomass.

Therefore, this research will be focused on four key aspects including (1) steam distillation of mallee leaves to extract high-value essential oil, (2) pyrolysis of the

raw and spent mallee biomass to investigate how steam distillation will affect the biomass fuel properties, its pyrolysis behaviour and the properties of pyrolysis products, (3) torrefaction of raw leaves to improve the properties of the solid fuel (4) combustion of mallee leaves, spent leaves and their chars to examine the particulate matter (PM) distribution and alkali alkaline earth metals (AAEM) transformation during combustion. Thorough understanding on these important aspects is essential to developing a feasible mallee-based bioenergy industry in Australia.

1.2 Scope and Objectives

The main objectives of this research are as follows:

1. To investigate the effect of steam distillation condition on eucalyptus oil extraction from mallee leaves including its distillation performance and kinetics, properties of spent leaves, particularly the evolution of biomass structure, fuel properties and inherent inorganic species.
2. To examine fuel properties of char produced from pyrolysis of spent leaves particularly the transformation of inherent inorganic species during pyrolysis.
3. To evaluate the combustion characteristic of spent leaves including distribution of particulate matter (PM).
4. To characterise the fuel properties of leaf char produced from torrefaction and its combustion characteristic.

1.3 Thesis Outline

This thesis consists of 8 chapters in total. The content of each chapter is outlined below followed by the thesis map which is arranged schematically in Figure 1-1.

Chapter 1 presents the background and aims of the current research;

Chapter 2 sums up literature review on the role of mallee trees in managing dryland salinity, eucalyptus oil in mallee leaf, extraction of eucalyptu soil from mallee leaf, technical challenges associated with biomass utilisation for fuels, direct and treated biomass combustion and its implications and the gaps identification followed by specific objectives for the current study;

Chapter 3 presents the methodology and techniques employed to achieve the research objectives, along with detailed explanation of the experimental equipment and materials used;

Chapter 4 discusses the extraction of cineole oil, fuels properties of spent leaf and transformation of inorganic components during steam distillation.

Chapter 5 reports the significant differences in the fuel and ash properties between biochars derived from raw leaf and spent leaf after steam distillation.

Chapter 6 evaluates combustion characteristic of raw leaf and spent leaf, particulate matter distribution and inorganic transformation during combustion.

Chapter 7 examines chars properties from torrefaction, combustion characteristics of char and its inorganic transformation; and

Chapter 8 summaries the results of the present study and give recommendations for future research.

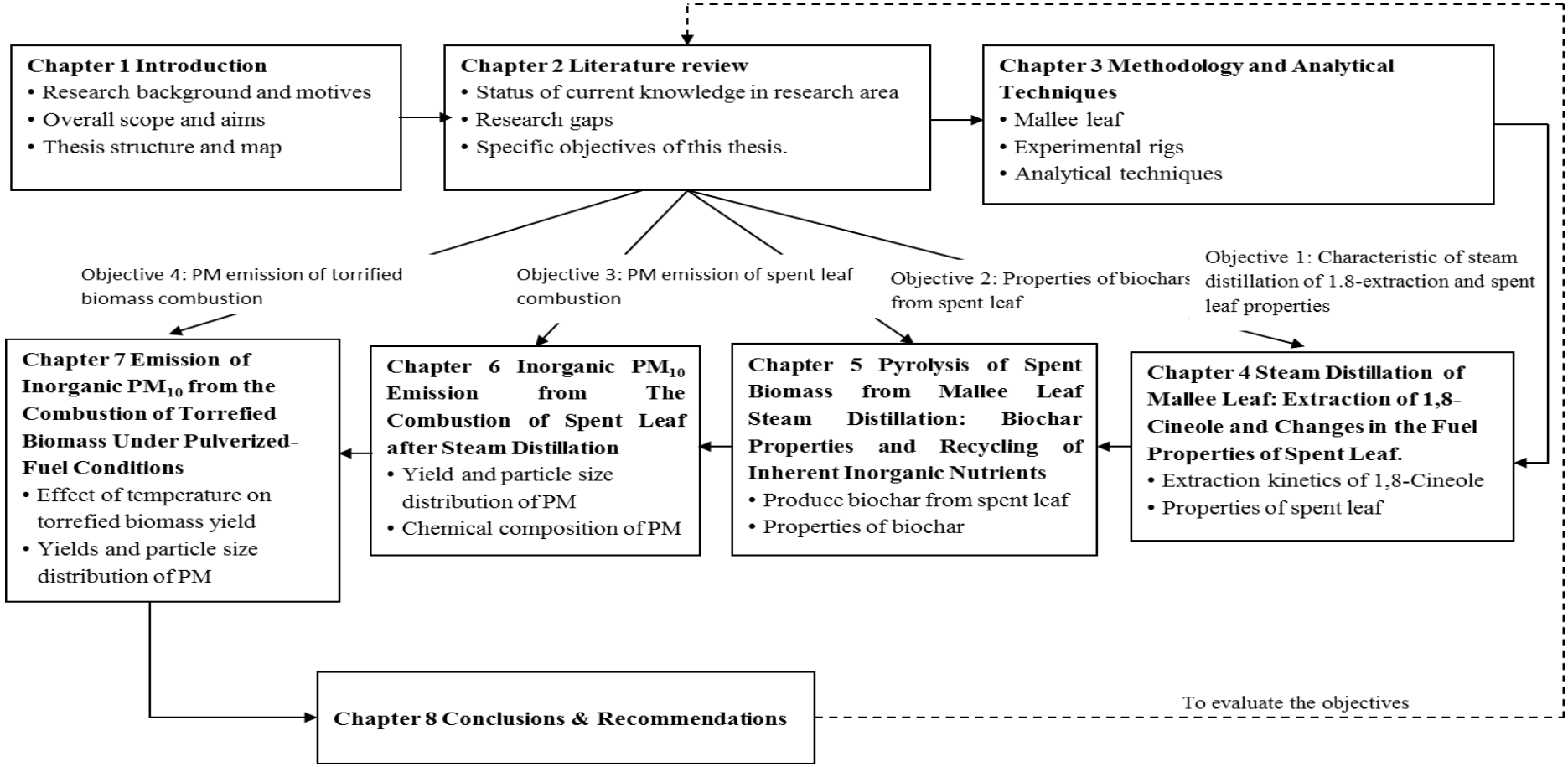

Figure 1- 1: Thesis map

CHAPTER 2 LITERATURE REVIEW

2.1 Introduction

Mallee trees are a native flora in Australia and can be found in all land as wild and planted trees. The latest mallee plantation program is aimed to help controlling the long-standing dryland salinity problem in the wheat-belt agriculture area of Western Australia (WA). The mallee plantation program may also provide feedstock for renewable chemicals and energy industries. Mallee leaf can be subjected to steam distillation for extracting essential oil which mainly contains cineole. Via thermochemical processes, mallee biomas and/or spent biomass can be used as feedstock for electricity generation, the production of biochar, liquid fuels (e.g. bio-oils) and synthesis gas (syngas).

However, there are challenges in utilizing biomass as a solid fuel for energy conversion. Biomass has several undesirable fuel properties including low energy density, high fibrous, high ash content (especially alkaline content), and high moisture content. These properties may lead to low pyrolysis/combustion efficiencies and limit the process equipment's design[8]. To address these issues, torrefaction is considered to be compromising due to its advantage in improving fuel volumetric energy density as well as increased grindability[9, 10]. Particulate matter (PM) generation during combustion of solid fuel is another significant issue which needs to be addressed, since the PM has been known to have a substantial impact on the process equipment, human health and environment[11, 12].

This chapter firstly gives a brief introduction of the important roles of mallee biomass as a potential feedstock of an essential oil industry and bioenergy resource in Australia, including a discussion of distillation methods to produce essential oil. Biomass properties with key technical challenges associated with direct utilisation of biomass is also discussed. The chapter then reviews biomass pre-treatment methods deployed to address these problems including steam distillation and torrefaction. Biomass pyrolysis to produce beneficiated fuels is subsequently discussed. Biomass combustion and issues related to inorganic particulate matter (PM) emission are also

reviewed. The chapter is concluded with summarizing the key research gaps identified and the scope of this PhD thesis.

2.2 Mallee Biomass as Potential Bioenergy Feedstock in Western Australia

2.2.1 Types of mallee biomass in WA

The development of large farming areas by replacement of deep-rooted plants with commercial crops and farming has increased problems of dryland salinity in Southern-Western Australia[13-15]. It is estimated that over 1.8 million hectares is currently salt-affected and will continue increase to 8.8 million hectares (33%) at risk by 2050[16]. The plantation of mallee trees, a deep-rooted and native plant of Australia, in wheatbelt agriculture land is considered as a key strategy for managing the dryland salinity problem.

The mallee plantation program has been implemented via alley farming in several farming land around Western Australia, for example in Kalannie, WA (Figure 2-1). The aims are to address the dryland salinity and to improve the environment in the current agricultural system. In particular, the objectives are to overcome the long-standing problem of dryland salinity; to provide shade, shelter and amenity, to control the erosion , to increase crop yields and to sequestrate the carbon as well as to support biodiversity through the provision of additional habitat for native animals and insects[17, 18]. The plantation also produces an abundant biomass as a byproduct which can be used as feedstock for biofuels and other valuable chemicals production.

Since early 1990s, the plantations of mallee eucalyptus in wheatbelt agriculture area, with low to medium rainfall category, have been developed in 14,000 ha land[2, 19]. In term of its harvest cycle, these plants can be harvested in every 3 years. As a result, the mallee plantations in WA could provide biomass as much as 10 million dry tons annually[20]. Apparently, the plantations could supply raw materials for large-scale malle-related industries.

The mallee biomass production rate for several species of mallee eucalyptus in detail has been investigated by several researchers. Sochacki et al.[21] and Harper et al.[22] estimated the production of mallee biomass for *E. globulus* and *E. occidentalis*

planted in lower landscape position with initial planting densities of 4000 stems/ha could produce approximately 5.5 and 7.4 t/haannually, respectively.

One of mallee species cultivated in WA wheatbelt area is *E. polybractea*. Currently in WA, a new plantation system for *E. polybractea* has been established at a nominal density of 5000 plants/ha compared to the natural system with only have a tree density of 750–1200 plants/ha[18]. Thus, among other mallee species, *E. polybractea* has an excellent prospect on biomass production in the WA wheatbelt area since this mallee tree grows effectively relative to other mallee species within the wheatbelt conditions. Furthermore, *E. polybractea* contains high cineole oil in its leaves[17, 18].

Figure 2- 1: Agriculture land with mallee plants for remediation of dryland salinity at Kalannie, WA.[23].

2.2.2 Carbon Footprint of Mallee Biomass

Since replacing fossil fuels with bioenergy produced from renewable biomass sources is popular, it is important to evaluate the environmental burdens related to biofuels productions by identification of the use of energy and materials as well as the discharge of waste and emissions to the environment. Nowadays, in a life cycle perspective, carbon footprint (CFP) has been used to quantify the impact of greenhouse gas (GHG) emissions on the climate change[24]. There are several factors influencing the CFP of a bioenergy system including feedstock, system boundaries, etc.[25].

The feedstock for bioenergy includes dedicated energy crops, byproducts, organic wastes, etc. In the case of dedicated energy crops, non-renewable energy inputs are required to produce those crops directly or indirectly through the fertilizer , harvest, transport, etc.[1, 25]. Therefore, from the life cycle perspective, bioenergy may not be fully carbon-neutral. However, in the case of the plantation of mallee trees in the wheatbelt agricultural area in Western Australia is aimed for managing serious dryland salinity problems. Mallee biomass is not a dedicated energy crop but a byproduct[26]. Therefore, it is expected that the carbon footprint of mallee biomass to be low.

Considering the land-use change (e.g. cutting down tree for biomass plantation), using biomass as a fuel can potentially release higher carbon emission than fossil fuels[27]. In the 1980s, the emissions of carbon in tropical Asia were approximately 75% from the land-use change [28]. Approximately one-fifth of the current greenhouse gas emission is contributed from land-use change[29]. Searchinger et al.[30] studied the emission of land-use change for corn-based ethanol production using a worldwide agricultural model, they concluded that the greenhouse emission is nearly doubles over 30 years.

For the plantation of mallee biomass, however, there has been a conversion from the wheat agricultural area to mallee tree plantations. The carbon stock may increase with the land-use change from agricultural area to tree plantations[31]. Therefore, the plantation of mallee trees may increase carbon stock in the soil which will enhance the carbon sequestration of mallee biomass when used as bioenergy feedstock. Yu and Wu[26] studied the carbon footprint of mallee biomass by assessing not only carbon sequestration in above-ground biomass (leaf, bark, trunk etc) but also carbon sequestration in under-ground biomass (root) as well as carbon sink caused by land-use change. They reported that the carbon footprint is a negative carbon suggesting that using mallee biomass as feedstock for energy conversions leads to reducing the net carbon emission.

2.2.3 Mallee Biomass as Biofuel Feedstock

Essentially, biomass is product of a photosynthesis process of green plants. The utilisation of biomass to produce energy could be achieved directly through combustion of biomass to produce energy or indirectly by converting the biomass to produce biofuel. As an organic material, the sunlight energy in biomass is kept in its chemical bonds of carbon, hydrogen and oxygen molecules. These bonds could be broken by digestion, combustion, or decomposition to produce chemical energy[32].

The quality of a certain type of biomass as a fuel depends on the chemical and physical properties of the biomass. Those properties include the contents of moisture volatiles, ash, fixed carbon, hydrogen, oxygen, nitrogen, sulphur, and cellulose/lignin ratio[33]. Biomass has been considered as a major source of energy; it is currently estimated to provide 10–14% of the total energy supply globally[32].Mallee biomass, including its leaf, bark, stem and wood has the potentiality to be used as feedstock for biofuel production. Apart from the raw mallee biomass, spent mallee biomass from other industries, such as essential oil industries, may be used as feedstock for biofuel production.

2.3 Properties of Mallee Biomass

2.3.1 Lignosellulosic and extractives in Mallee Biomass

Table 2-1 presents the contents of lignosellulosics and extractives in a type of mallee biomass. It can be seen that the contents of hemicellulose and cellulose in this type of mallee wood are significantly higher than in leaves, whereas the content of extractives in leaves is higher than in wood. The extractives in eucalyptus biomass include essential oil, proteins, ash and other chemical components. Thus, the essential oil in mallee biomass mostly can be extracted from its leaf.

Table 2- 1: Contents of lignin, hemicellulose, cellulose and extractives in mallee wood and leaves[34]

Compounds	Wood	Leaf
Lignin (wt.%)	24.9	25.9
Hemicellulose (wt.%)	40.7	14.8
Cellulose (wt.%)	22.2	14.6
Extractives (wt.%)	12.2	44.7

2.3.2 Essential oils in Mallee leaf and the extraction system

Most of mallee eucalyptus plants contain essential oil in their leaves. The essential oil contains mixtures of volatile organic compounds which include hydrocarbons, alcohols, aldehydes, ketones and acids as well as ethers and esters[35]. Table 2-2 shows the top 10 of chemical constituents of essential oils from four promising oil mallee plants from the Western Australian wheatbelt. It can be seen that 1.8-cineole dominates the compositions of essential oil extracted from four species of mallee in WA. The amount of 1.8-cineole in *E.polybractea* is quite high (87.3 wt%).

Eucalyptus leaves have been used as a traditional medicine by Australian aboriginal people. Furthermore, the first European settlers were also attracted to use eucalyptus oil.. Thus, it can be said that eucalyptus oil is the heritage of Australia.Eucalyptus was the first original Australian product export. Although there are many uses of eucalyptus oil, it is generally used in the following applications namely a natural antioxidant in the food industry[36], pest control [37], antibacterial[38], fumigant[39] and antimicrobial[40]. Commercially, according to their uses, eucalyptus oils can be categorized into three groups (as shown in Table 2-3), viz. medicinal, industrial and perfumery/flavouring oils. Table 2-3 shows that cineole is the main component of eucalyptus oil for medicinal/pharmaceutical industries. Due to the decrease of the sales of industrial and perfumery grade oil , pharmaceutical grade oil seems to be more popular in the market over the last few years[41].

Therefore, it is promising to extract cineole oil from cineole-containing mallee biomass.

Table 2- 2: Average composition of Eucalyptus oil (wt% of total oil) over six regional planting locations for four promising oil mallee species under alley culture in the Western Australian wheatbelt[42].

Oil constituent	*E. kochii* subsp. *plenissima*	*E. horistes*	*E. loxophleba* subsp. *lissophloia*	*E. polybractea*
1,8-Cineole	92.31	90.17	64.92	87.32
α-Pinene	0.6	1.83	12.95	1.51
Limonene	0.88	1.56	3.21	2.12
4-Methyl-2 pentyl acetate	0.01	0.04	6.12	0.03
p-Cymene	0.91	0.96	1.30	1.36
α-Terpineol	0.58	0.67	1.17	0.6
Terpinen-4-ol	0.7	0.79	0.57	0.81
trans-Pinocarveol	0.2	0.22	1.78	0.21
b-Pinene	0.36	0.45	0.22	0.7
Sabinene	0.47	0.48	0.07	0.66

Cineole is popular in medicinal/pharmaceutical industries since this compound has several important properties such as: biodegradable, low toxicity, good solvent for various materials, rapid tissue-penetration, mild bactericidal, insecticidal, synergistic combination with other materials, and generally acceptable odour[43]. As presented at Table 2-3, one of promising mallee species which has high total oil yield (0.7-5 wt%) with a high proportion of 1,8-cineole (60-93 wt%) in its leaf is *E. Polybractea*[41, 43, 44].

Table 2- 3: The main eucalyptus constituents of several eucalyptus species[45]

Species	Main leaves oil constituents (%)	Oil yield; (wt %)
Medicinal/pharmaceutical oils		
E. camaldulensis	cineole, 10-90	0.3-2.8
E. cneorifolia	cineole, 40-90	ca 2.0
E. dives (cineole variant)*	cineole, 60-75	3.0-6.0
E. dumosa	cineole, 33-70	1.0-2.0
E. elaeophora	cineole, 60-80	1.5-2.5
E. globulus	cineole, 60-85	0.7-2.4
E. leucoxylon	cineole, 65-75	0.8-2.5
E. oleosa	cineole, 45-52	1.0-2.1
E. ploybractea*	cineole, 60-93	0.7-5.0
E. radiata subsp. radiata (cineole variant)*	cineole, 65-75	2.5-3.5
E. sideroxylon	cineole, 60-75	0.5-2.5
E. smithii	cineole, 70-80	1.0-2.2
E. tereticornis	cineole, 45-45	0.9-1.0
E. viridis*	cineole, 70-80	1.0-1.5
Industrial oils		
E. dives (phellandrene variant)	phellandrene, 60-80	1.5-5.0
E. dives (piperitone variant)*	piperitone, 40-56	3.0-6.5
E. elata (piperitone variant)	piperitone, 40-55	2.5-5.0
E. radiata subsp. radiata (phellandrene variant)	phellandrene, 35-40	3.0-4.5
Perfumery and flavouring oils		
E. citriodora (citronellal variant)	citronellal, 65-80	0.5-2.0
E. macarthurii	geranylacetate, 60-70	0.2-1.0
E. staigerana	geranylacetate, 60-68	0.1-0.4
E. sp. nov. aff. Campanulata	citral (a + b), 16-40	1.2-1.5
E. methyl cinnamate	citral, 95	1.6-6.1

* Main Australian commercial species

The extraction of eucalyptus oil which contains 1,8-cineole from mallee biomass can be carried out using hydro-distillation or steam distillation process. Those distillation techniques use water to extract the essential oil from the biomass; the techniques are considered as user friendly, scale up easily and environmentally friendly[46-51].

The biomass feedstock for both hydro and steam distillation requires pretreatments including drying and size reduction. The feedstock is air dried to achieve a moisture content of ca 10%, and then it undergoes size reduction process to a particle size less than 500 µm to expose the oily fraction of the biomass[52].

In hydro-distillation, the biomass is boiled in water. Due to the water solubility of the essential oil, the oil is dissolve into the water. The water-oil mixture is then evaporated and rapidly cooled in a water condensation system (Figure 2-2). The condensed water-oil mixture is finally collected in the decanter to separate the oil rich and water rich products.

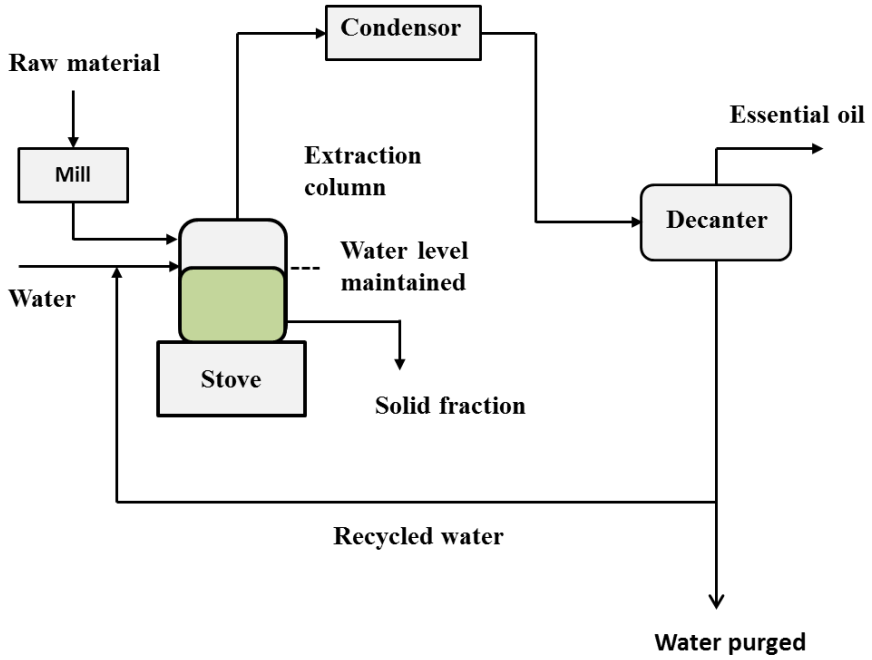

Figure 2- 2: Schematic diagram of hydrodistillation

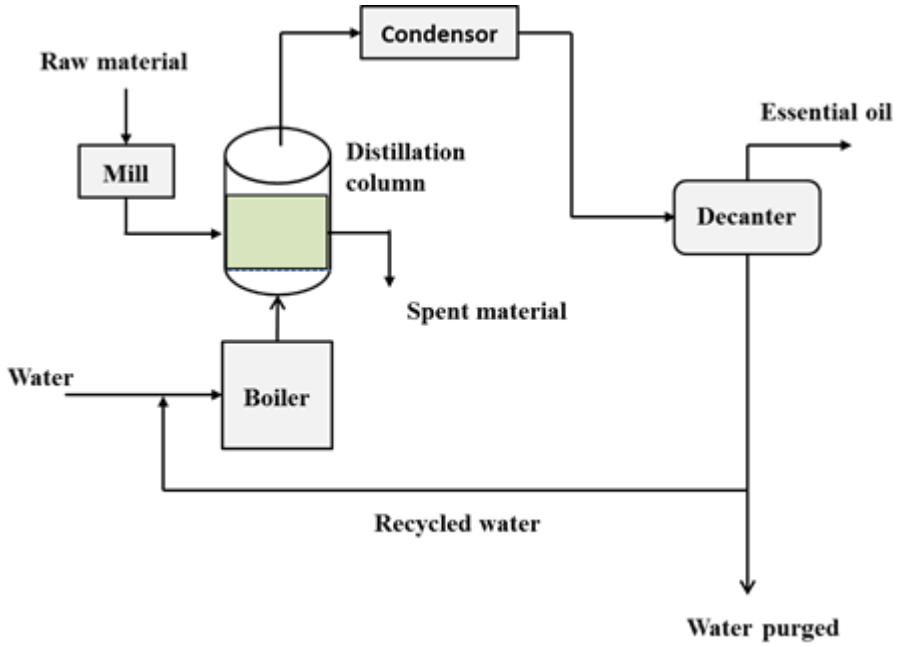

Figure 2- 3: Schematic diagram of steam distillation

On the other hand, in steam distillation, the biomass is not directly contacted with water but with steam. Figure 2-3 shows steam distillation process diagram. The biomass with reduced particle size is packed in a column. Subsequently steam generated in a boiler is passed through the bed, so that the essential oil in biomass is leached out to the steam. To prevent the degradation of oil quality, the steam temperature is controlled between 90 ºC and 100ºC at atmospheric pressure [52]. Then the steam-oil mixture is passed through a water condenser and the products are separated in a decanter.

Although, the separating agent for both hydro and steam distillation is water, steam distillation is reported to have a better performance than hydro distillation. Compared to hydro-distillation, steam distillation achieves higher oil yield with less impurities and minimizes the loss of polar compounds[53-55].

2.3.3 Inorganic Species in Mallee Biomass.

It has been generally known that the types and contents of inorganic elements in fossil fuel has a direct effect on ash formation during combustion. Similar to the fossil fuel, the types and contents of inorganic elements in biofuels has also a significant impact on the ash formation during combustion. The types and contents of

inorganic elements in biomass is affected by the chemical make-up and origin of the biomass and also how the biomass is collected for the energy conversion utilisation[56].

Table 2-4 shows contents of inorganic components and total ash in wood, leaf and bark of mallee biomass. The distribution of inorganics in wood, leaf and bark is distributed unevenly, however it is generally can be seen that the main elemental inorganics in mallee biomas minerals are Calcium (Ca), potassium (K), and sodium (Na) as well as magnesium (Mg). Na and K are alkali metals, while Ca and Mg are alkali earth metals. These inorganics are widely known as alkali and alkaline earth metals (AAEM). The minor constituents include silicon (Si), aluminum (Al), and iron (Fe)[7]. Phosphorus (P), sulfur (S), nitrogen (N), and chlorine (Cl) components are also found on various amounts in mallee biomass.

Table 2- 4: Contents of inorganics in mallee wood, leaf and bark [57]

Element (wt %)	Wood	Leaves	Bark
Na	0.0212	0.5537	0.2094
K	0.0744	0.3797	0.1105
Mg	0.0364	0.1447	0.0796
Ca	0.1236	0.7652	2.6591
Si	0.0026	0.0550	0.0099
Al	0.0025	0.0192	0.0028
Fe	0.0001	0.0142	0.0019
P	0.0182	0.1075	0.0235
S	0.0183	0.1181	0.0509
N	0.1910	1.4574	0.3918
Cl	0.0323	0.1839	0.2601
Ash content (wt % db)	0.4	3.8	5.5
On a dry basis (db) for Na, K, Mg,Ca, Fe, Si, Al, and P; On a dry-ash-free basis for S, Cl, and N			

2.3.4 The Form of Inorganic Species in Biomass

The inorganic species in biomass have various solubility patterns in water, acid and ion-exchange mode. Based on its predominate solubility pattern, the inorganic

components in biomass can be categorized into 4 groups[56], namely (1) predominant water soluble and/or ion-exchangeable components e.g., potassium, sodium and magnesium. (2) distributed among water and acid soluble and/or ion-exchangeable e.g., Ca, S and P; (3) evenly distributed in water, acid and ion-exchangeable e.g., iron; and (4) predominant acid insoluble e.g., aluminum and silicon.

The inorganics in mallee biomass may present in various chemical forms, including oxides, silicates, carbonates, sulfates, chlorides and phosphates[58]. Since in mallee biomass, the inorganic components including K, Na, Ca, and Mg (AAEM) along with S, Cl, P are present in significant amount, only the forms of those components will be discussed in the following paragraphs.

Potassium and sodium are alkali metal components which present significantly in most biomass fuels[59]. K is present more significantly in leaf and bark than in wood[60] . Its occurrence in the plants is mainly in the form of a univalent ion (K^+) which in the fluids the free K^+ may precipitate in the salt form , for example KCl, K_2SO_4, KOH, and K_2CO_3 during drying [61]. While some of the K in the plants are found in the form of organically bound structures such as carboxylic group[61].

Similar to potassium, sodium in biomass may present as salts and/or organically bound structures such as carboxylates[62]. For some plants, Na could act as a substitution for potassium in the osmoticum process [63]. Sodium can also stimulate plant's growth[63].

Chlorine in biomass has a significant role since Cl is identified as part of biomass nutrient cycle. Cl is also considered as a living portion of biomass materials. Furthermore, chlorine could act as a catalyst in the process of photosynthetic and enzymatic. In plants, chlorine presents mainly as a free anion or is loosely bound to exchange sites. It may also present in the form of chlorine-containing organic compounds such as quaternary ammonium chloride ($R\text{-}NH^{3+}$, Cl^-)[64].

Sulfur is an important micronutrient for plant's growth. S is incorporated in plants via two ways, namely S-adsorption via roots and S-absorption via aerial parts of the

plants [60]. The sulfur adsorbed by roots and aerial parts is mainly in the form of sulfate ($SO4^{2-}$)[65]. During the long migration of the sulfur in the plants, some of the sulfur is incorporated into the organic structure of the plant[65]. Therefore, sulfur can be present in plants as sulfates (inorganic S) and organic sulfur (organically associated S)[60, 66]. Leaching experiments suggest that organically associated S makes up approximately 50 wt % of the total S content of the material[67, 68].

Magnesium and calcium are alkaline earth divalent cations which occur almost exclusively bound to carboxylate group and observed in most biomass fuels in moderate amount[69]. They are macronutrients in plants that contribute to regulate plant growth[60, 66]. As a chlorophyll component, magnesium has an essential role on photosynthesis and protein synthesis[70]. The Calcium form is largely found as ion-exchangeable and acid soluble material. It may also be present as crystallized calcium oxalate ($Ca(COO-)_2$) in plants[71].

In biomass, phosphorus mostly occurs in the form of oxidized compounds[72]. The common form of P is dihydrogen phosphate ions (H_2PO_4); these P ions may remain in the form of inorganic P or be incorporated in organic P structures by forming esters or pyrophosphates[73].

2.3.5 Challenges in direct utilisation of biomass

Compared to the properties of coal as a fuel, biomass has poor fuel properties including high moisture content, low energy density, low bulk density, hydrophilic nature and poor grindability. These disadvantages lead to the difficulties to use raw biomass in direct combustion system[9]. The low energy density means that utilising biomass for energy conversion will need very high biomass volumes which may create problems related with storage, transportation, and handling[74]. High moisture content in raw biomass could lead to natural decomposition which results in the decrease in a product quality. In addition, high moisture content could also be related to off-gas emission, cause ignition problem during combustion[75], reduce the process efficiency and increase fuel production costs[76]. In the case of mallee, the green mallee biomass has a very high moisture (45%) and very low energy density (10 GJ/ton)[77].

Furthermore, the bulky and fibrous nature properties of biomass lead to poor grindability, causing a significant increased in size reduction cost and other associated operating and maintenance costs[78]. In conventional coal-based power plants, poor grindability of biomass is one of the key limiting factors of the use of biomass as a co-firing fuel. It can cause incomplete burn out, blockage of the feeding system, sedimentation, and insufficient mixing[79].

The abundance of inorganic species in biomass is also another important issue of consideration during biomass utilisation. Some inorganic species are responsible for various ash-related issues during biomass combustion[75, 80]. The low melting point of ash from biomass thermochemical processing causes ash fouling and slagging problems in the equipment[75].

Torrefaction is an important technology for addressing the aforementioned drawbacks. Furthermore, because eucalyptus oil in mallee leaf is a high-value product, its co-production via steam distillation of mallee leaf may be a vital strategy to increase the economic performance of a mallee-based bioenergy supply chain. In a way, the distillation process can also be considered as a pretreatment process of mallee biomass. Therefore, it is important to have a systematic understanding on the effect of steam distillation on these aforementioned issues associated with biomass. Consequently, these two pretreatment technologies (steam distillation and torrefaction) are reviewed in the next sections.

2.4 Biomass steam distillation

As described in section 2.3.2 steam distillation is commonly used to extract essential oil from biomass. Mechanical, chemical and thermal processes happen during distillation process. Cutting and grinding of the feedstock may disrupt the biomass physical structure. Furthermore, the contact between steam and biomass during distillation destroys the structure of biomass chemically and thermally. It was reported that the inorganic components in spent biomass after hydro distillation was reduced signifantly[7]. The inorganics have a significant contribution on the ash production during combustion.

There is a very limited study on the fuel properties of spent biomass after steam distillation. Since the principle of hydro distillation is quite similar with steam

distillation, it is reasonable to speculate that the steam distillation can improve the properties of spent biomass as a solid fuel particularly in mitigation of ash-related problems.

2.5 Biomass torrefaction

Torrefaction technique has been practiced for many thousands of years to produce charcoal as the first convenient solid fuel as well as a feedstock for iron extraction. Recently, the utilisation of char produced from biomass torrefaction is used in large field area such as cofiring with coal for power plant, fuels for decentralized or residential heating system, fuels for gasification, feedstock for chemical industries and material substitution for coke in blast furnace.

Torrefaction is conducted by heating a solid material at temperature below 300 ^{o}C in the absence of oxygen or in limited supply of oxygen. Torrefaction process is influenced by several parameters including temperature, heating rate, residence time, ambient pressure, feedstock moisture and feedstock particle size. Torrefaction in an absent of oxygen can potentially produce a very high quality of solid fuels[81-83].

The process reaction during torrefaction at different temperature may be divided into three regimes[74]. Firstly, a nonreactive drying regime which occurs at temperatures between 50 and 150 ^{o}C where there is a loss in physical moisture in biomass but no change in its chemical composition. The lignin component becomes softer in this step[84]. Secondly, a reactive drying regime happens at temperatures of 150 – 200 ^{o}C. In this regime, the structural deformity of the biomass initiates breakage of hydrogen and carbon bonds and depolymerisation of hemicellulose occurs[85]. Finally, a destructive regime undergoes at temperatures of 200–300 ^{o}C. In this regime, the process reaction of extensive volatilisation and carbonation of hemicellulose take a place, followed by a limited amount of depolymerisation and devolatilisation of lignin. A slight depolimerisation and devolatilisation of cellulose also occurs in this regime[86]. As a result, biomass cell structure is completely destroyed in this final regime making it brittle and nonfibrous.

In comparison with raw biomass, torrefied biomass possesses higher degree of carbon to oxygen (C/O) content ranging from 102% to 120%, makes the torrefied

biomass increase the energy density significantly[84]. The breakdown of hemicellulose due to torrefaction yield lower strength of the torrefied biomass and improves its grindabiliy[84]. In relation to the improving hydrophobicity of torrefied biomass, it is presumably due to the following factors. Firstly, the loss of the OH functional group from hemicellulose during torrefaction reduces the ability of the biomass to form hydrogen bonds with water. Secondly, the destruction of the chains between the cellulose and lignin as a result of hemicellulose breakdown makes the water molecules could not be stored in the cell.

In addition, tar condensation inside the pores during torrefaction may have a non-polar character and also obstruct the passage of moist air to condense through the solid resulting low moisture of the material[87]. The low moisture content of the torrefied biomass makes the material more stable, especially against chemical oxidation and microbial degradation. The improved properties of torrefied biomass make the material more suitable as a cofiring material in power plants, upgraded gasification feedstock[74], and other energy conversion technologies.

2.6 Biomass pyrolysis

2.6.1 Biochar production via biomass pyrolysis

There are various thermochemical processes for converting biomass into various energy and fuels products, including combustion, gasification, liquefaction, pyrolysis and torrefaction. Pyrolysis is a flexible thermochemical technology[88] in which biomass is thermally processed either in the absence of air or in a limited supply to produce biochar, bio-oil and pyrolytic gas via thermal cracking of lignocellulosic macromolecules[89] as represented by equation 2-1.

$$C_nH_mO_p(\text{biomass}) \rightarrow \sum(C_xH_yO_z)_{Liquid} + \sum(C_aH_bO_c)_{gas} + H_2O + C(\text{char}) \ldots\ldots (2\text{-}1)$$

In general, pyrolysis can be classified into two categories, i.e. slow and fast pyrolysis. Slow pyrolysis is mainly used for char production, while fast pyrolysis is carried out for bio-oil and gas production [88, 90-94]. The pyrolysis product yields are influenced by several factors including biomass properties and operating conditions, for example heating rate, pyrolysis temperature and pyrolysis residence time.. Individual components including cellulose, hemicelluloses, and lignin

(including inherent inorganic species) exhibit different characteristics and products distributions during pyrolysis[95]. Qu et al.[96] reported that bio oil extracted from cellulose and lignin mainly contain carbohydrates and phenols, respectively. Whereas, bio-oil from hemicellulose are consists of acids, ketones, aldehydes and phenols. The roles of lignocellulosic individual components in thermal decomposition activity during pyrolysis have also been investigated by Yang et al[97]. They found that the highest level of activity in thermal decomposition is hemicellulose followed by cellulose and lignin. The research carried out by Lv et al.[98] show that the pyrolysis rate, tar and gas yield increased with the increased in cellulose content, whereas the char yield decreased. On the other hands, the pyrolysis rate was slower in the biomass with higher lignin content.

Biomass particle size also influences the pyrolysis process[99]. The particle size is related to the heat and mass transport effects in the biomass during pyrolysis. In general, the total gas yield decreases as the biomass particle size increases. The mass transfer resistance is larger in a big biomass particle.

The effects of temperature during pyrolysis have been widely investigated[99-109]. The results showed that temperature is the key factor which affects the distribution of the liquid and gas yields, as well as the fraction of phenolic components within the range of their experimental conditions. Pyrolysis conducted at low temperature (below 400 ^{o}C) yield the pyrolysis products are dominated by char. Liquid yield increases with increase in pyrolysis temperature, reaching the peak at ca 400-500 $^{\circ}$C then gradually decreases. The gas yield, however, increases with the increase in the temperature. Wang et al.[110] proposed the biomass decomposition reactions at different temperature regime during pyrolysis as shown in figure 2-4. Biomass pyrolysis at below 250ºC produces mostly char and pyrolysis gas is mostly dominated the pyrolysis products at pyrolysis temperature above 700ºC.

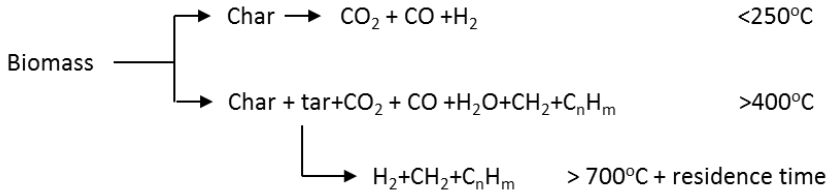

Figure 2- 4: Reaction mechanism of biomass during pyrolysis at different temperature regimes[110].

Heating rate is another important operation condition affecting yield of pyrolysis products and compositions. Numerous studies have been done and reported in literatures focus on the influence of heating rate in pyrolysis process[105, 111-113] and the results show that with increasing the heating rate the char yield decreases , however increases liquid and gas yields. The production of biochar is favoured at slow heating pyrolysis.

The presence of AAEM species such as K, Na, Mg and Ca in biomass is more significant than in most bituminous coals[114]. The current biomass utilisation processes are largely based on experiences from coal conversion system[114]. Many studies have been done to investigate the roles and chemical forms of AAEM in coals pyrolysis, gasification, combustion and liquefaction[115-118]. They found that these cations play an important role in coal conversion process particularly in the volatilisation stage at high temperature.

Many studies have been conducted on the role of inorganic matter including AAEM species in biomass during thermal conversion processes. AAEM elements in combination with the organic matters play an important role in determining pyrolysis product distribution and product properties[119].

AAEM is also reported to play as a catalyst during pyrolysis. Hosokai et al.[120] studied the effect of the alumina particle by depositing it into the coke and the results showed that alumina played as a catalyst to reduce polyaromatic hydrocarbon, a heavy tar representative component. Fahmi et al.[121] found that there was a strong catalytic effect by the AAEM species particularly potassium during pyrolysis.

The yield and properties of biomass pyrolysis products are affected by pyrolysis process conditions and feedstock features including physical and chemical properties of the biomass, including mallee biomass. Therefore studies of mallee biomass pyrolysis will help to determine suitable conditions for the applications of mallee biomass as a renewable energy source.

2.6.2 Nutrient recycling of biochars product

There has been a growing concern related to t the uncontrolled of the use of non-renewable soil resources which has fashioned land degradation problems around the world. In order to minimize these problems, the remediation concept using biochar as a renewable materials became popular. The application of biochar by returning to soil may improve soil quality[122-124], achieve carbon sequestration to mitigate the effects of global warming and recycle some of inherent inorganic nutrients in biochar to soil.[125-130] Considering a biochar application rate of 5−50 tonnes per hectare of land[131], recycling at least part of inorganic nutrients in biochar to soil is particularly important to improve the sustainability of biochar industry. The returning of biomass and/or its derived product such as biochar to the field can potentially increase agricultural productivity[132-135].

The ability of biochars on improving soil performance is due to its unique properties. In general, biochar has a large specific surface area; it also has high porosityas well as a high resistance level to be mineralized to CO_2 [127]. The large of cation exchange capacity (CEC) of biochar is believed as one of the main factors took place on improving soil properties; thesedue to the large-negative charge surface area and charge density of the biochar[128, 136-139]. A high water holding capacity (WHC) plus water absorption are also important properties of biochar to improve soil performance. A previous study shows that there is a wood char found in aquifer materials[140]. The WHC of the soil can be increased significantly by addition of biochar to soil[141, 142].

Biochar may also offer an alternative to return nutrients to the soil[143]. Biochar produced at low pyrolysis temperatures (< 500°C) has the greatest effect on biochar characteristics that impact agricultural productivity such as cation exchange capacity and nutrient content[144].

Several studies investigated the availability of nutrients in biochars by application of biochars into the soil and measuring the nutrients contents in the plants. Chan et al.[145] in their pot study found that biochar of poultry litter could increase the concentrations of N, P, S, Na, Ca, and Mg concentrations of radish plants (*Raphanus sativus variety Long Scarlet*) indicating that these nutrients are plant available[145]. However, the application of greenwaste biochar on their pot only increased concentrations of P, K, and Ca in radishes[146]. Steiner et al.[147] investigated the effect of addition secondary forest products biochars in a weathered Amazonian soil without other fertility amendments, they found that this biochar did not affect the nutrient concentration in rice (*Oryza sativa L.*) nor sorghum (*Sorghum bicolor L. Moench*).

Thus, it appears that data related to the nutrient retention in biochar after water leaching in various biomass feedstock and pyrolysis condition become essential, particularly in returning biochar to the soil for recycling of nutrients as well as carbon sequestration. There are only few studies on the leaching process of inherent inorganic elements in the pyrolysis biomass char. For example, Jensen et al.[148] characterised straw char by water leaching and they found that there were three fractions of potassium in straw char viz. dissolved very fast, slow release and not be removed with pure water. Wu et al.[57] investigated the recycling of inherent inorganic nutrient elements during water leaching of biochars produced from mallee biomass under slow heating pyrolysis. They reported that there were significant reductions in the overall recycling by water leaching of most nutrient species in biochar which originally present in biomass.

To improve understanding on the inherent inorganic species leachability of biochar, further study on biochar leaching characteristics from various feedstocks under different pyrolysis conditions is needed.

2.7 Biomass combustion

2.7.1 Ash-Related Problems of Pulverized Biomass combustion

The inorganic species in solid fuels are believed as components which produce ash during combustion. The alkali and alkaline earth metal inorganics combine with other inorganics elements such as silica, sulfur and chlorine are known as the key elements for many unwanted reactions in a combustion furnace and boiler[149], causing adverse impacts such as slagging, fouling, corrosion and bed material agglomeration in fluidized beds[59, 64, 65, 68, 149-156].

During combustion, the inorganic components are responsible for ash deposition and the release of particulate matter (PM). PM evolution from the fuel to the gas phase during combustion contributes significantly to the negative effects of human health and environment as will be discussed in the following section. From this point of view, it is crucial to understand the principle of transformation of the inorganic species and its ash mechanisms formation during combustion. Therefore, the next section also reviews the transformation and release of the key inorganic species during biomass combustion including its reaction system in gas and gas-solid phase.

2.7.2 Issues related to Particulate Inorganic Matter (PM) emission

Biomass combustion releases a significant emission of particulate matter (PM)[157-162] and recently become one of the major environmental issues[163]. This emission contributes to deterioration of atmospheric visibility[164] and correlated to negative health effects[165]. Studies on epidemiology have shown that increased concentrations of PM in ambient air correlates with negative health effects. When inhale, PM could penetrate into the lung alveolar regions[166-168]. Particulate matter was also correlated with cardiopulmonary as well as mortality due to lung cancer [169, 170]. It was also reported that particulate matter are responsible for the initial pulmonary injury[171] and increased risk of cardiovascular disease (CVD)[172].

2.7.3 Formation Mechanisms of Particulate Matter (PM)

Biomass combustion emits relatively high particulate matters in a various fine particle size distribution[80]. The size of particulate matters emitted is mainly classified on aerodynamic particle size since these particles are generally an imperfect spherical form. The range of particle sizes in submicron (< 1 μm) and supermicron (> 1 μm) are usually emitted with respect to technology used[173, 174] and biomass feedstock properties[175, 176].

In general, the particulate emissions during combustion can be emitted from the incomplete particle combustion such as soot, tar and char which could be easily controlled by adjusting the operating parameters. PM also can be emitted from the inorganic material (AAEM, S, and Cl) in the fuel via a complex transformation mechanisms, e.g. nucleation, coagulation and homo- or heterogeneous condensation in gas phase[69, 149, 163, 174, 177, 178]. The formation of submicron particles is generally through nucleation mechanisms while the supermicron (coarse) particles are formed from incomplete ash coalescence caused by the relatively low temperature of ash formation[165, 179]. During combustion pulverized wood, submicron particles mainly contain alkali, sulphur and chlorine, while supermicron particles were enriched in Ca, Mg, Si, P and Al [180, 181].

It is well documented that the gaseous release of the inorganic elements as known as the main key in particulate matter formation during combustion can be linked with the two stages of material conversion, namely fuel particle devolatilisation and char combustion[69]. In general, devolatilisation occurs at relatively low temperatures (during torrefaction and pyrolysis) releasing loosely bound free ions, salts and organically associated alkali minerals. While, the stronger bonded alkalis and part of alkaline earth metal will mostly be released during the char combustion at high temperatures[182]. Taking all this into consideration, it is very important to understand the path ways of inorganic components released during torrefaction, pyrolysis, and combustion; particularly for Cl, K, Na, Mg, Ca, and S components as presented in the next sections.

2.6.3.1 Chlorine release

Several investigations in relation to releasing Cl to gas phase during torrefaction and pyrolysis have been conducted by several researchers. Figure 2-5 shows a schematic of transformation and Cl release during biomass combustion based on the finding from several previous studies. It shows that the Cl release to the gas phase through a two-steps mechanisms which is related to its chemical forms and the influence of temperature during thermal conversion.

At temperature below 200 ^{o}C, the release of Cl to the gas phase is insignificant[183, 184]. While, a significant effects on the release of Cl occurs above this temperature. For example, Khazraie et al.[185] found that during torrefaction and pyrolysis of birch wood, chlorine to some extents are emitted to the gas phase at temperatures below 500 °C. It was around 25% and 85% of Cl has been released at temperature 240 ^{o}C and 280 ^{o}C, respectively.

Jensen et al.[184] conducted experiment with large range temperature pyrolysis using straw biomass and they found that chlorine was released in two steps viz. at the range temperature between 200 to 400 ^{o}C, there was approximately 60% Cl released and most of the residual chlorine was released between 700 and 900 °C. It was suggested that Cl to be released as HCl gas as the result of ion-exchange reactions with functional groups in the organic matrix at initial low temperature[65, 186]. While at high temperature the residual chlorine release most likely due to the evaporation metal chlorides as a result of the degradation reaction of alkaline carboxylate formed from interaction with the organic material[187].

Saleh et al.[188] found that Cl released to the gas phase during straw torrefaction and pyrolysis was majority in the form of methyl chloride (CH_3Cl). Hamilton et al.[189] also found a similar phenomenon on releasing Cl in the form of methyl chloride at ranging temperature 150 ^{o}C to 300 ^{o}C. They proposed that pectin took place as a CH_3 donor to react with Cl forming CH_3Cl and release to the gas phase. They found by analysis of released gases from straw that pectin can react with chloride ions to form methyl chloride and the gas phase release of the methyl chloride has already been completed at a temperature of 300 °C.

The roles of Cl component to enhance of K and Na in biomass during pyrolysis and combustion are still debatable. It was reported that Cl content in biomass was important to facilitate alkali release during combustion[64, 66]. Baxter et al.[66] reported that the Cl concentration controlled the amount of alkali vaporisation stronger than the alkali concentration in the fuel during combustion. It was also found that there is a close correlation between the release of K and Cl. The amount of Cl seems to control the final high temperature K release. The release of Cl occurs at low temperatures, thus at elevated temperature there is a reduce amount of Cl which then limits the K release. The analysis of ash phase components has proven that K is retained in the ash phase, it was not released as KCl.

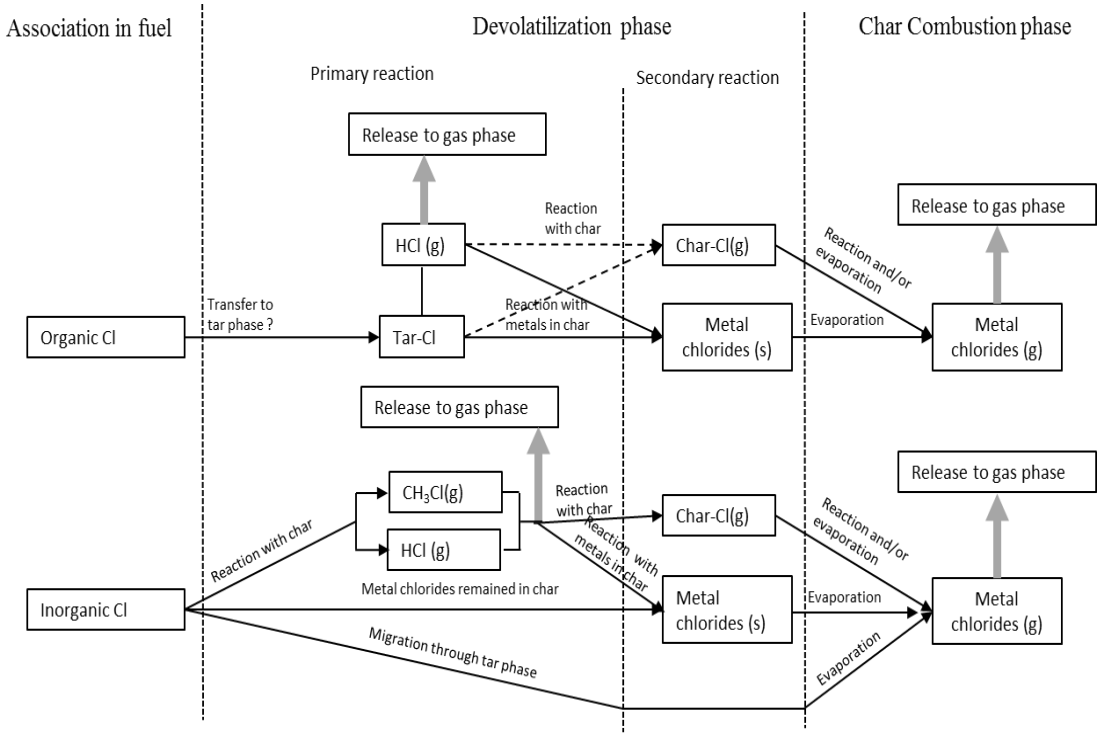

Figure 2- 5: Transformation of Cl during devolatilisation and combustion[190].

2.6.3.2 S release

As discussed in section 2.3.4, the occurrence of S can be present in organically bound forms or inorganic forms. These forms cause the transformations of S are complex. Inorganic and organic S in the biomass could be released to the atmosphere or captured into the char bed during thermal energy conversion processes both at low and high temperatures.

Several studies have been done related to release and transformation of S during torrefaction and pyrolysis which is conducted at temperature below 500 ^{o}C. Shoulaifar et al.[185] run torrefaction of birch wood at temperature 240 ^{o}C and 280 ^{o}C and they found that S content decreased approximately by 40% and 55%, respectively. The S decrease was mostly seen in the insoluble fraction. This suggests that organic sulphu is emitted. Similar finding was also found by Yan et al.[191] during wet biomass torrefaction which showed that the sulfur release at 260 ^{o}C was twice higher than at 230 ^{o}C.

Lith et al.[61] studied the release of S during pyrolysis of four types of fuels with various ash and inorganic contents. Their results exhibited that at temperature 500 ^{o}C, the release of S was in the range of 50–70%. Knudsen et al.[65] studied the release of S during pyrolysis, their results show that at 500 °C, the amount of total S emitted to the gas phase is 25-35%, while at the interval temperature of 500-800 °C, the S emission increases to 40-50%. Other study[192] showed that the fraction of sulfates in the char remains constant up to 500-600 °C, in contrast the total S content in the char decreased in this temperature ranges during pyrolysis. This result suggests that the release of S is caused by the decomposition of organic Sulphur components, it is not caused by the decomposition of inorganic sulfates.

A significant amount of S released at low temperature (500 ^{o}C) is mainly as SO_2 which is caused by the decomposition of organic S components that are thermally unstable, rather than the decomposition of inorganic sulfates during the pyrolysis stage[61, 68, 193]. The release of organic sulfur during devolatilisation may also then be captured by reactive sites of the char matrix and attached to the char[192]. It was also postulated that during devolatilisation, inorganic sulfate (e.g. K_2SO_4) may

undergo partial reaction with char and become bound to the char matrix or converted to CaS/K_2S.

As discussed above, the release of S during torrefaction and pyrolysis is mainly in the form of organic sulfur and the inorganic S form predominantly remains stable. However, inorganic sulfides and sulfur attached to the char matrix has been recognized to be emitted to the gas phase at high temperature during char burnout[61, 65, 190]. Knudsen et al.[65] highlighted that the release of S increases significantly during combustion of annual biomass at temperature above 800 ^{o}C and completed at 1150 °C. The sulfur release in this temperature range is believed to be mainly due to the decomposition and/or alkali metal sulfate evaporation releasing SO_2 to the gas phase[61, 65, 186] or transformed into solid in the form metals sulfide e.g. $CaSO_4$ and K_2SO_4[192].

2.6.3.3 Potassium and Sodium Release

The release of K and Na during energy conversion processes is mainly influenced by the occurrence of its forms and process temperature[65, 186, 194]. As discussed in previous section (section 2,6.2), the forms of K and Na can present as organically and inorganically bound and/or a free bound.

Pyrolysis of several biomass (bichwood[195], wood waste[196], and annual fuel crops[68, 194, 196, 197]) at low temperature were only released a small fraction of K. The K released is organically associated ascarboxylates or phenols which decomposed at ca 300 and 400 ^{o}C, respectively[61]. The release mechanisms of K in the form of carboxylates and phenols groups at low temperature was proposed by van Lith[61] as presented by Equation (2.2) and (2.3), respectively. It seems that the K release of devolatilsation of carboxylates seems to be in the atomic form. However, in the case of phenols, only a small fraction of K is released from phenols and phenol groups were still present in the char.

Char-COOK → Char + CO_2(g) + K (300 ^{o}C) …….….(2-2)

Char-C_6H_5-OH + K → Char-C_6H_5-OK + H ……..…(2-3)

The K release phenomena might be related to a higher diffusional resistance as a result of the organic matrix intact which still occur during low temperature pyrolysis[198]. The intercalation of the existing organic matrix can also potentially affect the net K release at low to moderate temperatures[184, 199] and prevent vaporisation of K during char combustion[200].

The K release of various biomass above 500 – 700 ^{o}C during pyrolysis and combustion has been investigated in several studies e.g. birchwood[195], wood waste[196], and annual fuel crops[65, 68, 184, 194, 196, 197]. Their findings show that the K released mainly due to vaporisation of potassium salts. This is suggested by the finding that the K release during devolatilisation of water-leached biomass fuels at high temperature is greatly reduced[196].

The release of K in the form of KCl which is originally present in most biomass has been identified at pyrolysis temperature above 700 ^{o}C[184]. The K which released at the high temperature may react with the organic-char-matrix functional groups . This results in the formation of HCl(g) and subsequently K is bound into the char matrix[190]. This char-bound K together with K_2SO_4(s) which is also originally present in biomass could react with Si, Al, and probably Ti elements in the ash during char burnout which then will form a stable elements(up to 1150 °C) and release SO_2(g)[190]. The vaporisation of condensed alkali sulfates during combustion was also identified from wood fuels which contain low Cl and alkali metal[201].

Wu et al.[118] proposed that the contribution of volatile-char interaction also took place on releasing alkali metal during fast heating pyrolysis in a fluidized-bed at high temperature (>500 ^{o}C). They observed the interaction between char and reactive species (hypothesized as free radicals, especially H radicals) produced from thermal cracking allowing the release of alkali species as a result of substitution reaction. The interaction between reactive species (R) and char alkali matrix (CM-X) is given in equation (2.4) below:

$$R + CM\text{-}X \rightarrow CM\text{-}R + X \quad \text{.....(2-4)}$$

where CM is the char matrix, X is the alkali species and R is reactive species (hypothesized as free radicals, including H radicals) in the volatiles.

At higher temperature, sodium may be incorporated in the char structure with an interaction with other species. It was reported that Na might be incorporated in the aluminosilicate structure during combustion at high temperature (around 1200 ^{o}C). The interaction between sodium and alumina during combustion to form aluminosilicate was proposed in equation (2.5)[182].

$$2NaCl + Al_2O_3.xSiO_2 + H_2O \rightarrow Na_2O.Al_2O_3.xSiO_2 + 2HCl \quad \text{.....(2-5)}$$

2.6.3.4 Alkaline Earth Metals (Mg and Ca) Release

As discussed in section 2.3.3, mallee biomass contains alkaline earth metal particularly Mg and Ca in a moderate amount. It has been also pointed out in section 2.3.4 that these components dominantly bound to carboxylate group. The decrease of carboxylic acid sites during biomass torrefaction has been identified in earlier study by Shoulaifar et al.[202]. In another investigation[203], it was found that the alkaline earth metal bound associated to carboxylate group in biomass has been destructed during torrefaction. However, there is no report on the release of alkaline earth metals during torrefaction.The release of Mg and Ca was detected during pyrolysis at temperature around 500 ^{o}C[114]. The decomposition of Mg and Ca-containing organic structure yielded light carboxylate, following the path way of the release mechanism of alkalis Na and K[114]. Due to the difference of valences between K (and Na) and Mg (and Ca) made the amounts of K and Na release were generally higher than Mg and Ca[114, 204].

During biomass combustion, there are strong indications that the release ofCa from the solid fuels is mainly in the form of CaO at temperature >800 ^{o}C and $CaCO_3$ at temperature <800 ^{o}C[180]. Mg and Ca can also be incorporated in the aluminosilicate structure for the solid fuels with high content of Al and Si[182]. The reaction of Ca and Mg with alumina-silicate has been found more appropriate compared to alkalis[69]. For that reason, it is reasonable to speculate that higher content of Ca in the fuel will cause more alkalis to emit in gas phase during combustion.

2.7 Conclusions and Research Gaps

Long-term economic and environmental concerns regarding the dryland salinity in the wheatbelt agricultural area of WA have led to the plantation program of mallee eucalyptus trees. Mallee biomass as the byproduct of the plantation program has the potentiality to be utilized through steam distillation to produce 1,8-cineole oil for pharmaceutical industries as well as to be used as feedstock for energy conversion processes. Steam distillation and torrefaction are considered to be suitable to pre-treat raw mallee biomass so that the pretreated biomass is easy to be further utilized in energy conversion technology and has less impact to the equipment and environment due to less content of inorganics in the pretreated biomass. The inorganic components in solid fuels are responsible on the formation of particulate matter (PM) during combustion. Biomass pyrolysis produces biochar, liquid and gas. Biochar produced from pyrolysis is potentially used as solid fuel, remediation of agriculture land and source of plant nutrients.

Based on the summary above, there are no reports on data of kinetics of the extraction of 1,8-cineole from mallee leaves via steam distillation. There are also no data reported on the fuel properties of the spent leaves after steam distillation. It is also largely unknown how the roles and transformation of inherent inorganic species especially alkali and alkaline earth metal (AAEM) species during distillation and pyrolysis. In addition, there is also no data reported related to the inorganic PM emission during combustion of spent biomass and biomass torrefied. Therefore, further study is needed to improve the fundamental understanding of integrating the utilisation of mallee biomass as renewable chemical and energy sources including:

1) Extraction kinetics of the main components in mallee biomass during steam distillation.

2) Characterisation of spent mallee biomass as a fuel after steam distillation process.

3) Characterisation of chars from spent mallee biomass pyrolysis. A more detail study of this issue is needed including an assessment of the molecular forms in mallee biomass before and after process.

4) Emission behavior of inorganic PM from spent mallee biomass during combustion.

5) Emission behavior of inorganic PM from torrefied mallee biomass during combustion.

6) Roles of inorganic species in mallee biomass on the formation of PM during combustion.

2.8 Research objective of the Present study

Based on the literature review above, various research gaps have been identified. However, those gaps can not be filled in all by conducting research due to the limitation of PhD study period. Therefore, this study will focus on distillation of mallee leaves for eucalyptus oil extraction and pyrolysis behavior of the spent biomass and its combustion characteristics. The main objectives of this thesis are listed as follows:

1. To investigate the extraction behaviours of 1,8-cineole during steam distillation and the effect of such steam distillation on the fuel properties of spent biomass.

2. To examine the effects of steam distillation on the biochar yields, the retention of inorganics in the biochars during spent leaves pyrolysis, and their subsequent release during biochar water leaching.

3. To examine the combustion characteristic of spent leaves particularly its particulate matter (PM) behavior.

4. To carry out a systematic investigation into the emission behaviour of inorganic PM_{10} from torrefied biomass combustion under pulverized-fuel conditions.

CHAPTER 3 RESEARCH METHODOLOGY AND ANALYTICAL TECHNIQUES

3.1 Introduction

The overall research methodology and detailed analytical techniques employed in this PhD study are elucidated in this chapter in order to accomplish the thesis objectives which were outlined in Chapter 2.

3.2 Methodology

Mallee leaves were separated from mallee trees and prepared by drying and cutting. Spent leaves were obtained from steam distillation process and biochar was produced from fixed-bed and drop tube reactor system. Raw and spent leaves used as feedstock for pyrolysis were grounded using a ball-mill system as well as torrefied leaves from torrefaction system. All fine fuels from raw leaves, spent leaves and torrefied leaves were subjected as feedstock for further combustion experiments and compositional/elemental analysis. Unground spent leaf was subjected to image analysis and scanning electron microscopic (SEM) analysis. An array of advanced analytical instruments such as thermogravimetric analysis (TGA), elemental analyser, total organic carbon (TOC), ion chromatography (IC) cation and IC anion were employed to characterise feedstock and its utilisation products. In this research, experiments or analytical analysis were replicated to ensure reproducibility of results.

The overall methodology to achieve the objectives in Chapter 2 is shown in Figure 3-1 with further explanations in the following sections.

3.2.1 Steam Distillation of Mallee Leaves: Extraction of 1,8-Cineole and Changes in Fuel Properties of Spent Biomass

In this study, steam distillation apparatus (see section 3.4.2) was employed to extract 1,8-cineole component from prepared mallee leaves sample (see section 3.4.1). A series of distillation experiments were carried out at various distillation times at a fixed sample mass and steam flow rate. The raw leaves and spent leaves after steam distillation were characterised their morphological structures and quantified their 1,8-

cineole and inorganic contents. Proximate and ultimate analysis were also carried out to those samples.

The ground raw leaves and spent leaves samples were also subjected to semi-continuous leaching (as described in section 3.4.3) and the leachate samples collected at various leaching times were then quantified for their total organic carbon (TOC), alkali and alkaline earth metal (AAEM) species and chlorine (Cl) content. Chapter 4 presents the results and discussion for this work.

3.2.2 Pyrolysis of Spent Biomass from Mallee Leaves Steam Distillation: Biochar Properties and Recycling of Inherent Inorganic Nutrients

Pyrolysis at slow heating and fast heating at various temperatures were conducted to produce the biochar from the ground raw leaves and selected spent leaves. (See detailed descriptions on sample preparations in Section 3.4.1 and pyrolysis condition in Section 3.4.4. The ground raw leaves and biochars were then quantified their elemental compositions including proximate and ultimate analysis.

The biochar samples were also leached in Milli-Q water under batch conditions at room temperature in order to quantify its water-soluble inorganic nutrients. The detailed results and discussion for this work are presented in chapter 5.

3.2.3 Inorganic PM_{10} Emission from the Combustion of Spent Leaf after Steam Distillation

For this work, the ground raw leaves and selected spent leaves produced from steam distillation were combusted in a drop tube furnace (DTF) system , followed by PM sampling and appropriate analysis(See Section 3.4.6). Chapter 6 presents the results and discussion for this work.

3.2.4 Emission of Inorganic PM_{10} from the Combustion of Torrefied Biomass under Pulverized-Fuel Conditions

Torrefied leaf samples were produced in a fixed bed reactor with slow heating condition process and an absent of oxygen at relatively low temperature (220 °C to 280 °C). The ground torrefied samples were then subjected in combustion system (similar method in Section 3.3.3). The results and discussion for this work are presented in Chapter 7.

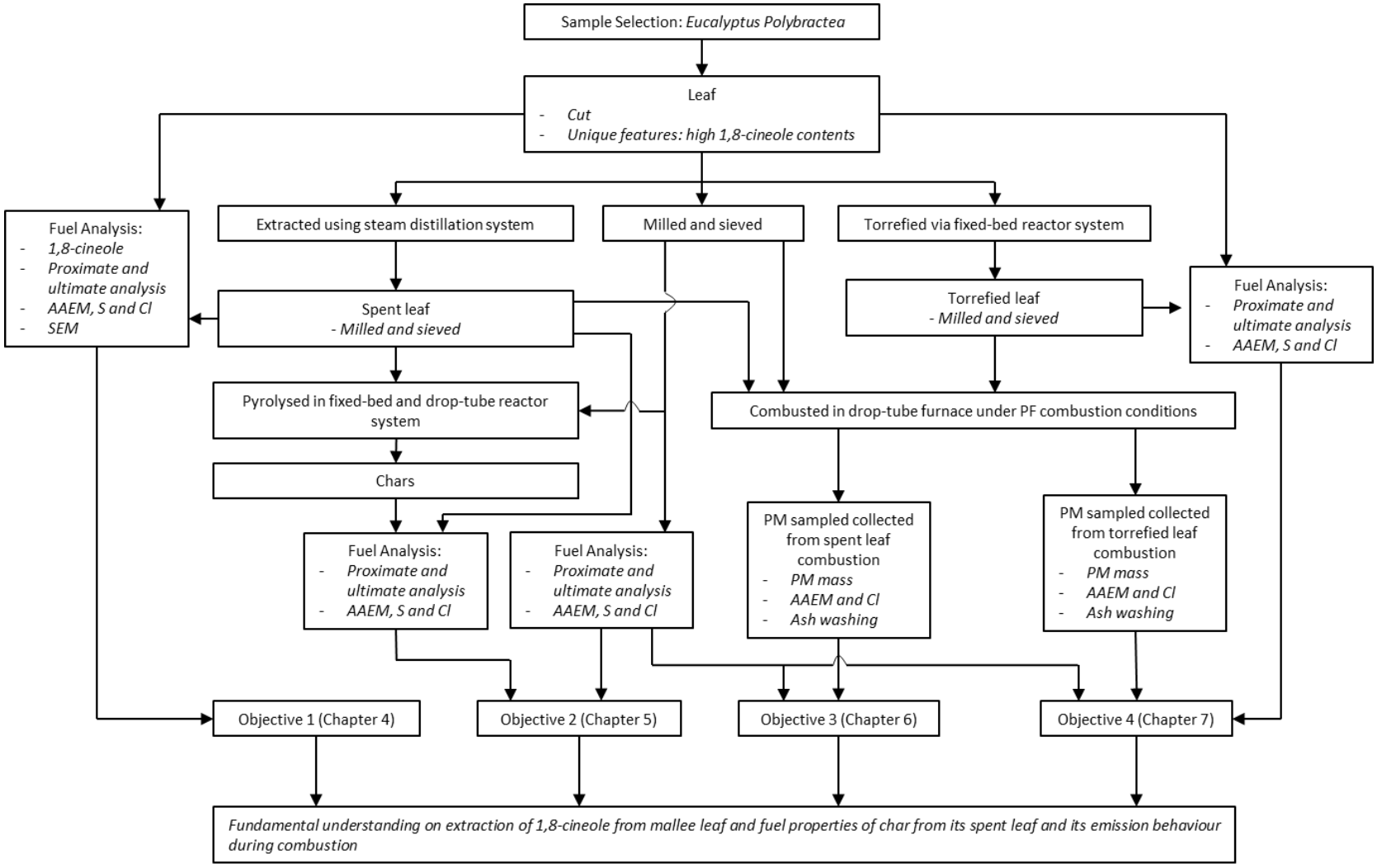

Figure 3- 1: Research methodology

Table 3- 1: Summary of methodology

Sub section	Experiment	Instrument and analytical technique
Sub section 3.2.1 Extraction of 1,8-Cineole by steam distillation from mallee leaves and Changes in the Fuel Properties of Spent Leaves. *(Results reported in Chapter 4)*	• Mallee leaves were extracted by steam distillation in various steam distillation time.	• The mass of raw leaves and spent leaves before and after steam distillation were weighed. • Elements composition of raw leaves and spent leaves were analysed. • Images and SEM analysis were carried out.
Sub section 3.2.2 Biochar from spent leaves after steam distillation for nutrients recycling. *(Results reported in Chapter 5)*	• Spent leaves were pyrolised at various temperatures and heating rates then the chars were washed with water.	• Spent leaves and chars before and after pyrolysis were weighed. • Elements composition of raw leaves, spent leaves and extracted water were analysed.
Sub section 3.2.3 In organic PM_{10} emission from the combustion of spent leaf after steam distillation. *(Results reported in Chapter 6)*	• Spent leaves were combusted in drop tube furnace.	• The mass of spent leaves and ash produced during combustion were weighed of each stage. • Elements composition of ash for each stages and extracted water were analysed.
Sub section 3.2.*4* Emission of inorganic PM_{10} from the combustion of torrefied biomass under pulverized-fuel conditions. *(Results reported in Chapter 7)*	• Raw leaves were pyrolised at low temperature and heating rate then its chars were combusted in drop tube furnace reactor.	• Raw leaves and chars produced from torrefaction were weighed. • The mass of chars and ash produced during combustion were weighed of each stage. • Elements composition of ash for each stages and extracted water were analysed.

3.3 Experimental

3.3.1 Sample Preparation

Leaves were collected from mallee trees (five-year old, E. polybractea) cultivated in the Narrogin region in the wheatbelt area of WA. The leaves were then dried overnight in an oven at 40 °C to reduce the moisture content to ~5% and cut to approximately 1 cm x1 cm (length x width). Hereafter, the leaves sample after drying and cutting is referred as "raw leaves". The retained leaves after steam distillation and torrefaction are referred as "spent leaves" and "torrified biomass", respectively. Both spent leaves and torrefied biomass were then ground to reduce their particle sizes ranging from 63 – 150 µm. The ground spent leaves were then used as feedstock for both pyrolysis and combustion process. However torrefied biomass was used as feedstock for combustion process only.

3.3.2 Steam Distillation

Steam distillations were carried out using a laboratory scale equipment which consists of an extraction column (inner diameter: ~9 cm), a flask, a heating mantle and a condenser as can be seen at Figure 3.2. Milli Q water was heated in the flask to continuously produce steam which flowed through the distillation column containing the mallee leaves. In each experiment, ~10 g of the raw leaves sample was charged into the extraction column. In all experiments, the steam flow was maintained at 1.3 kg/min/m2, the highest steam flow value allowed by the experimental system. A series of extraction experiments were carried out at various distillation times ranging from 1 to 180 min. In all experiments, the distillation column was wrapped with heating tape and insulation in order to maintain the temperature inside the column at 105 °C. Once each distillation was completed, the flask and the column were separated immediately and the spent leaves were leaves then collected.

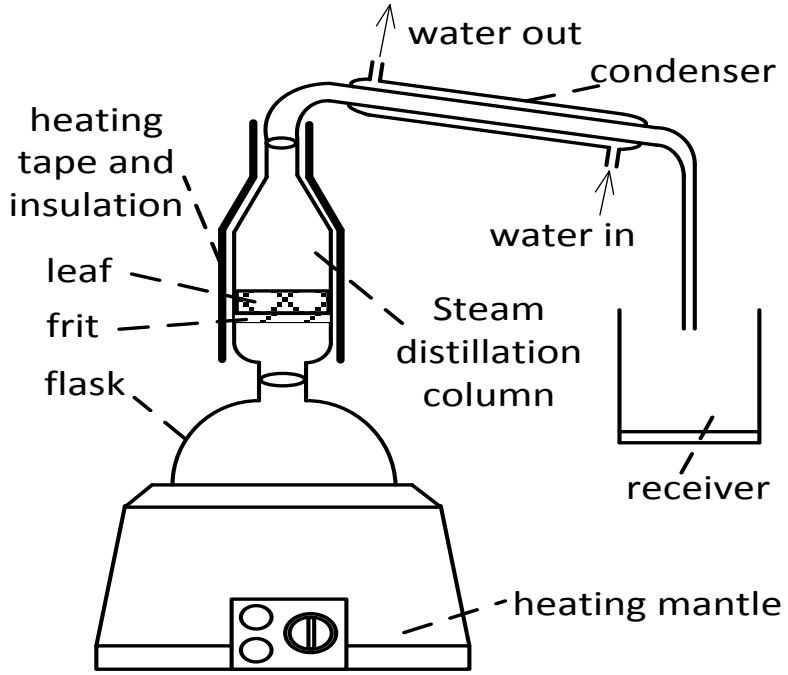

Figure 3-2: A steam distillation setup

3.3.3 Leaching Experiments

Water leaching of the raw, spent leaves, torrefied biomass and chars samples were carried out using a semi-continuous leaching apparatus, similar to the one used in a previous study[205]. Briefly, a high performance liquid chromatography (HPLC) pump (Alltech model 627) was used to deliver a stream (100 mL/min) of ultrapure water through a tubular reactor cell. In each experiment, ~25 mg of the raw or spent leaves were loaded into the reactor cell. The leachate samples were collected at the exit of the reactor cell at various leaching times for subsequent quantification of total organic carbon (TOC), alkali and alkaline earth metallic (AAEM, mainly Na, K, Mg, and Ca) species, and chlorine (Cl).

3.3.4 Pyrolysis Experiments

Pyrolysis was conducted in a quartz drop-tube/fixed-bed reactor as shown in Figure 3-3, similar to the one used by previous studies[176, 206]. The pyrolysis is performed under slow heating and fast heating rates at temperatures ranging from 400−700 °C. The feedstocks used for the pyrolysis experiments to produce biochars were raw leaves as well as spent leaves obtained from 30 min distillation (spent leaves−30) and spent leaves obtained from 60 minute-distillation (spent leaves−60).

A quartz drop-tube/fixed-bed reactor was employed in this pyrolysis experiment as shown in Figure 3-3.

For the slow pyrolysis to produce biochars, firstly approximately 1.0 g of a sample were loaded into the reactor, secondly the reactor was purged with argon of ultra-high purity -at flow rate of 2 L/min for 15 min. The reactor then was heated in an electrical furnace to achieve a certain temperature at a heating rate of ~10 °C/min (or ~0.17 °C/s) for 10 min before being lifted up and cooled down to room temperature with the argon flow continuously passing through.

For the fast pyrolysis, the rector was pre-heated to the desired temperature and the feedstock was then fed into the hot reactor at approximately 0.1 g/min feeding rate for 10 min. The particle residence time in the isothermal zone is maintained as ~1.2 s by adjusting the carrier gas flow rate. The heating rate of the feedstock particles was estimated from ~300 °C/s at 400 °C to ~1000 °C/s at 700 °C, based on a method reported elsewhere[207]. Rapid pyrolysis occured once the feedstock was fed into the hot reactor. The formed biochar particles were retained on the quartz frit of the reactor whereas the volatiles were swept away from the biochar bed. The holding time of the reactor in the furnace after feeding was 10 min. Finally the reactor was lifted up and cooled down to room temperature with argon flowing through it.

3.3.5 Torrefaction Experiments

Biomass torrefaction to produce torrefied biomass was conducted in a a drop-tube/fixed-bed quartz reactor system which was similar to the equipment used for pyrolysis experiments showing at Figure 3-3. Torrefaction process was performed similarly to the slow pyrolysis process, however the torrefaction was run at a low temperature range of 220-280 ^{o}C.

The feedstock for torrefaction was raw leaves. Firstly, the quartz reactor was preloaded with ~20 g of raw leaves. The following steps were similar to slow pyrolysis steps (Section 3.4.5) with the different was only that the temperatures of the torrefaction were at 220-280 ^{o}C.

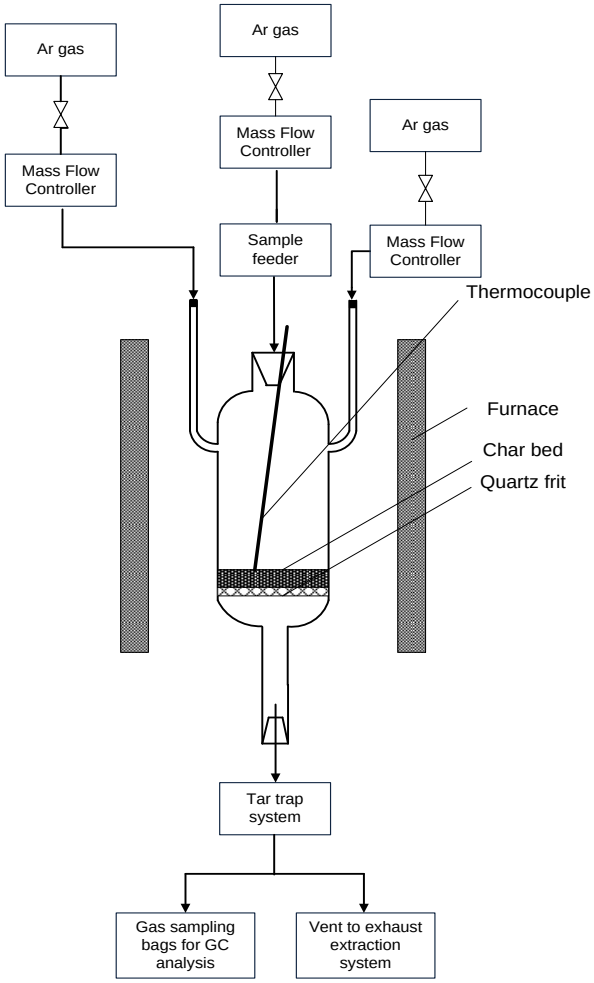

Figure 3-3: A Drop-tube/fixed-bed quartz reactor system

3.3.6 A High-Temperature DTF System

The combustion experiments were carried out using a laboratory-scale high temperature drop tube furnace (DTF) system. The experiment system consists of a drop tube furnace which was facilitated with a feeding system and a PM sampling system, as shown in Figure 3-4, similar with the DTF system was used in previous combustion studies[176, 208]. Briefly, the furnace temperature was kept at a temperature of 1400 °C. The flow rates of primary air and secondary air were ~1.0 and ~3.6 L/min, respectively. The feedstock was fed at a feeding rate of ~0.05 g/min and the residence time in the isothermal zone of the DTF was ~1.7 s. The values of λ

(i.e., the ratio of actual air-fuel ratio to stoichiometric air-fuel ratio) are ca14−17, depending on the combustion feedstock.

The inorganic particulate matter (PM) produced from combustion was sampled via a cyclone and a Dekati low-pressure impactor (DLPI) which was kept at 115 ^{o}C in order to avoid condensation of the flue gas and prevent the coagulation of particles during the sampling process, following a method detailed elsewhere[209]. The mass of PM_{10} collected in the DPLI was measured using a Mettler MX5 microbalance (the accuracy is 0.001 mg). At least five repeated tests were conducted under each condition to ensure the repeatability of all the combustion experiments.

3.4 Instruments and Analytical Techniques

3.4.1 Proximate and Ultimate analysis

Proximate analysis of the raw leaves, spent leaves, torrefied leaves and biochar samples were conducted using a thermogravimetric analyser (TGA) METTLER model in accordance with American Society for Testing and Materials (ASTM) international standard ASTME870-82[210] with an appropriate temperature program. Briefly, approximately 10 mg of the solid fuel sample was loaded into a TGA sample crucible and purged with Argon gas for 15 min followed by heating the sample to 110 ^{o}C. This temperature was held for 20 min until no further weight loss was observed. The moisture content of the sample was referred to the total weight loss in these steps. The sample was then further heated to 950 ^{o}C at a heating rate of 50 K min^{-1} in Ar and held at the temperature for 20 min, followed by decreasing the temperature to 600 ^{o}C. The weight loss was recorded as volatile matter and the remaining material as char. The char residue was then exposed to air to be oxidized for 30 min until no weight loss was observed. The weight of the residual ash in the sample crucible was used to calculate the ash content of the fuel, while the difference between the weight of the char and residue ash is calculated as the fixed carbon content of the fuel.

For ultimate analysis, the contents of carbon (C), hydrogen (H), and nitrogen (N) of the raw leaves and the biochars were determined using a CHNO elemental analyser (model: Perkin Elmer 2400 Series II). The oxygen (O) contents in these samples

were determined by difference, on a dry and ash-free (daf) basis. Cl in these samples was quantified via a two-step method recently developed[211]. The content of S was quantified following the method previously used[212].

3.4.2 Scanning Electron Microscope (SEM)

Morphological characterisations were carried out using a scanning electron microscope (SEM, model: Zeiss EVO 40XVP). The working distance and voltage use for the SEM were 5 mm and 15 kV, respectively. Cross-sections were prepared from the raw and spent leaves by setting them in epoxy resin which was then solidified, polished and coated with carbon for SEM characterisation, following a similar procedure used in a previous study[213].

3.4.3 Quantification of 1,8-cineole

The concentrations of 1,8-cineole in the raw and spent leaves samples were determined using a previous method[7] combining solvent extraction and quantification using Gas Chromatography (GC). Briefly, approximately 3g of leaves were boiled under reflux for 90 min in a weighed aliquot of approximately 50mL absolute ethanol containing 0.25% methyl isobutyl ketone (MIBK) as an internal standard. A Hewlett-Packard 5890 GC fitted with a split injector, a flame-ionisation detector and capillary column AT-35 (Grace Davidson Discovery Sciences) of 60m x 0.25mm x 0.25uM was used to determine the concentration of cineole in the extracts using both internal and external standard calibration. The relative standard error of 1,8-cineole extraction via steam distillation estimated as ±3% based on at least duplicated experiments under each condition.

3.4.4 Total Organic Carbon (TOC) Analyser

The total carbon in raw leaves, spent leaves, torrefied biomass, biochars and PM samples were quantified by extracting these samples in MilliQ water for 24 hours then subjected into TOC analyser (Shimadzu TOC-VCPH). The basic principle of this analysis is oxidized the carbon in the sample to CO_2 then introduced to non-dispersive infrared detector (NDIR) for carbon detection.

3.4.5 Quantification of Ash-forming Species in Solid and aqueous samples

The contents of inorganic species in the raw, spent leaves, torrefied and biochars samples were determined based on a previous method described elsewhere[7, 194]. Briefly, ~10 mg of a solid fuel sample was ashed in a muffle furnace according to a designed temperature-time program that avoided ignition during the ashing process. The ash was then digested in a Pt crucible using a mixture of concentrated acids ($HF:HNO_3$=1:1) at 120 °C for 12 h. After the evaporation of the excessive acid, the residue remaining in the crucible was then dissolved in 0.02 M methanesulfonic acid solution. The inorganic species in the solution was then quantified via an ion chromatography (IC, model: Dionex ICS-3000; column: IonPac CS12A; guard column: IonPac CG12A) equipped with suppressed conductivity detection system. The concentrations of AAEM species in the aqueous leachates of the raw and spent leaves samples were quantified via direct injection of the solutions into the IC system. Anions (e.g. Cl^-) were analysed using another IC (model: DIONEX ICS-1100; column: IonPac AS22; guard column: IonPac AG22).

3.4.6 Summary of Methodology

A series of experimental procedures and analytical techniques have been developed to achieve the fundamental understanding on the extraction of 1,8-cineole from mallee leaves and the energy conversion processes of raw leaves, spent leaves and torrefied biomass. Steam distillation was applied to extract essential oil containing1,8-cineole. Raw leaves and spent leaves from steam distillation were then pyrolysed using a quartz drop-tube/fixed-bed reactor at slow and fast heating rate processes in an absent of oxygen. Torrefaction was also performed to produce torrefied biomass. Spent leaves and torrefied biomass were then combusted using a high-temperature DTF system. The ash particles produced from this combustion were collected in a cyclone and DLPI. The solid fuels and ash particle were then characterised using various analytical techniques.

CHAPTER 4 STEAM DISTILLATION OF MALLEE LEAVES: EXTRACTION OF 1,8-CINEOLE AND CHANGES IN THE FUEL PROPERTIES OF SPENT LEAVES

4.1 Introduction

Biomass as a renewable energy source plays significant role in future sustainable energy supply[214, 215]. In Western Australia (WA), mallee eucalypts are planted in agricultural land for managing dryland salinity that seriously threatens the State's sustainable food production[20]. As a biomass, mallee can be produced at low cost, on a large scale and with low energy and carbon footprints[1, 216] hence potentially an important feedstock for energy applications (e.g. via various technical routes[78, 217-221]). The leaves of mallees contain eucalyptus essential oil that is widely used in medicinal, perfumery and flavouring applications and 1,8-cineole is the most abundant (up to 96%) constituent in the oil[37, 222-227]. Therefore, producing 1,8-cineole as a value-added product from mallee leaves is an important strategy to further improve the economic performance of an envisaged mallee-based biomass supply chain in WA[2, 20, 228].

Extraction of essential oil containing 1,8-cineole from mallee leaves can be commonly done via hydrodistillation or steam distillation, both of which are environmentally friendly, safe to operate and easy to scale up[7, 40, 42, 46-48, 50, 51, 229-236]. In comparison to hydrodistillation, steam distillation achieves higher oil yield and minimises the extraction of impurities and the loss of polar compounds[53, 54]. In addition, the spent leaves following the extraction of 1,8-cineole is potentially an important feedstock in a future mallee-based bioenergy supply chain system[7]. Previous studies reported that the extraction of 1,8-cineole from eucalyptus leaves via steam distillation is slow and requires a long period of steam distillation (typically at a scale of several hours)[231, 232]. Unfortunately, to the best of the author knowledge, no kinetic data on the extraction of 1,8-cineole from mallee leaves via steam distillation has

been reported. There are also no data reported on the fuel properties of the spent leaves after steam distillation.

Therefore, this chapter is focused on the extraction behaviour of 1,8-cineole during steam distillation and the effect of such steam distillation on the fuel properties of spent biomass. A series of experiments have been conducted to investigate the steam distillation of mallee leaves at various extraction time (1–180 min). The extraction kinetics of 1,8-cineole are then derived and the fuel properties of spent leaves samples are also characterised. The effect of steam distillation on the loss of fuel materials and the occurrence of inorganic species in the spent leaves are also studied.

4.2 Extraction Kinetics of 1,8-cineole during Steam Distillation of Mallee Leaves

The data on the extraction of 1,8-cineole are presented in Figure 4-1. The raw leaves contains ~5.3 wt% of 1,8-cineole on a dry basis. The extraction of 1,8-cineole via steam distillation is fast within the first 15 min but slow afterward. Over 50% of the total 1,8-cineole in the raw leaves has been extracted after steam distillation for 4 min. Further increasing the steam distillation to 15 min extracts ~90% of 1,8-cineole from the raw leaves. The extraction of residual (~10%) 1,8-cineole becomes slow after 15 min and is virtually completed after steam distillation for 60 min.

The different 1,8-cineole extraction rates before and after 15 min observed in Figure 4-1 suggest that the steam distillation is governed by two different mechanisms. Based on the steam distillation process under the experimental conditions in this study, the fast step within the first 15 min can be described by zero-order kinetics, as evidenced by the straight line within the first 15 min. However, the extraction of 1,8-cineole is much slower at extraction time longer than 15 min and does not follow a straight line (see Figure 4:1). To understand the kinetics of the slow step after 15 min, the extraction data in Figure 4:1 was further evaluated according to first-order kinetics:

$$-\ln(\frac{C_t}{C_0}) = kt \quad \text{..... (4-1)}$$

where C_0 is the maximum amount (based on weight) of 1,8-cineole which can be extracted, C_t is the total amount (based on weight) of 1,8-cineole retained in the spent leaves after steam distillation for time t, k (min^{-1}) is the extraction rate of 1,8-cineole and t is distillation time (min). The correlation between $-ln\ (C_t/C_0)$ and extraction time t during steam distillation is presented in Figure 4-2. The straight line shown in Figure 4-2 indicates that the extraction of residual 1,8-cineole from the raw leaves after 15 min follows first-order kinetics

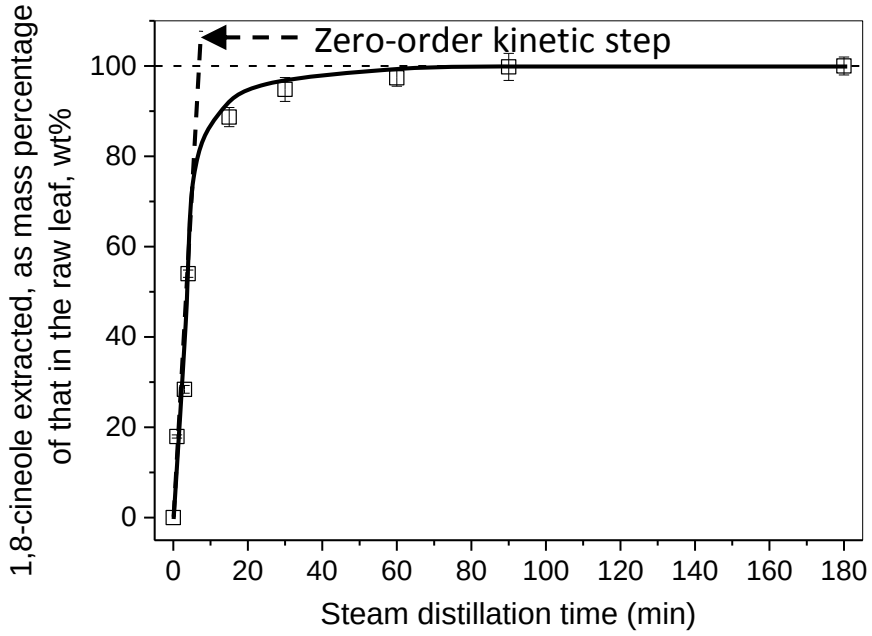

Figure 4-1: Extraction (on a weight basis) of 1,8-cineole from the mallee leaves sample as a function of steam distillation time. The initial concentration of 1,8-cineole in the raw leaves is 5.3 wt% on a dry basis.

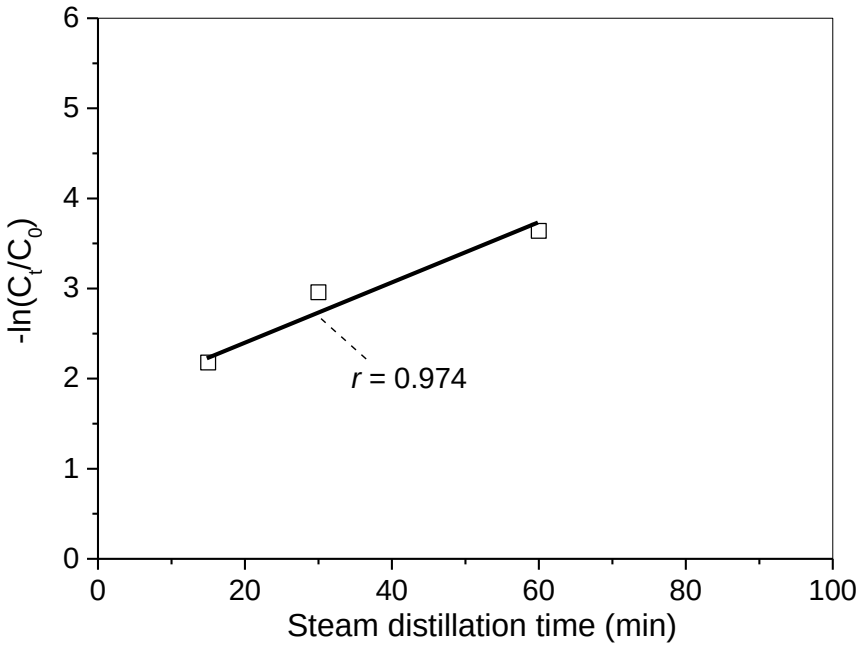

Figure 4-2: Correlation between –ln (C_t/C_0) and steam distillation time (t) for the extraction of 1,8-cineole from the mallee leaves sample in the slow step ($t \geq 15$ min), on a basis of weight. Correlation coefficient (r) is also shown.

The two governing mechanisms can be explained by the fundamental process of steam distillation. During the initial stage of steam distillation, hot water condensed on the leaves surfaces results in a diffusion process after penetrating cutaneous layers of the leaves. Subsequently, 1,8-cineole originally secreted in oil glands diffuses rapidly to the leaves surfaces because of its hydrophilic nature[237], forming numerous small circular patches on the leaves surfaces[238]. It is reported that the evaporation of the 1,8-cineole only takes place from the perimeters of these patches where steam is condensed to raise the temperature[238]. This means that, under the steam flow rate used in this study, only part (not all) of the 1,8-cineole on the leaves surface can be evaporated by the steam within the first 15 min. Therefore, the zero-order fast extraction within the 15 min appears to be regulated by the latent heat (provided by steam) that supports the evaporation of 1,8-cineole from the leaves surfaces[238]. In this study, the set of experiments used the highest steam flow rate allowed by the experimental setup. It is

expected that an increasing steam flow rate would accelerate the extraction of 1,8-cineole in this step as previously reported on the extraction of 1,8-cineole from tea tree[237] and other essential oils from lavender flowers[239]. On the other hand, at steam distillation longer than 15 min, the amount of 1,8-cineole on the leaves surface continuously decreases whereas the ability of steam in evaporating 1,8-cineole remains unchanged at the given flow rate. As the 1,8-cineole diffused to the leaves surface can be immediately carried away by the steam, the extraction of 1,8-cineole is therefore governed by the slow internal diffusion of the residual 1,8-cineole from oil glands to the leaves surface[240].

4.3 Loss of Total Organic Carbon, AAEM Species, and Cl from Mallee Leaves during Steam Distillation

Figure 4-3 presents the data on the loss of total organic carbon during steam distillation of the raw leaves, expressed on a carbon basis, benchmarking with the carbon in form of 1,8-cineole. Clearly, within the first 15 min, the loss of total organic carbon is rapid and identical to that in form of 1,8-cineole, following zero-order kinetics (see the straight line in Figure 4-3). This indicates that the extraction of 1,8-cineole, which is more hydrophilic than many other organic carbon compounds[237], is the main mechanism responsible for the initial rapid loss of total organic carbon during steam distillation within the first 15 min. However, unlike the extraction of carbon in forms of 1,8-cienole, the loss of total organic carbon continues to increase (but at a lower rate) after 15 min and reaches the maximum value of ~17% after steam distillation for 150 min. Therefore, there are additional loss of organic carbon from the raw leaves during steam distillation and the extraction of such additional organic carbon is considerably slower than the extraction of organic carbon in the form of 1,8-cineole during the first 15 min.

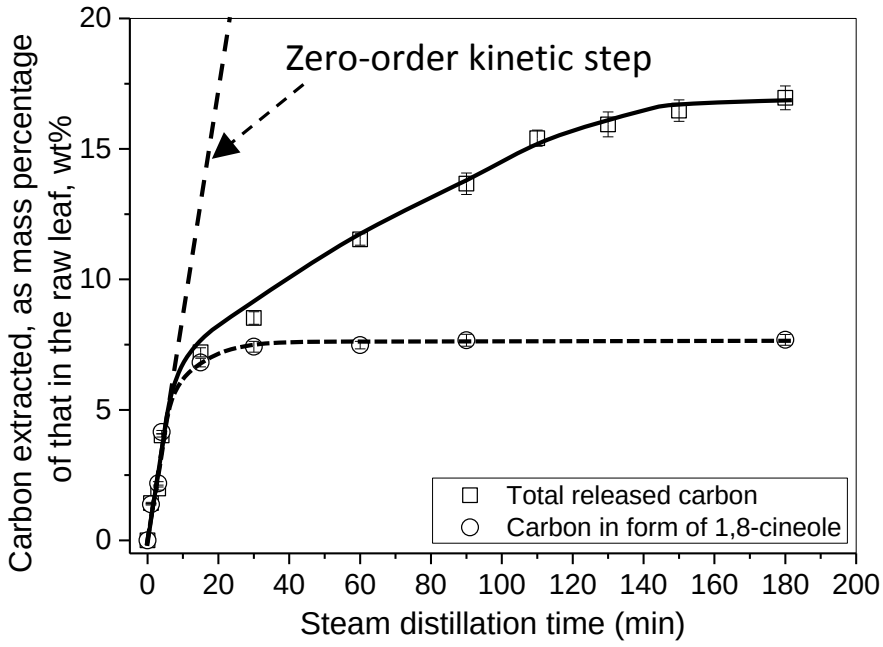

Figure 4-3: Loss (on a carbon basis) of the total organic carbon and that in form of 1,8-cineole from the raw leaves during steam distillation.

As the profile of total organic carbon loss after 15 min does not follow a straight line (see Figure 4-3), further analysis similar to eq1 was then conducted, assuming that the total organic carbon loss in this step follows first-order kinetics. Such data are illustrated in Figure 4-4, the straight line shown in which clearly suggests that the loss of total organic carbon after steam distillation for 15 min follows first-order kinetics. This step may correspond to the leaching of other organic carbon compounds, which are less hydrophilic, via possible reflux effect due to the formed hot water condensed on the leaves surfaces. The extraction of residual 1,8-cineole after 15 min is unlikely the main mechanism responsible for the loss of total organic carbon in this step because only ~10% of 1,8-cineole (equivalent to ~0.8% of total carbon) is left in the spent leaves.

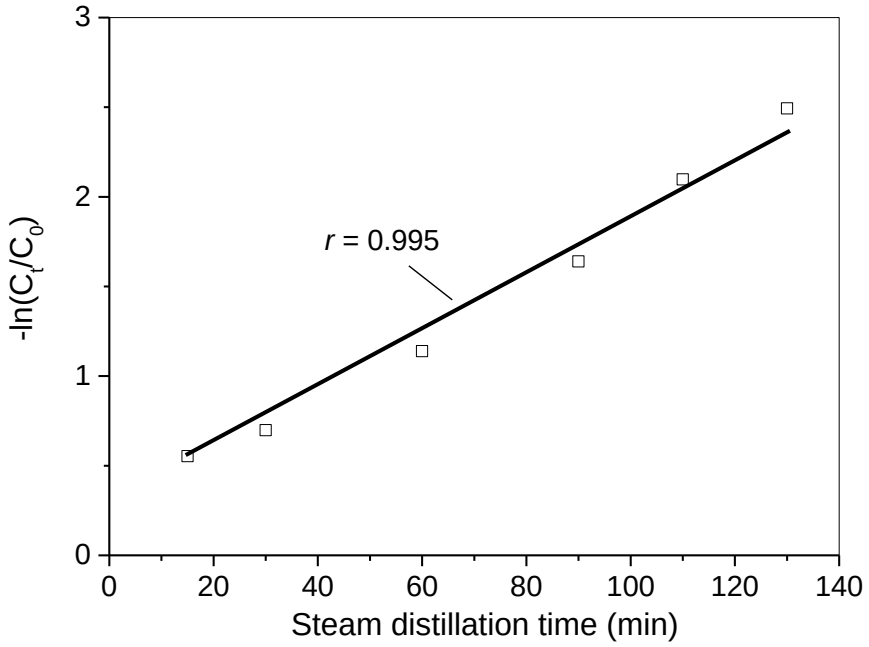

Figure 4-4: Correlation between –ln (C_t/C_0) and extraction time (≥ 15 min) for the loss of total organic carbon from the raw leaves during steam distillation, on a basis of the total organic carbon extracted. Correlation coefficient (*r*) is also shown.

As a result of the reflux effect, there are also some losses of AAEM species and Cl from the leaves during steam distillation, in addition to the loss of total organic carbon. Figure 4-5 presents the data on the retention of AAEM species and Cl in the spent leaves samples as a function of steam distillation time, considering the weight loss of the spent leaves samples during steam distillation. The retention of Na, K, Mg, Ca, and Cl in the spent leaves samples reduces from 100% in the raw leaves to ~85%, ~84%, ~83%, ~65%, and ~70% in the spent leaves after steam distillation for 15 min, respectively, and then levels off with further increasing steam distillation time up to 180 min. There are two possible mechanisms responsible for the removal of AAEM species and Cl from the raw leaves during steam distillation. One is that parts of originally water-soluble AAEM species and Cl in the raw leaves are leached out by the hot water that is condensed on the leaves surface and then flows downward (i.e., the reflux). This is plausible as it is supported by the extraction profile of 1,8-cineole (see Figure 4-1). During the rapid

extraction of 1,8-cineole within the first 15 min, more steam is condensed on the leaves surfaces to provide latent heat for the evaporation of 1,8-cineole. As a result, considerable amounts of AAEM species and Cl are leached out during steam distillation within the first 15 min. Further increasing steam distillation time leads to little changes in the retention of these inorganic species because majority (~90%) of 1,8-cineole has been extracted within 15 min and thereby little water is further condensed on the leaves surfaces. The other mechanism is that steam distillation may have also changed the structures of the raw leaves and occurrence forms of inorganic species in it, converting parts of water-insoluble inorganic species into water-soluble ones. Semi-continuous water leaching experiments were then conducted to quantify water-soluble inorganic species in the samples, with the data presented in Figure 4-6. As shown in Figure 4-6d, only ~5% of Ca in the raw leaves is water-soluble, which is considerably lower than that (up to ~35%, see Figure 4-5d) removed during steam distillation. This clearly demonstrates that the occurrence forms of Ca in the raw leaves must have been changed during steam distillation, converting part of water-insoluble Ca into water-soluble one that can be immediately leached out by the hot reflux. The retention profile of Ca in the spent leaves samples during steam distillation is similar to that of hydrodistillation reported in our previous study.[7]

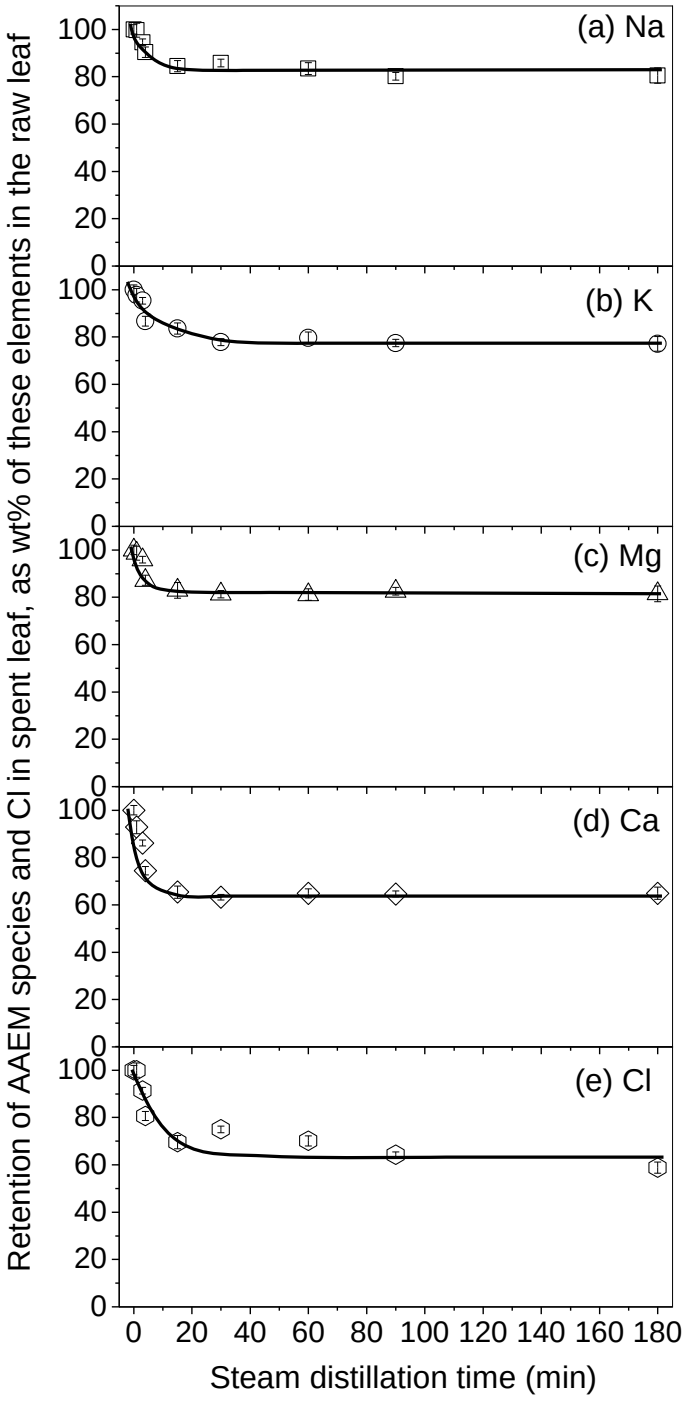

Figure 4-5: Retention of Na, K, Mg, Ca, and Cl in the spent leaves samples after steam distillation for different time.

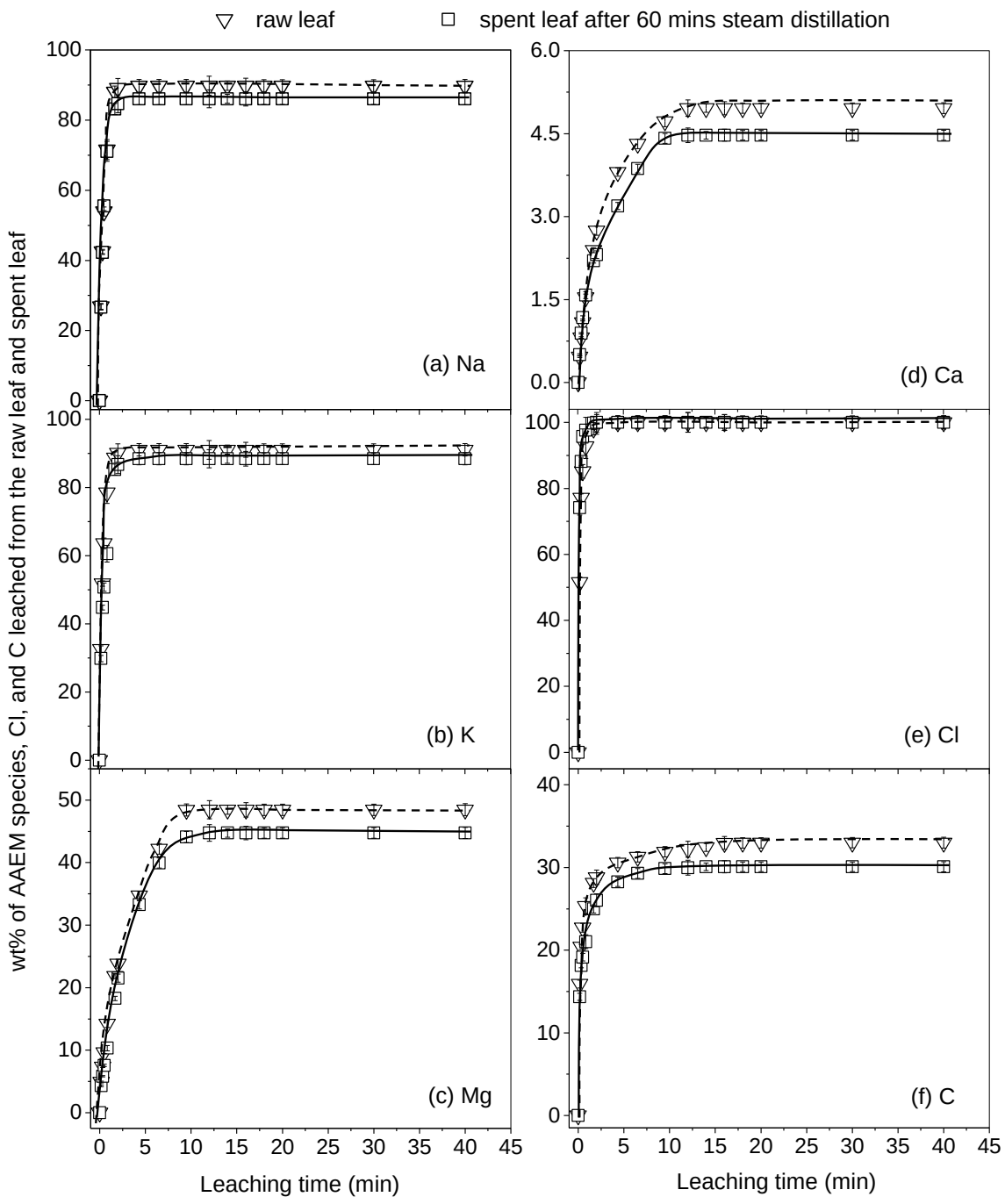

Figure 4-6: Removal of Na, K, Mg, Ca, Cl and C from the raw leaves and the spent leaves after 60 min steam distillation via semi-continuous water leaching.

Overall, steam distillation not only extracts 1,8-cineole into gas phase, but also removes considerable amount of total organic carbon, AAEM species, and Cl in the raw leaves as a result of reflux and interactions between the leaves and steam (and/or hot water condensed on the leaves surface). The amounts of Na, K, and Cl removed by steam distillation (see Figure 4-5) are much lower than those removed by semi-continuous water leaching (see Figure 4-6), suggesting that there are some effect of reflux during steam distillation but such effect is limited.

4.4 Changes in Morphology and Fuel Properties of Spent Leaves due to Steam Distillation

The data in Figure 4-3 clearly show that the extraction of 1,8-cineole virtually completes after 60 min but the loss of organic carbon continues with further increasing distillation time over 60 min. This suggests the changes in the structures of the spent leaves as a result of steam distillation, as supported by the visual differences in the colour of the raw and spent leaves samples shown in Figure 4-7. The colour of the spent leaves produced from steam distillation for a longer time is darker.

The SEM images in Figure 4-7 also show the changes in cross-sectional morphologies of the raw and spent leaves samples after steam distillation. There are abundant oil glands (for essential oil storage) present in the raw leaves. These oil glands are depicted in circular shapes. However, as a result of steam distillation, most of oil glands have experienced deformation in shape. The oil glands are no longer in circular shape and transformed to more destructive forms in the spent leaves samples, particularly after prolonged steam distillation (e.g., 60 and 180 min). The results suggest that the interactions between steam and the leaves as well as the release of essential oils from oil glands during steam distillation lead to disruption and destruction of the oil glands.

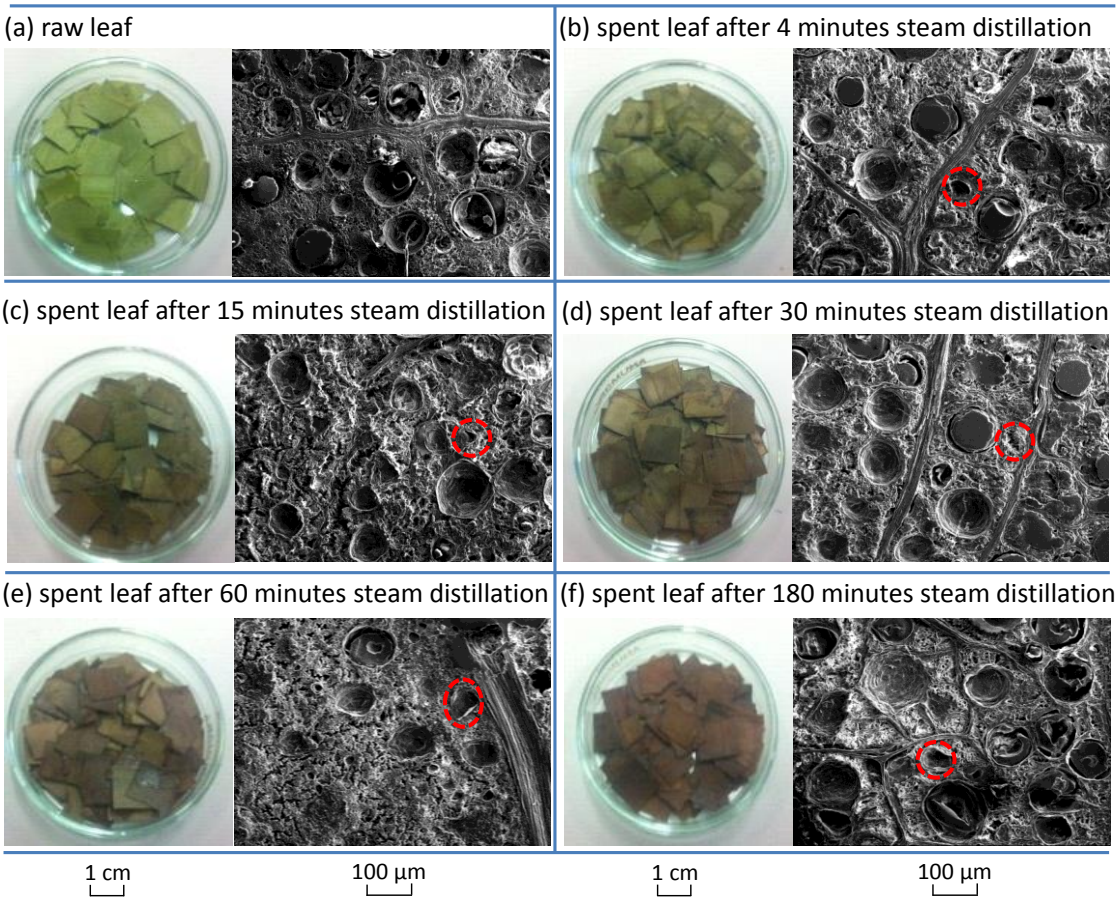

Figure 4-7: Morphologies of the raw mallee leaves and the spent leaves samples after steam distillation for 4, 15, 30, 60 and 180 min. Examples on the destruction of oil glands in spent leaves are shown in red circles.

For fuel applications, it is important to assess the effect of steam distillation on fuel properties of the spent leaves. The fuel properties include proximate and ultimate analyses, mass energy density, the contents of key ash-forming species (i.e., AAEM species and Cl) and their forms of occurrence. Such results are presented in Table 4-1. Steam distillation simultaneously removes parts of organic and inorganic species (see Figs. 4 and 6) and thereby results in little change in the proximate and ultimate analyses data of the raw and spent leaves samples. As a result, steam distillation also has little effect on the mass energy density (or calorific value), which is expressed as higher

heating value (HHV) and estimated from the ultimate analysis data[241] of the raw and spent leaves samples. Table 4-1 also shows that, whereas steam distillation results in little changes in the content of Na and K in the raw and spent leaves samples, concentrations of Mg, Ca, and Cl in the spent leaves samples are considerably lower than those in the raw leaves. This implies that, using the spent leaves as a fuel is likely to lead to less ash-related problems (e.g., fireside corrosion, ash deposition, and fine inorganic aerosol emission[176, 209, 242]) associated with Cl.

It is also known that during thermochemical conversion process, the transformation of AAEM species and Cl strongly depends on their occurrence forms in the fuel used[243]. Therefore, further experiments were also performed to investigate the leaching characteristics of AAEM species, Cl and C in spent leaves using a semi-continuous leaching apparatus. Along with the raw leaves, the spent leaves−60 was selected because the extraction of 1,8-cineole is completed after steam distillation for 60 min. The data are presented in Figure 4-6, with two important findings. One is that the majority (~86−100%) of Na, K, and Cl in the raw leaves and the spent leaves−60 can be rapidly leached out, reaching equilibrium values within the first 2 min while only <5% of Ca, <50% of Mg and <32% of C in the raw leaves and the spent leaves−60 can be leached and the leaching is much slower, taking over 10 min to reach equilibrium. The other is that except for Cl that is completely water-soluble, leaching equilibrium values of other elements (i.e., Na, K, Mg, Ca, and C) in the spent leaves−60 are slightly lower than those of the raw leaves. The results suggest that at least parts of the water-soluble species (that contain these elements) are leached out during steam distillation.

Table 4- 1: Properties of the Raw Leaves and the Spent Leaves Samples (Legend: SL−xxx, the Spent Leaves Collected after the Steam Distillation of the Raw Leaves for xxx min)

Samples	raw leaves	SL−1	SL−3	SL−4	SL−15	SL−30	SL−60	SL−90	SL−180
Proximate analysis									
Moisture (wt%, ad)	5.0	4.6	4.7	5.0	4.4	4.0	3.9	3.8	3.3
Ash (wt%, db[b])	4.2	3.9	3.6	3.7	3.7	3.6	3.8	3.9	3.9
VM (wt%, db[b])	77.7	78.2	77.5	78.4	78.4	78.4	77.4	78.4	77.4
FC (wt%, db[b])	18.1	17.9	18.9	17.9	17.9	18.0	18.8	17.7	18.7
Ultimate analysis (wt%, daf[c])									
C	56.2	56.7	57.7	57.7	56.5	56.9	57.5	57.9	57.2
H	7.1	7.0	6.9	6.9	8.1	7.6	7.8	7.6	7.4
N	1.33	1.64	1.84	2.02	1.50	1.19	1.58	1.40	1.51
S	0.13	0.12	0.13	0.11	0.12	0.12	0.13	0.12	0.12
Cl	0.24	0.24	0.23	0.17	0.18	0.19	0.19	0.18	0.17
O[d]	35.0	34.3	33.2	33.1	33.6	34.0	32.8	32.8	33.6
HHV[e] (MJ/kg, db[b])	21.3	21.5	21.8	21.7	22.2	22.0	22.2	22.0	21.9
Alkali and alkaline earth metallic (AAEM) species content (wt%, db[b])									
Na	0.6027	0.6166	0.6017	0.5777	0.5559	0.5772	0.5850	0.5805	0.5984
K	0.3529	0.3538	0.3551	0.3243	0.3220	0.3067	0.3273	0.3281	0.3356
Mg	0.1831	0.1806	0.1756	0.1597	0.1519	0.1490	0.1486	0.1512	0.1492
Ca	0.8964	0.8539	0.8153	0.7080	0.6396	0.6324	0.6773	0.6957	0.7177

VM = Volatile matter. FC = Fixed carbon [a]Air dried basis. [b]Dry basis. [c]Dry and ash-free basis. [d]By difference. [e]Higher heating value

Further efforts were then made to investigate the leaching kinetics of AAEM species, Cl, and C from the raw leaves and the spent leaves−60, following the method in eq 1. The data in Figure 4-8 lead to at least four findings. First, the leaching of Na, K, Mg, Ca, and Cl from the raw leaves and the spent leaves−60 follows first-order kinetics whereas that of C exhibits two first-order leaching steps, consistent with the finding in our previous study[205]. Second, the leaching rates of Na, K, Mg, and Ca from the spent leaves−60 are slightly lower than those of the raw leaves (see Figure 4-8a-d), possibly because parts of these inorganic species that can be easily and rapidly washed have been removed during steam distillation. Third, the leaching rate of Cl in the spent leaves−60 is faster than that of Cl in the raw leaves (see Figure 4-8e). All Cl in the raw leaves or the spent leaves−60 can be rapidly leached out once it is in contact with water, as demonstrated in Figure 4-6e. Steam distillation for 60 min increases the surface area of pores in the spent leaves−60 as a result of the depletion of 1,8-cineole. Therefore, Cl in the spent leaves−60 is more accessible to water and thereby leached at a rate faster than that of the raw leaves. Fourth and last, the fast leaching of C in the spent leaves−60 observed is identical to that of C in the raw leaves. However, in the slow step, the leaching rate of C in the spent leaves−60 is considerably higher than that of C in the raw leaves. The data suggest that after 1,8-cineole has been completely extracted, the water-leachable organic carbon in the spent leaves becomes more easily accessed by water during leaching.

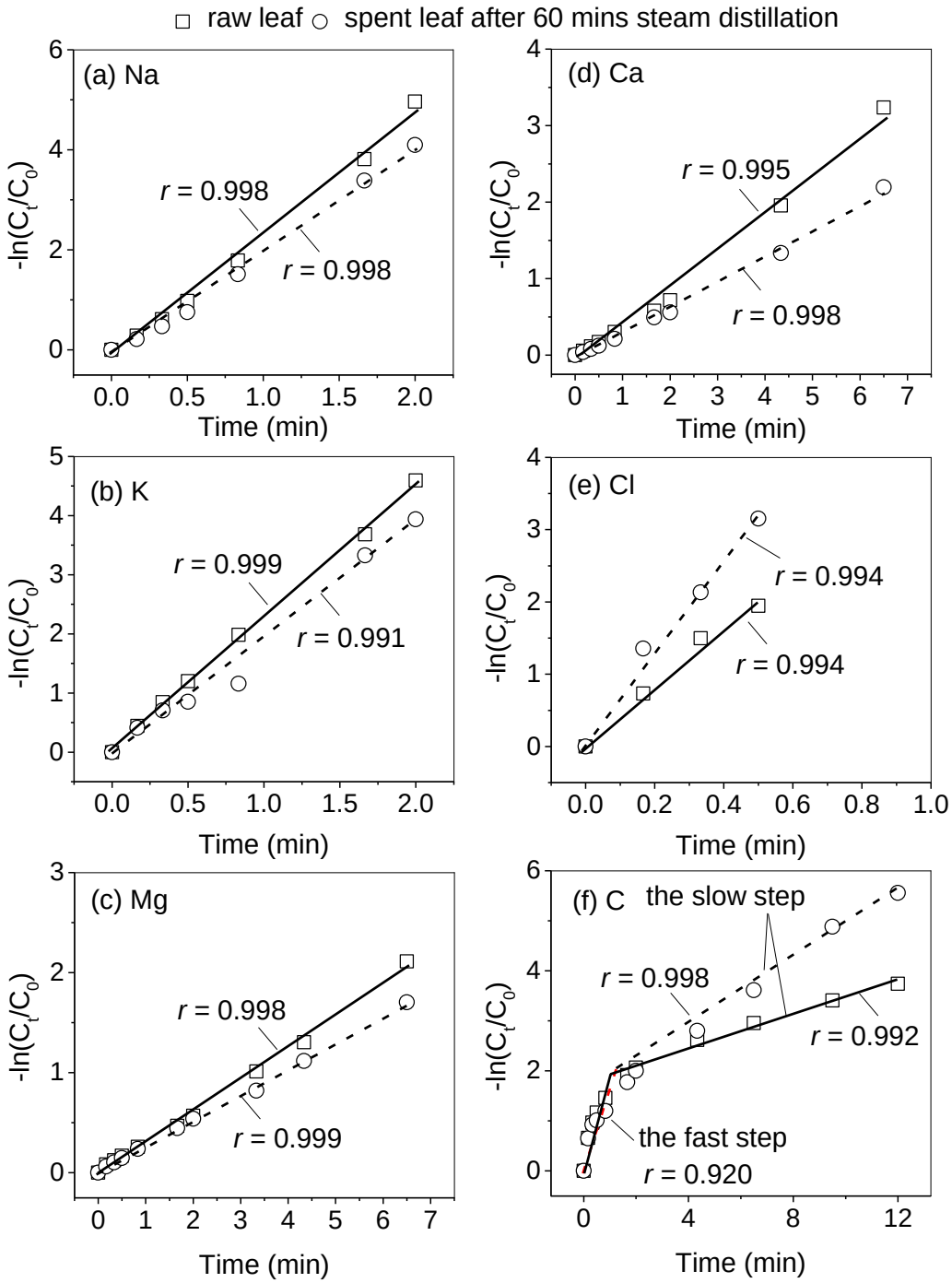

Figure 4-8: Correlation between –ln (C_t/C_0) and leaching time for Na, K, Mg, Ca, Cl, and C from the semi-continuous water leaching of the raw leaves and the spent leaves after steam distillation for 60 min. Correlation coefficient (*r*) is also shown.

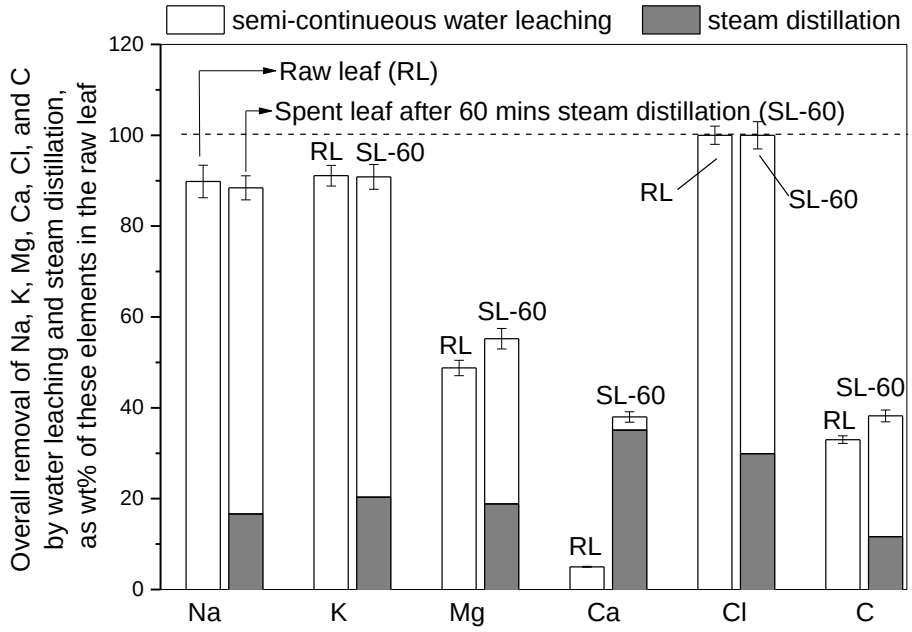

Figure 4-9: Overall removal of Na, K, Mg, Ca, Cl, and C from the spent leaves after 60 min steam distillation, including those removed during steam distillation and those from the semi-continuous water leaching of the spent biomass. The data on the semi-continuous leaching of the raw leaves directly are also plotted for comparison.

Figure 4-9 further presents the overall removal of these elements via steam distillation for 60 min followed by semi-continuous water leaching. For comparison, the removal of AAEM species, Cl, and C in the raw leaves during single semi-continuous water leaching is also plotted in Figure 4-9. If the occurrence forms are not affected by steam distillation, the removal of these elements via the two-step process (i.e., steam distillation followed by semi-continuous water leaching) should be identical to that of the direct (one-step) semi-continuous leaching of the raw leaves. This is exactly the case for the overall removal of Na, K, and Cl, indicating that steam distillation removes part of these species that are originally water-soluble in the raw leaves. On the other hand, the overall removal of Mg, Ca and C via the two-step process is higher than that of a single leaching process, indicating that the chemical structure of the organic compounds

in the leaves are being changed by the interactions with the steam and/or the condensed hot water so that Mg, Ca and C are released in water-soluble forms.

4.5 Conclusions

The extraction of 1,8-cineole from the mallee leaves is fast within the first 15 min, becomes slow afterward and is almost completed after steam distillation for 60 min. The fast step is likely regulated by the rate of latent heat for the evaporation of 1,8-cineole and thereby follows zero-order kinetics under the experimental conditions. The slow step appears to be governed by the internal diffusion of residual 1,8-cineole in the leaves, following first-order kinetics. Steam distillation has little effect on the proximate and ultimate analyses as well as mass energy density of the spent leaves. However, it removes a considerable amount of total organic carbon from leaves and leads to substantial reductions in the concentrations of Mg, Ca, and Cl in the spent leaves. Water leaching of AAEM species and Cl in the raw leaves and the spent leaves−60 follows first-order kinetics whereas the leaching profile of C exhibits two different first-order rates. The leaching equilibrium values and the leaching rates of AAEM species in the spent leaves−60 are considerably lower than those of the raw leaves. While Cl in both the raw leaves and the spent leaves−60 is completely water-soluble, the leaching rate of which in the spent leaves−60 is considerably higher than that of the raw leaves. The fast leaching step of C in the spent leaves−60 is identical to that of C in the raw leaves whereas the leaching rate of C in the slow step for the spent leaves−60 is higher. The overall removals of Mg, Ca, and C after steam distillation for 60 min followed by water leaching are considerably higher than those of water leaching only, indicating the changes in the occurrence forms of Mg, Ca, and the organic structure in the leaves during steam distillation.

CHAPTER 5 PYROLYSIS OF SPENT BIOMASS FROM MALLEE LEAVES STEAM DISTILLATION: BIOCHAR PROPERTIES AND RECYCLING OF INHERENT INORGANIC NUTRIENTS

5.1 Introduction

As a byproduct of managing dryland salinity in Western Australia (WA)[20, 22], mallee biomass is potentially an important bioenergy feedstock because of its economic and large-scale production, low energy input and small carbon footprint[1, 216]. In addition, mallee leaves contains abundant eucalyptus essential oil (mainly 1,8-cineole)[7] that has wide applications[37, 222, 227]. Because 1,8-cineole is a value-added product, its co-production may further improve the economic performance of a mallee-based bioenergy supply chain in WA[2, 20, 228]. As discussed in Section 4.1, the extraction of 1,8-cineole is commonly conducted via steam distillation that produces oil-depleted spent leaves as bioenergy feedstock. As illustrated in Figure 5-1, the spent leaves can be subjected to pyrolysis that produces bio-oil and/or biochar. In particular for fast pyrolysis, whereas bio-oil is upgraded or refined to produce green liquid transport fuels or chemicals[244], biochar can find various applications. For example, biochar can be used as feedstock for electricity generation via thermochemical processing[78, 176, 219] and as carbon materials[245]. Additionally, biochar may also be returned to soil to enhance soil quality[122, 123], achieve carbon sequestration and recycle some of inherent inorganic nutrients in biochar to soil[125, 126], although the particulate matter within the biochar needs to be taken into consideration[175]. Considering a biochar application rate of 5−50 tonnes per hectare of land[131], recycling at least part of inorganic nutrients in biochar to soil is particularly important to improve the sustainability of biochar industry.

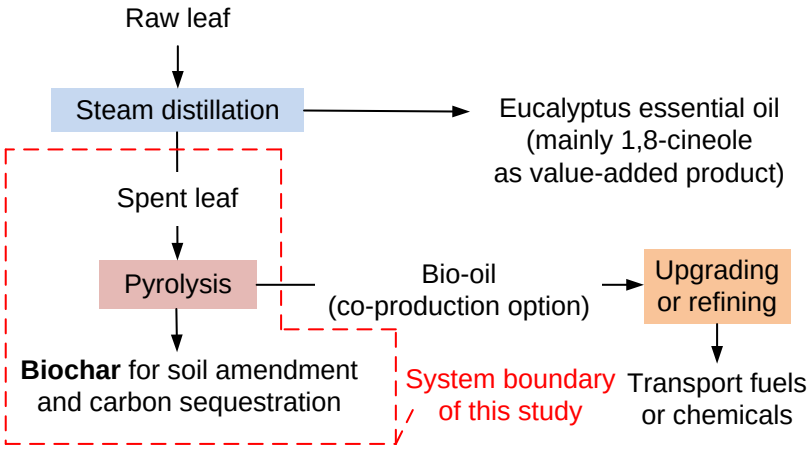

Figure 5- 1: Conceptual diagram of the proposed process that simultaneously produces eucalyptus essential oil, biochar and/or bio-oil.

For a mallee-based supply chain, previous studies have systematically investigated water-leaching characteristics of inorganic nutrients, including Na, K, Mg and Ca, in the biochars produced from slow and fast pyrolysis of major mallee compounds (i.e., wood, leaves, and bark)[57, 246]. As discussed in Section 4-3 that steam distillation not only removes considerable amounts of Na, K, Mg, Ca, Cl and C in the raw leaves, but also alters the association of Mg and Ca with organic structure in the spent leaves. Therefore, the effects of steam distillation on the biochar yields, the retentions of inorganic species in the biochars during spent leaves pyrolysis, and their subsequent release during biochar water leaching are largely unknown. This is the first objective of this chapter. In addition, it is desirable to determine the optimised steam distillation and pyrolysis conditions for biochar production from the spent leaves, in terms of maximizing the yield of stable biochar and the amounts of inherent inorganic nutrients returned to soil. This is the other objective of this chapter. Spent leaves were firstly prepared via steam distillation of the raw leaves for 30 and 60 min. The raw and spent leaves were then subject to both slow pyrolysis and fast pyrolysis at 400−700 °C to produce biochars that were subsequently leached via water under batch condition. The overall recycling rates of Na, K, Mg, Ca, Cl and C in the biochars from the raw and spent leaves via water leaching were discussed.

5.2 Yields and Properties of the Biochars

Figure 5-2 shows the yields of the biochars produced from slow pyrolysis and fast pyrolysis of the raw leaves, the spent leaves−30, and the spent leaves−60 at 400−700 °C. Regardless of pyrolysis conditions, similar biochar yields are achieved from the pyrolysis of the raw leaves and the spent leaves. The results suggest that most essential oil and other organic compounds, which are extracted from steam distillation of the raw leaves, are readily released into volatiles during its pyrolysis. Therefore, co-production of eucalyptus oil via steam distillation is not at a cost of biochar yield. As expected, pyrolysis temperature and heating rate have considerable effect on the biochar yields. For example, the biochar yields from slow pyrolysis decrease from ~32 wt% (db) at 400 °C to ~22 wt% (db) at 500 °C and then level off when further increasing pyrolysis temperature to 700 °C, indicating that the release of volatiles is virtually completed at temperatures ≥500 °C. Similar trend is also observed for the biochar yields from fast pyrolysis. However, the biochar yields from fast pyrolysis are generally ~5 wt% (db) lower than their counterparts from slow pyrolysis because fast pyrolysis suppresses intra-particle recombination reactions that promotes biochar formation[244].

Table 1 presents the proximate and elemental analyses of the raw and spent leaves as well as their derived biochars. Compared to those in the feedstock, the contents of ash and fixed carbon in the biochars increase by ~8−15 wt% (db) and ~23−47 wt% (db), respectively, at the expense of a reduction of ~31−58 wt% (db) in volatile matter contents. The biochars produced from the raw and spent leaves have similar data on proximate analysis whereas such data are sensitive to pyrolysis temperature and heating rate. Pyrolysis at a higher temperature produces biochar with higher contents of ash and fixed carbon but lower contents of volatile matter. The biochars from fast pyrolysis generally have higher contents of ash and volatile matter but lower contents of fixed carbon, compared to their counterparts from slow pyrolysis.

In comparison with the contents of C, H, and O in the raw leaves, steam distillation results in little changes in the contents of these elements in the spent leaves. The biochars produced from the raw and spent leaves under identical pyrolysis conditions

also have similar contents of these elements. On the contrary, pyrolysis temperature and heating rate have significant effects on the contents of C, H, and O in the biochars. The contents of C in the biochars increase by ~9−13 wt% (daf) whereas those of H and O decrease by ~3−4 wt% (daf) and ~5−10 wt% (daf), respectively, when increasing pyrolysis temperature from 400 to 700 °C. The biochars from slow pyrolysis generally have higher C contents but lower O contents compared with those in their counterparts from fast pyrolysis, indicating that the slow pyrolysis biochars have higher degrees of carbonisation possibly due to intensified intraparticle secondary reactions[244].

The contents of C, H, and O in the biochars can also be used to examine the biochar's degree of maturity[247] by plotting van Krevelen diagram (see Figure 5-3). Pyrolysis at 400 °C leads to a substantial reduction in the molar ratios of O/C and H/C in the biochars compared to those in the feedstock, as a result of the preferential release of H and O into volatiles during pyrolysis. Increasing pyrolysis temperature further reduces the two molar ratios in the biochar, grouping the biochar closer to the origin. A close examination reveals that the major reduction in the molar ratios of O/C and H/C in the biochars takes place when increasing pyrolysis temperature from 400 to 500 °C, consistent with the biochar yields profiles (see Figure 5-2). Except those in the biochars produced at 400 °C, the molar ratios of O/C and H/C in the biochars produced at ≥500 °C are all within the ranges set by the European Biochar Certificate Guidelines[215], indicating that these biochars are sufficiently stable to be used as soil amendment.

Table 1 also shows that, the contents of AAEM species in the feedstock and the biochars are in the order of Ca>Na>K>Mg. As discussed in Section 4-2, the contents of these species in the spent leaves are ~5−22% lower than those in the raw leaves because some of these elements were removed by hot reflux, which flows downward, during steam distillation. As a result, the contents of AAEM species in the biochars from the raw leaves are also slightly higher than those in the biochars from the spent leaves. Consistent with the trend of the ash contents, increasing pyrolysis temperature results in higher contents of AAEM species in the biochars.

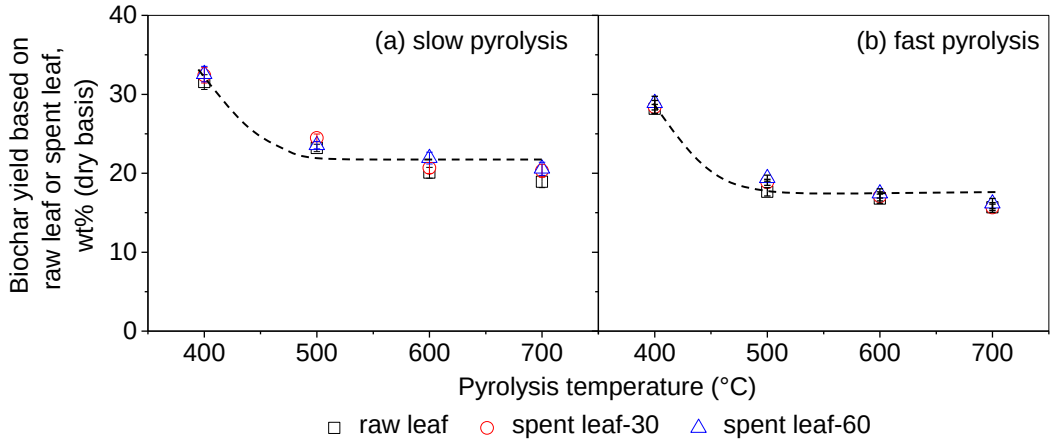

Figure 5- 2: Yields of the biochars produced from (a) slow pyrolysis and (b) fast pyrolysis of the raw leaves, the spent leaves−30, and the spent leaves−60 at 400−700 °C. The spent leaves−30 (or 60) means the spent leaves collected after steam distillation of the raw leaves for 30 (or 60) min.

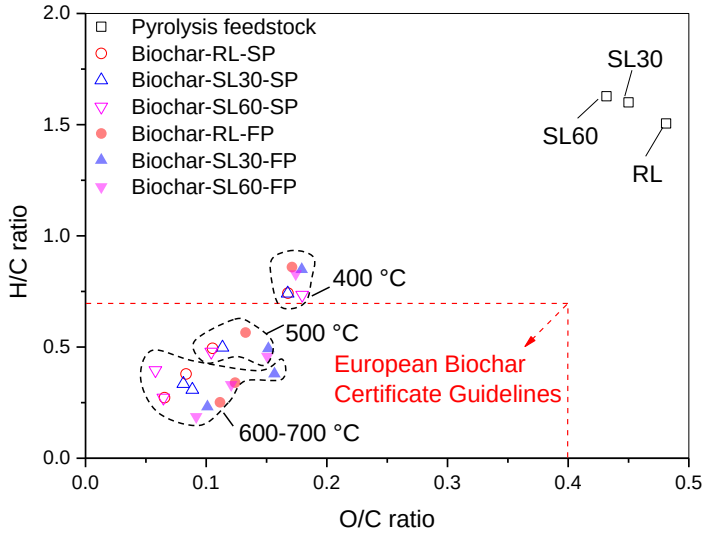

Figure 5- 3: Van Krevelen diagram of the raw leaves (RL), the spent leaves−30 (SL30), the spent leaves−60 (SL60), and their derived biochars. The spent leaves−30 (or 60) means the spent leaves collected after steam distillation of the raw leaves for 30 (or 60) min. Biochar−xx−SP (or FP) stands for the biochar produced from slow pyrolysis (or fast pyrolysis) of feedstock xx.

Table 5- 1: Properties of the raw leaves (RL), the spent leaves, and their derived biochars [SLxx = Spent Leaves Collected after Steam Distillation of the RL for xx min; Biochar−yy−SP (or FP)−zzz = Biochar Produced from the Slow Pyrolysis (or Fast Pyrolysis) of Feedstock yy at zzz °C]

Samples	Moisture (wt%, ad[a])	Proximate analysis (wt%, db[b])			Elemental analysis (wt%, daf[c])				Contents of inorganic species (wt%, db[b])				
		Ash	VM[d]	FC[e]	C	H	N	O[f]	Na	K	Mg	Ca	Cl
RL	5.0	4.1	77.9	18.0	55.8	7.0	1.4	35.8	0.608	0.351	0.159	0.808	0.22
SL−30	4.1	3.7	78.1	18.2	57.0	7.6	1.2	34.2	0.555	0.326	0.153	0.611	0.19
SL−60	3.9	3.8	77.6	18.6	57.5	7.8	1.6	33.1	0.523	0.315	0.150	0.655	0.18
Biochar−RL−SP−400	4.9	11.5	38.4	50.1	76.0	4.7	2.3	17.0	1.855	1.027	0.495	2.421	0.06
Biochar−RL−SP−500	4.9	15.2	25.9	58.9	82.6	3.4	2.4	11.6	2.358	1.311	0.609	2.921	0.08
Biochar−RL−SP−600	4.6	15.6	21.9	62.5	85.5	2.7	2.3	9.5	2.499	1.449	0.678	3.021	0.08
Biochar−RL−SP−700	6.0	16.8	20.7	62.5	88.1	2.0	2.2	7.7	2.533	1.552	0.702	3.232	0.06
Biochar−SL30−SP−400	4.8	11.6	38.0	50.4	76.1	4.7	2.2	17.0	1.660	0.924	0.466	1.957	0.02
Biochar−SL30−SP−500	4.3	14.1	25.4	60.5	81.9	3.4	2.3	12.4	2.186	1.228	0.590	2.383	0.03
Biochar−SL30−SP−600	4.8	15	21.9	63.1	86.0	2.4	2.3	9.3	2.279	1.320	0.626	2.563	0.03
Biochar−SL30−SP−700	5.6	16.6	19.4	64.0	85.6	2.2	2.1	10.1	2.342	1.409	0.687	2.709	0.02
Biochar−SL60−SP−400	4.8	12.0	39.0	49.0	75.2	4.6	2.2	18.0	1.676	0.800	0.468	1.930	0.01
Biochar−SL60−SP−500	4.6	14.6	25.4	60.0	82.8	3.3	2.4	11.5	2.066	1.140	0.580	2.585	0.02
Biochar−SL60−SP−600	5.3	15.1	21.9	63.0	88.0	2.9	2.3	6.8	2.193	1.234	0.625	2.690	0.02
Biochar−SL60−SP−700	6.1	16.5	20.5	63.0	88.3	2.0	2.1	7.6	2.287	1.301	0.680	2.914	0.02
Biochar−RL−FP−400	4.9	13.3	42.7	44.0	75.4	5.4	2.0	17.2	1.913	0.935	0.415	2.327	0.14
Biochar−RL−FP−500	5.3	17.9	30.6	51.5	79.7	3.8	2.4	14.1	2.997	1.340	0.664	3.455	0.48
Biochar−RL−FP−600	3.9	18.6	24.8	56.6	82.3	2.3	1.8	13.6	2.986	1.320	0.770	3.972	0.74
Biochar−RL−FP−700	5.0	18.2	21.2	60.6	84.1	1.8	1.6	12.5	2.703	1.099	0.734	4.076	0.77
Biochar−SL30−FP−400	4.3	12.1	46.2	41.7	74.9	5.3	1.9	17.9	1.586	0.795	0.384	1.870	0.04
Biochar−SL30−FP−500	4.8	16.2	28.3	55.5	78.7	3.2	2.2	15.9	2.530	0.967	0.593	3.215	0.29
Biochar−SL30−FP−600	4.2	16.6	22.5	60.9	79.0	2.5	2.0	16.5	2.472	0.949	0.670	3.352	0.52
Biochar−SL30−FP−700	4.2	17.6	22.7	59.7	85.3	1.6	1.6	11.5	2.179	1.031	0.800	3.476	0.48
Biochar−SL60−FP−400	4.2	12.5	46.5	41.0	75.3	5.2	2.0	17.5	1.683	0.744	0.427	2.146	0.04
Biochar−SL60−FP−500	4.7	16.9	28.8	54.3	79.2	3.0	1.9	15.9	2.514	0.947	0.635	3.243	0.35
Biochar−SL60−FP−600	3.7	18.1	23.9	58.0	82.6	2.3	1.8	13.3	2.643	1.072	0.690	3.615	0.51
Biochar−SL60−FP−700	3.7	18.9	21.1	60.0	86.6	1.3	1.5	10.6	2.315	1.122	0.754	3.967	0.48

[a]air dried basis. [b]dry basis. [c]dry and ash-free basis. [d]volatile matter. [e]fixed carbon. [f]by difference.

5.3 Inorganic Nutrients Retained in the Biochars

Figure 5-4 presents the retention of AAEM species and Cl in the biochars, expressed as wt% of corresponding elements in the raw and spent leaves. Overall, ~61−100% of Na, ~49−92% of K, ~71−100% of Mg, and ~75−100% of Ca are retained in the biochars over the whole temperature range studied. Whereas having insignificant effect on the retentions of Na, K, and Mg in the biochars, steam distillation appears to increase the retention of Ca in the biochars from the spent leaves by ~13−16%. This is because that steam distillation has removed part of Ca in the raw leaves, which can be easily released during the raw leaves pyrolysis. As shown in Figure 5-5, ~30−32% of Ca in the raw leaves has been removed via hot reflux during steam distillation.

At 400 °C, up to ~19% of Na, ~32% of K, ~29% of Mg, and ~19% of Ca have been released, possibly due to the thermal decomposition of the carboxylates of AAEM species followed by the release of their light carboxylates[248]. An increase in the pyrolysis temperature up to 700 °C leads to different retention profiles of AAEM species in the biochars, depending on pyrolysis heating rate and the nature (e.g., valence) of these inorganic species. For the slow pyrolysis biochars, the retentions of Na, Mg, and Ca decrease by ~13%, ~12%, and ~6−20%, respectively, when increasing pyrolysis temperature from 400 to 600 °C, and then level off with further increasing pyrolysis temperature to 700 °C. However, the retention of K in the slow pyrolysis biochars stabilize at ~87% across the whole temperature range studied. This is possibly due to the nature of K being more electropositive than Na[199], which enables the formation of K-containing intercalation compounds with carbon and thereby causes its retention in biochars[200]. For the biochars from fast pyrolysis, increasing pyrolysis temperature from 400 to 600 °C causes little changes in Na retention, whereas a considerable reduction of ~15% is observed when further increasing pyrolysis temperature to 700 °C as a result of the interactions between volatiles and nascent char, known as volatiles−char interactions[118]. However, the volatiles−char interactions

result in little changes in the retention of K because of the potential formation of K-containing intercalation compounds in biochar matrix and those of Mg and Ca because of their divalent nature[116]. The retention of AAEM species, particularly Na, K and Mg, in the fast pyrolysis biochars are generally lower than those in their counterparts from slow pyrolysis, due to the aforementioned volatiles-char interactions[118] and the suppression of intra-particle secondary reactions during fast pyrolysis that favours the retention of AAEM species in biochars[248].

The retention profiles of Cl in the biochars follow different trends with those of AAEM species. During slow pyrolysis, up to ~98% of Cl has been released at 400 °C and therefore increasing pyrolysis temperature up to 700 °C results in little changes in the Cl retention. The release of Cl at 400 °C is possibly due to the interactions between inorganic chlorides and organic structures (e.g., cellulose) in the raw and spent leaves[249]. For fast pyrolysis, however, the Cl retention increase first from ~5−18% at 400 °C to ~42−56% at 600 °C and then level off with further increasing pyrolysis temperature to 700 °C, indicating the recombination of Cl in volatiles with organic biochar matrix[117] and/or inherent metals[250] (e.g., AAEM species) in the biochars. Such recombination appears to be enhanced as the temperature increases, possibly due to intensified thermal cracking reactions of both biochar and volatiles[117]. These reactions may produce more Cl-bonding sites on biochar surface[117] and convert Cl-containing volatiles into forms (e.g., gaseous HCl) that can be easily captured in the biochar. While following similar trend, the retention of Cl in the biochars from the spent leaves are ~9−16% lower than those in their counterparts from the raw leaves. This can be attributed to the removal of considerable amounts of AAEM species during steam distillation (i.e., ~18−26% of Na, ~17−23% of K, ~14−19% of Mg, and ~30−32% of Ca, see Figure 5-5). The inorganic species appear otherwise to act as bonding sites for the recombination of Cl hence increase the Cl retention. This is supported by the fact that ~100% of Cl in the fast pyrolysis biochars is water-soluble (see discussion below in

Section 3.3) because Cl is predominantly recombined with metals (as water-soluble metal chlorides) in the biochars.

5.4 Release of Inorganic Nutrients in the Biochars from Water Leaching

Figure 5-6 illustrates the quantity of water-soluble AAEM species and Cl, expressed as wt% of corresponding elements in the biochars. Overall, ~69−100% of Na, ~53−88% of K, ~4−43% of Mg, ~4−13% of Ca, and ~60−100% of Cl in the biochars can be leached out via water, depending on the nature of these elements, the feedstock, and pyrolysis temperature. Compared to divalent Mg and Ca, monovalent Na, K, and Cl in the biochars are easier to be released via water leaching. Apart from those of Mg in the slow pyrolysis biochars, steam distillation has insignificant effect on the quantities of water-soluble Na, K, Ca, and Cl in the biochars.

However, pyrolysis temperature has considerable effect on the quantities of water-soluble inorganic elements in the biochars and such effects are dependent on the nature of these inorganic elements and heating rate. For example, whereas pyrolysis temperature leads to little changes on the quantities of water-soluble K and Ca in the biochars, that of Na, Mg, and Cl is sensitive to pyrolysis temperature. The quantity of water-soluble Na in the biochars decreases by ~13% for slow pyrolysis and by ~21% for fast pyrolysis when increasing pyrolysis temperature from 400 to 500 °C, and then stabilizes with further increasing temperature to 700 °C. Mg follows similar trend with that of Na but the temperature at which the quantity of water-soluble Mg levels off increases to 600 °C. The reduction in the quantity of water-soluble Na and Mg with increasing pyrolysis temperature can be attributed to the higher degrees of carbonisation[251], which results in more Na and Mg being bound to biochar structure and thereby becoming water-insoluble. Whereas Cl in the slow pyrolysis biochars follows similar trend with that of Na, ~100% of Cl in the fast pyrolysis biochars is water-soluble, indicating the formation of water-soluble chlorides in the biochars.

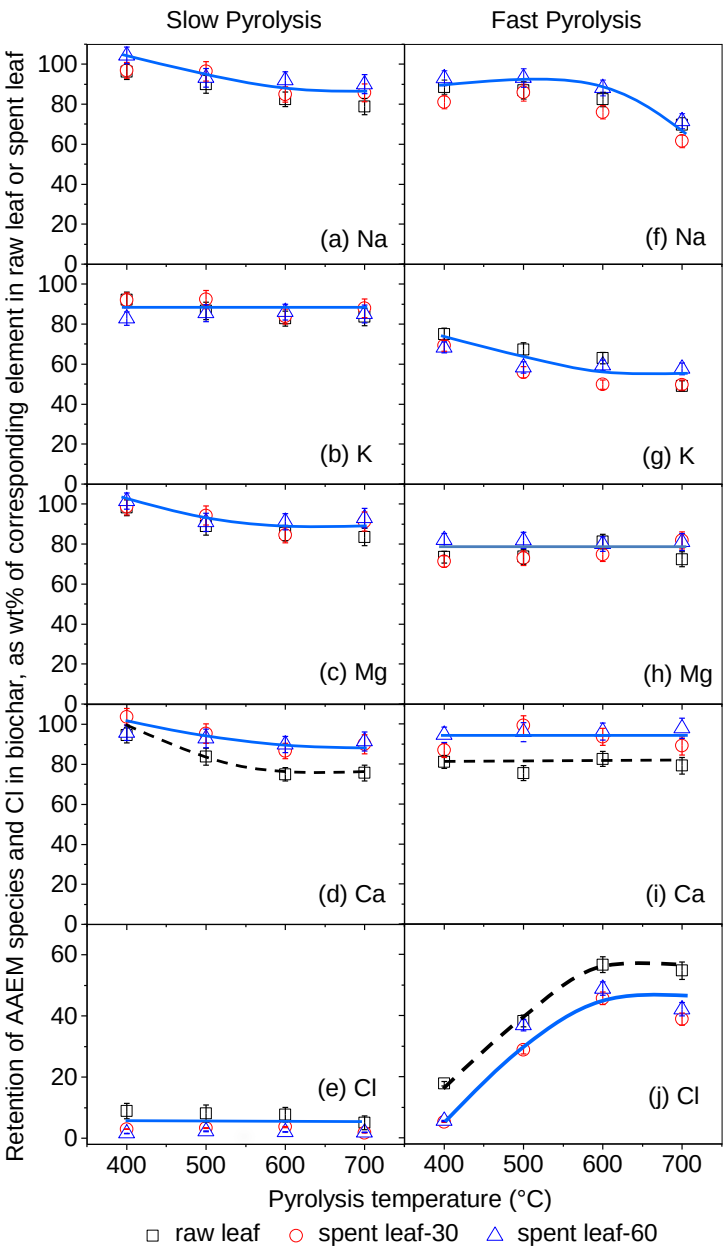

Figure 5- 4: Retentions of Na, K, Mg, Ca, and Cl in the biochars produced from slow pyrolysis (a-e) and fast pyrolysis (f-j) of the raw leaves, the spent leaves−30, and the spent leaves−60 at 400−700 °C, expressed as wt% of corresponding elements in the raw and spent leaves. The spent leaves−30 (or 60) means the spent leaves collected after steam distillation of the raw leaves for 30 (or 60) min.

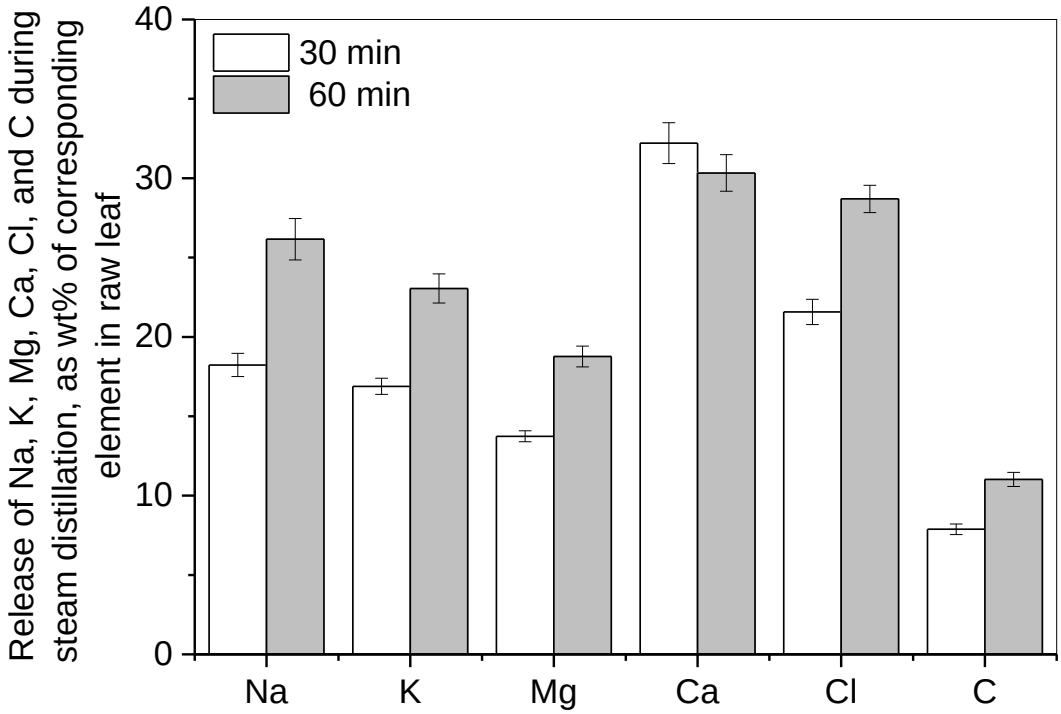

Figure 5- 5: Release of Na, K, Mg, Ca, Cl, and C in the raw leaves after steam distillation (due to hot reflux) for 30 and 60 min, expressed as wt% of corresponding elements in the raw leaves, considering the weight loss of ~10 wt% (db) and ~14 wt% (db) after steam distillation for 30 and 60 min, respectively.

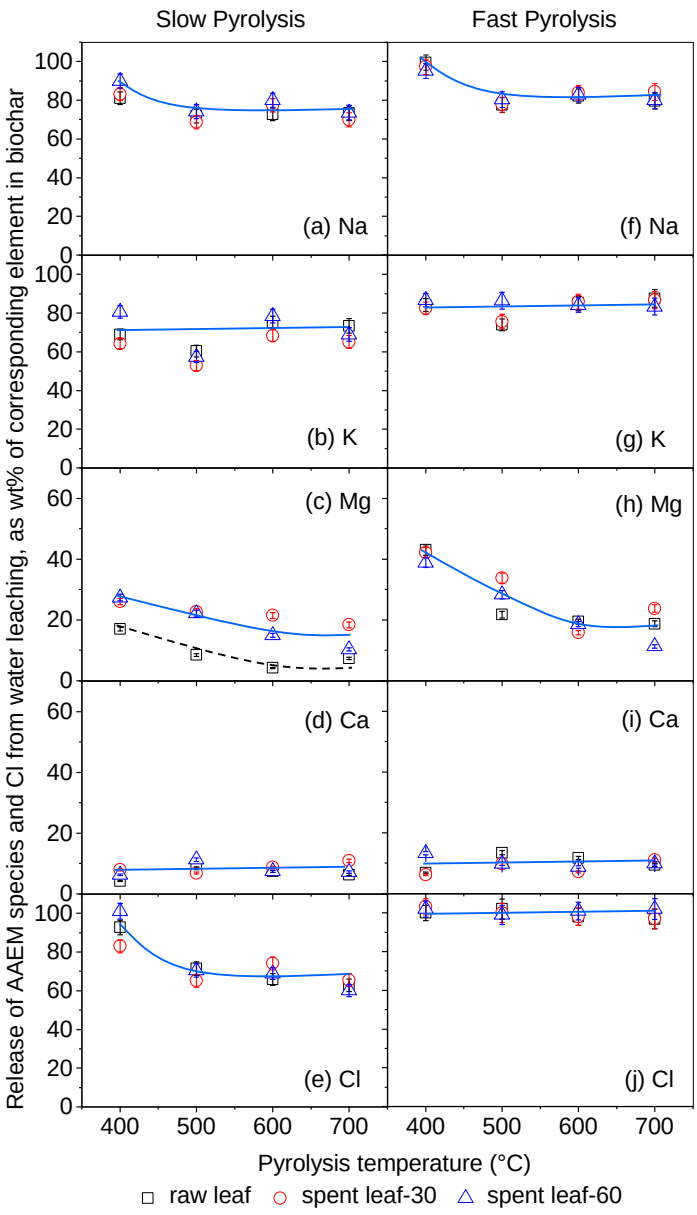

Figure 5- 6: Quantity of water-soluble Na, K, Mg, Ca, and Cl in the biochars produced from slow pyrolysis (a-e) and fast pyrolysis (f-j) of the raw leaves, the spent leaves−30, and the spent leaves−60 at 400−700 °C, expressed as wt% of corresponding elements in the raw and spent leaves. The spent leaves−30 (or 60) means the spent leaves collected after steam distillation of the raw leaves for 30 (or 60) min.

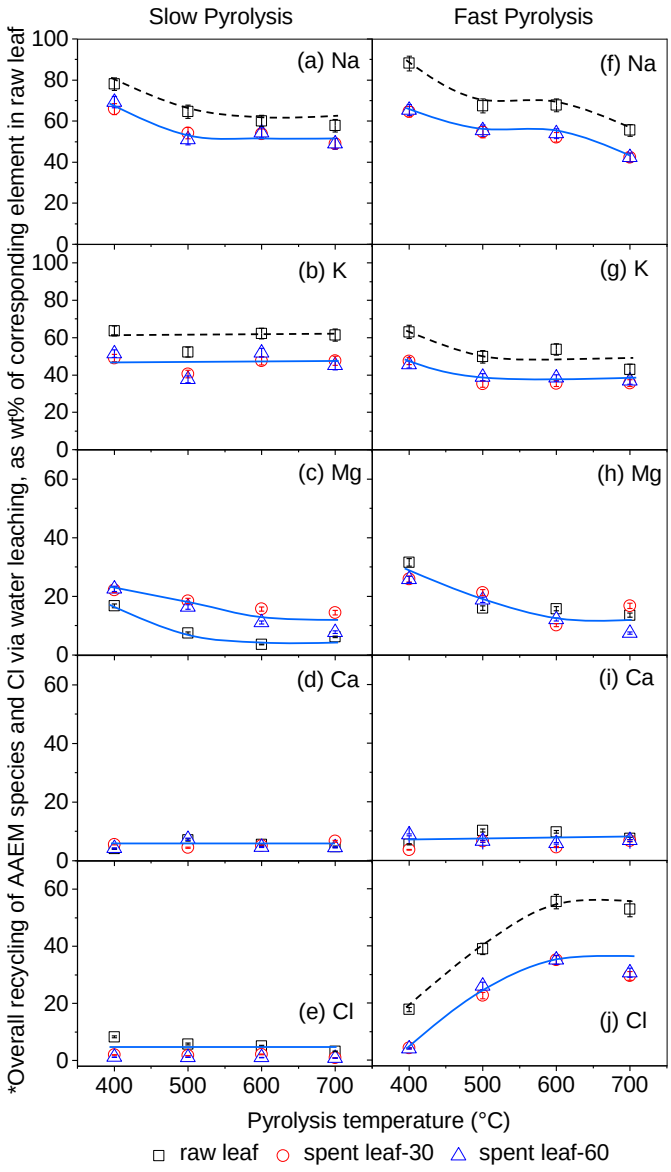

Figure 5- 7: Overall recycling of Na, K, Mg, Ca, and Cl in the biochars produced from slow pyrolysis (a-e) and fast pyrolysis (f-j) of the raw leaves, the spent leaves−30, and the spent leaves−60 at 400−700 °C. The spent leaves−30 (or 60) means the spent leaves collected after steam distillation of the raw leaves for 30 (or 60) min. *Expressed as wt% of corresponding elements in the raw leaves, considering the release of these elements from steam distillation and pyrolysis.

Considering the fate of AAEM species during steam distillation, pyrolysis, and water leaching (i.e., data in Figures 5-6), the overall recycling of these inorganic species via water leaching are illustrated in Figure 5-7, expressed as wt% of corresponding elements in the raw leaves. Overall, ~42−88% of Na, ~35−64% of K, ~4−32% of Mg, ~4−10% of Ca, and ~1−56% of Cl in the original leaves can be recycled to soil via water leaching, depending on the feedstock and pyrolysis conditions.

Steam distillation of the raw leaves appears to have considerable effect on the overall recycling of Na, K, Mg, and Cl via water leaching. Regardless of pyrolysis conditions, the overall recycling rates of Na and K in the biochar from the raw leaves are ~6−24% and ~6−18% higher than those in the biochars from the spent leaves, mostly due to the removal of considerable amounts of Na and K during steam distillation (see Figure 5-5). On the contrary, the slow pyrolysis of the raw leaves leads to lower (up to ~12%, see Figure 5-7c) overall recycling rates of Mg, compared to those in their counterparts from the spent leaves, primarily because of the poor solubility of Mg in the biochars from the slow pyrolysis of the raw leaves (see Figure 5-6c). The effects of the feedstock on the overall recycling rates of Cl depend on heating rate. For slow pyrolysis, the overall recycling rates of Cl in the biochars are consistently low (<10%) because over ~90% of Cl has been released during pyrolysis. For fast pyrolysis, the overall recycling rates of Cl in the biochars from the spent leaves are considerably lower (up to ~23%) than those in the biochars from the raw leaves due to the release of Cl during steam distillation (see Figure 5-5) and the lower retention of Cl in the biochars from the spent leaves (see Figure 5-4j).

Pyrolysis conditions (i.e., temperature and heating rate) also considerably affect the overall recycling rates of AAEM species and Cl, depending on the nature of these species. For example, the overall recycling rates of Na decrease by ~10−21% with increasing pyrolysis temperature from 400 to 500 °C. Further increasing pyrolysis temperature leads to little changes in its overall recycling rates in the slow pyrolysis biochars. However, a further reduction of ~10−12% in those of Na in the fast pyrolysis

biochars is observed when increasing pyrolysis temperature from 600 to 700 °C, primarily due to the release of Na during pyrolysis (see Figure 5-5-4f). The overall recycling rates of K in the fast pyrolysis biochars and those of Mg in all the biochars follow similar trend with those of Na. Oppositely, the overall recycling rates of Cl in the fast pyrolysis biochars increase drastically by ~31−38% when increasing pyrolysis temperature from 400 to 600 °C and then stabilize with further increasing pyrolysis temperature to 700 °C, consistent with its retention in the fast pyrolysis biochars (see Figure 5-5-4j).

5.5 Fate of Carbon in the Raw Leaves from Steam Distillation, Pyrolysis, and Water Leaching

When producing biochar from the raw and spent leaves for soil application, the fate of C during steam distillation, pyrolysis, and water leaching is important because its release upon leaching affects the evaluation of C sequestration credits, poses potential soil contamination, and alters the soil organic carbon composition[252]. Figures 8a and 8b show the retention of C in the biochars from slow pyrolysis and fast pyrolysis, respectively. Clearly, the retention of C in the slow pyrolysis biochars decrease from ~39% at 400 °C to ~28% at 500 °C and then levels off with further increasing pyrolysis temperature to 700 °C. Similar trend is also observed for the fast pyrolysis biochars. However, the retention of C in the fast pyrolysis biochars are ~5−7% lower than those in the slow pyrolysis biochars because slow pyrolysis leads to higher degrees of carbonisation. Although steam distillation removes ~8−11% of C in the raw leaves (see Figure 5-5), it has little effects on the C retention in the biochars from the raw and spent leaves because pyrolysis at ≥400 °C easily volatilises the C that can be extracted via steam distillation.

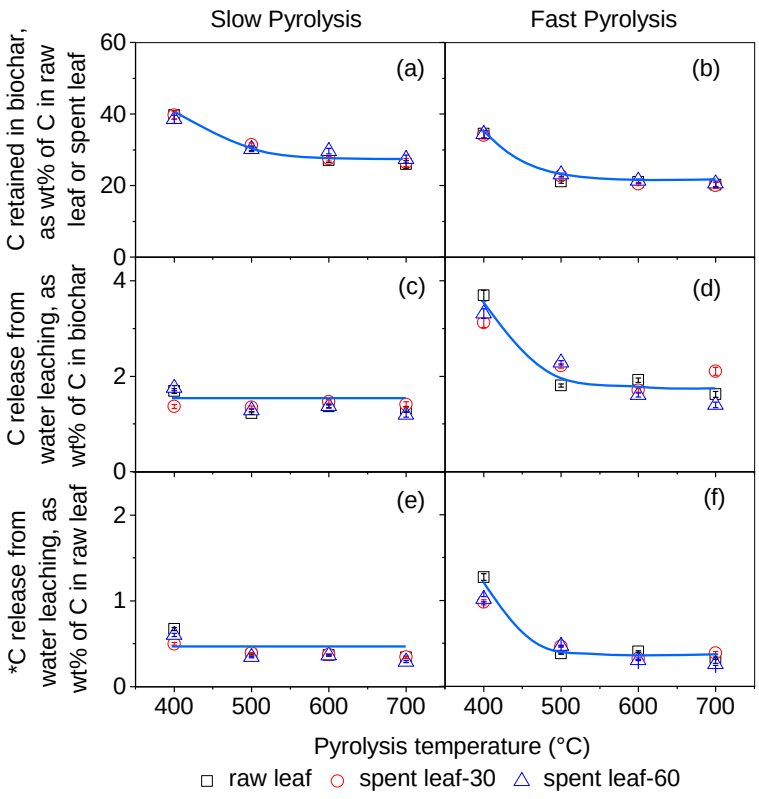

Figure 5- 8: Retention of carbon (a-b) and the quantity of water-soluble carbon (c-d) in the biochars produced from slow and fast pyrolysis of the raw leaves, the spent leaves−30, and the spent leaves−60 at 400−700 °C as well as (e-f) the overall removal of carbon from pyrolysis and water leaching. *Expressed on the basis of carbon in the raw leaves, considering the carbon release during steam distillation, pyrolysis and water leaching.

Figures 5-8c and 5-8d illustrate the quantity of water-soluble C in the biochars from slow pyrolysis and fast pyrolysis, respectively. Regardless of the feedstock, the quantity of water-soluble C in the slow pyrolysis biochars is stabilized at ~1.4% across the whole pyrolysis temperature range studied. On the contrary, that of C in the fast pyrolysis biochars decreases by ~1.5% when increasing pyrolysis temperature from 400 to 500 °C and then terminates at ~1.9% with further increasing pyrolysis temperature to 700 °C. As expected, the biochars from fast pyrolysis have a higher quantity of water-soluble C

than their counterparts from slow pyrolysis because the fast pyrolysis biochars tend to adsorb volatile organic compounds[253] that can be removed during water leaching. It is therefore reasonable to speculate that the quantity of water-soluble C in the biochars may correlate with their relative volatile matter contents. Such correlation is plotted in Figure 5-9. Indeed, the C released during biochar water leaching is proportional to the relative contents of volatile matter in the biochars, particularly for those from fast pyrolysis. This implies that simple and inexpensive proximate analysis can provide basic information on the quantity of water-soluble C in biochars. Considering the C released during steam distillation, pyrolysis and water leaching together, Figures 5-8e and 5-8f present the overall quantity of C that ends up in the leachate, on the basis of C in the raw leaves. Regardless of the feedstock and temperature, that of C in the slow pyrolysis biochars stabilizes at ~0.4%. However, the overall leaching of C in the fast pyrolysis biochars decreases from ~1.1% at 400 °C to ~0.5% at 500 °C and then levels off with further increasing pyrolysis temperature to 700 °C.

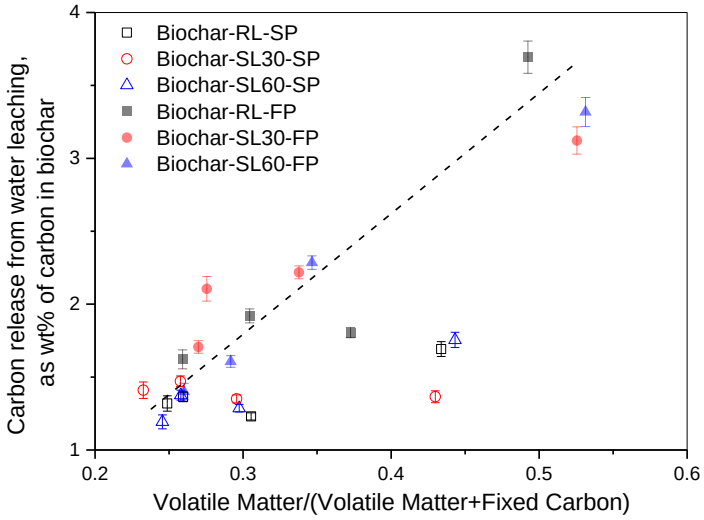

Figure 5- 9: Correlation between the quantity of water-soluble organic carbon and the fraction of volatile matter contents (based on the data in Table 1) in the biochars.

5.6 Further Discussion and Implications

Practically, the production of biochar from the spent leaves after steam distillation of mallee leaves may consider at least four factors. First, it appears that the spent leaves−60 will likely be the pyrolysis feedstock because the complete extraction of 1,8-cineole from the raw leaves requires 60 min. Second, stable biochar is favoured for soil application to ensure the sequestration of stable carbon and lower the risks of potential soil contamination. Therefore, the biochars produced at 400 °C should be excluded because their O/C and H/C molar ratios are higher than those regulated by the European Biochar Certificate Guidelines (see Figure 5-3). The instability of C in the biochars from fast pyrolysis at 400 °C is further evidenced by their high quantity of water-soluble C (see Figure 5-8d). Third, biochar production must be economically feasible. Based on the current knowledge on techno-economic analysis of pyrolysis systems, biochar from fast pyrolysis is economically favourable than that from slow pyrolysis because of the production of transportation fuels via bio-oil upgrading[254]. Therefore, fast pyrolysis should be employed for biochar production. In addition, maximum bio-oil yields are generally achieved from fast pyrolysis at temperatures around 500 °C[244]. Fourth and last, the maximum overall recycling rates of AAEM species in the fast pyrolysis biochars are achieved at 500 °C, compared to those produced at higher temperatures. Therefore, the fast pyrolysis of the spent leaves-60 at 500 °C is recommended to produce the biochar that is sufficiently stable and economically favourable and returns maximum inherent inorganic nutrients (mainly AAEM species) to soil.

In addition, considering the data in Figures 5-8 together, mass balance analysis suggests that steam distillation removes ~26.2% of Na, ~23.1% of K, ~18.8% of Mg, ~30.3% of Ca, 28.7% of Cl, and ~11.0% of C in the raw leaves via hot reflux whereas the remaining elements are retained in the spent leaves−60. Fast pyrolysis of the spent leaves−60 at 500 °C leads to 45.0% of Cl and ~68.5% of C being released into volatiles whereas the majority of AAEM species (~44.9−68.8%) are retained in the biochar. After water leaching, ~55.4% of Na, ~38.8% of K, ~18.8% of Mg, ~6.5% of Ca, ~26.0% of Cl,

and ~0.5% of C in the raw leaves end up in the leachate and are therefore able to be recycled to soil via water leaching.

5.7 Conclusions

Under identical pyrolysis conditions, whereas the effects of the feedstock on the yields, proximate analysis, and elemental analysis of the biochars are negligible, the contents of Na, K, Mg, Ca and Cl in the biochars from the raw leaves are generally higher than those in the biochars from the spent leaves. The feedstock has little effects on the retention of these inorganic species except for Ca in all the biochars and Cl in the fast pyrolysis biochars. However, expressed as wt% of corresponding elements in the raw leaves, the quantities of water-leachable Na, K, and Cl in the biochars from the mallee leaves are considerably higher than those in the biochars from the spent leaves whereas those of Mg in the slow pyrolysis biochars follow an opposite trend. Regardless of the feedstock, increasing pyrolysis temperature from 400 to 500 or 600 °C leads to considerable decreases in the overall recycling rates of Na and Mg in all the biochars as well as those of K and C in the fast pyrolysis biochars. The fast pyrolysis of the spent leaves−60 at 500 °C seems to be suitable to simultaneously produce 1,8-cineole, bio-oil, and biochar. The biochar has favourable properties for returning its inherent inorganic nutrients to soil.

CHAPTER 6 INORGANIC PM10 EMISSION FROM THE COMBUSTION OF SPENT LEAF AFTER STEAM DISTILLATION

6.1 Introduction

In Chapter 4, it was discussed that steam distillation has an impact on the composition and chemical association of inorganic elements, especially alkali and alkaline earth metal (AAEM, mainly Na, K, Mg and Ca) species and Cl. A significant amount of AAEM components was removed from the raw leaf during steam distillation. Those inorganic components are known as key components on the formation of ash and particulate matter (PM) with an aerodynamic diameter of <10 μm (PM_{10})[158, 161, 255]. PM_{10} contributes significantly to the adverse impact on both human health and environment[164-169, 171, 172]. Reducing inorganic component concentrations in solid fuels can potentially reduce the ash formation. Therefore spent leaves could be seen as a promising feedstock in biomass fuel based power generation plants particularly in reducing ash forming problem and particulate matter (PM) emissions.

In a conventional technical practice, mallee spent leaves have been used as a source of boiler fuel to produce steam by several distilleries[256]. However, to the best of the author's knowledge, no data has been published related to the ash formation during spent leaves combustion under pulverized-fuel conditions. Furthermore, a thorough understanding on PM properties and formation during spent leaf combustion is required for minimizing PM emissions which is important on designing and developing biomass based power generation equipment. Therefore, this chapter will thoroughly discuss the emission behaviour and characteristics inorganic PM during combustion of spent leaves. A series of experiments has been developed to study the behaviour of PM_{10} during combustion of spent leaves from steam distillation. Raw and spent leaves were

pulverised and then combusted at 1400 ^{o}C in air using a laboratory-scale drop-tube furnace (DTF). The inorganic PM_{10} was then collected and characterised to investigate its emission behaviour.

6.2 Properties of spent leave and its inorganics

During steam distillation, only a small fraction of the total material is extracted from the raw leaf even at long extraction time. As discussed in section 4.4 of Chapter 4, the spent leaf is still retained approximately 86% and 81% on dry basis (db) at steam distillation time of 60 (spent leaf-60) and 180 (spent leaf-180) min, respectively. For further investigation, along with the raw leaf, only the spent leaf−60 was selected as combustion feedstock because after which the extraction of 1,8-cineole is completed.

As discussed in Chapter 4, the fuel properties of raw leaf are affected by steam distillation process. It is shown in Table 4-1, the contents of moisture, ash, volatile matter, and oxygen in spent leaf-60 decreased by ~22, ~9.5, ~0.4%, and ~3%, respectively, compared to that of the raw leaf. However, the content of fixed carbon, C, and H increase by ~4, ~2.3, and ~10%, respectively. Consequently, steam distillation has an effect on the mass energy density (or calorific value), which is expressed as higher heating value (HHV) and estimated from the ultimate analysis data[241] of the raw and spent leaf samples. The HHV of spent leaf-60 is 4.2% higher than that of the raw leaf.

Figure 6-1(a) presents the retention of inorganics in spent leaf-60. It can be seen from the figure that steam distillation results in reductions in the contents of AAEM species and Cl. Affected by the reflux during steam distillation, considerable amounts of Na, K, Mg, and Ca are leached out during steam distillation, resulting in lower contents of these inorganic species in the spent leaf-60, compared to those of the raw leaf. The retention of these species in the raw leaf is ~77-89%. While for Cl, a significant amount of Cl (~32%) is removed during the distillation process.

One possible mechanism in governing the removal of AAEM and Cl during steam distillation is the contact between parts of water soluble inorganic materials with the condensed steam on the surface of the leaves. The inorganics are then dissolved in the hot water and are washed out from the leaves. Another possible mechanism is that steam distillation has changed the structure of the leaves, which makes inorganic materials being more water-soluble. It is shown in Figure 6-1 that the portion of water-soluble Ca is enhanced by steam distillation process. This finding is in accordance with previous study on mallee leaf hydrodistillation[7].

Overall, steam distillation has affected the spent biomass, resulting in a higher energy density and lower contents of AAEM species and Cl. This suggests that using spent leaves from steam distillation could be promising especially in mitigating ash related problems such as slagging, fouling, corrosion, bed material agglomeration in fluidized beds as well as mitigating problems related to fine inorganic aerosol emission[59, 64, 65, 68, 69, 149, 156, 163, 174, 177, 178].

The forms of inorganic components, in term of the water solubility, in the fuel are an important aspect during thermochemical process[243]. Water leaching is one of the most popular techniques to evaluate the inorganic water soluble form in solid fuel. In this investigation, a semi-continuous method which has been developed by Liaw et al.[205] was employed and the results are presented in Figure 6-1 (b). It can be seen that Cl in both raw and spent leaf is completely soluble in water. The figure also shows that a majoritiy of Na and K in the raw leaf and the spent leaf−60 could be easily leached out. On the other hand, only <5% of Ca and <50% of Mg in the raw leaf and the spent leaf−60 could be leached out.

The concentration and form of the inorganic species in spent leaf may affect the formation and behaviour of PM during combustion, which will be discussed in the following sections.

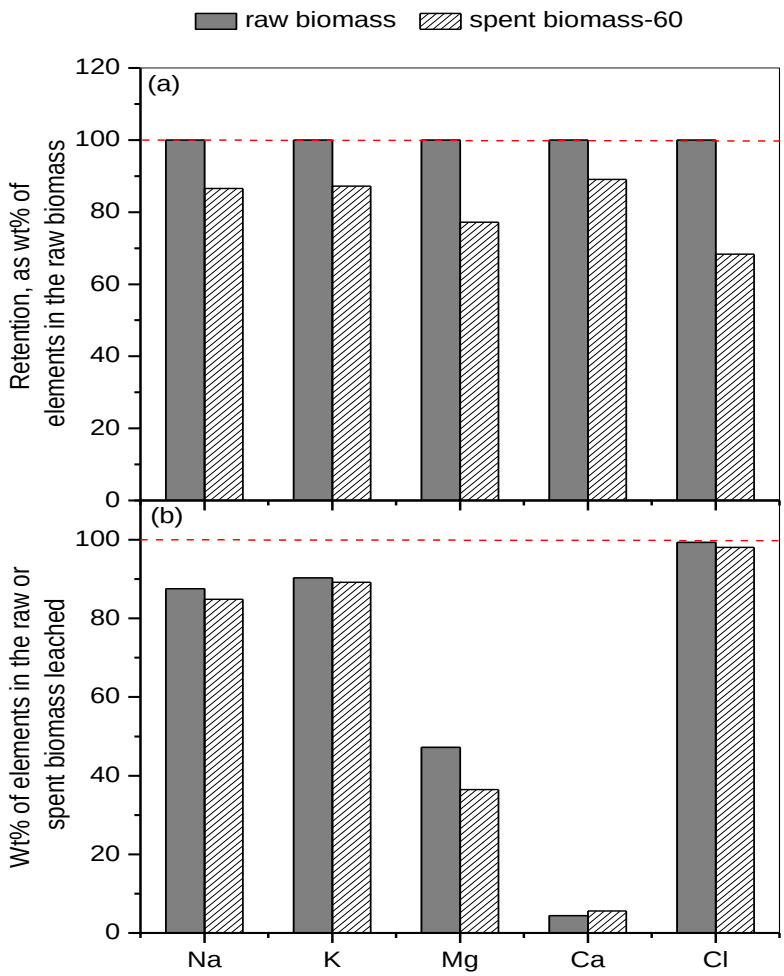

Figure 6- 1: (a) Retention of Na, K, Mg, Ca, and Cl in spent biomass at 60 min and (b) water-leachable fractions of these elements in the raw and spent biomass.

6.3 Particle Size Distributions and Yields of PM_{10}

The particle size distributions (PSDs) and yields of the inorganic PM_{10} produced from the combustion of raw leaf and spent leaf-60 at 1400 ^{o}C are presented in Panel a and b of Figure 6-2, respectively, on the basis of unit mass (dry basis) of the combustion feedstock fed into the DTF reactor. From Figure 6-2(a), the PSDs of PM_{10} both raw leaf and spent leaf-60 follow a bimodal distributions, with two peaks at ~0.02 and ~4.09 μm, respectively.

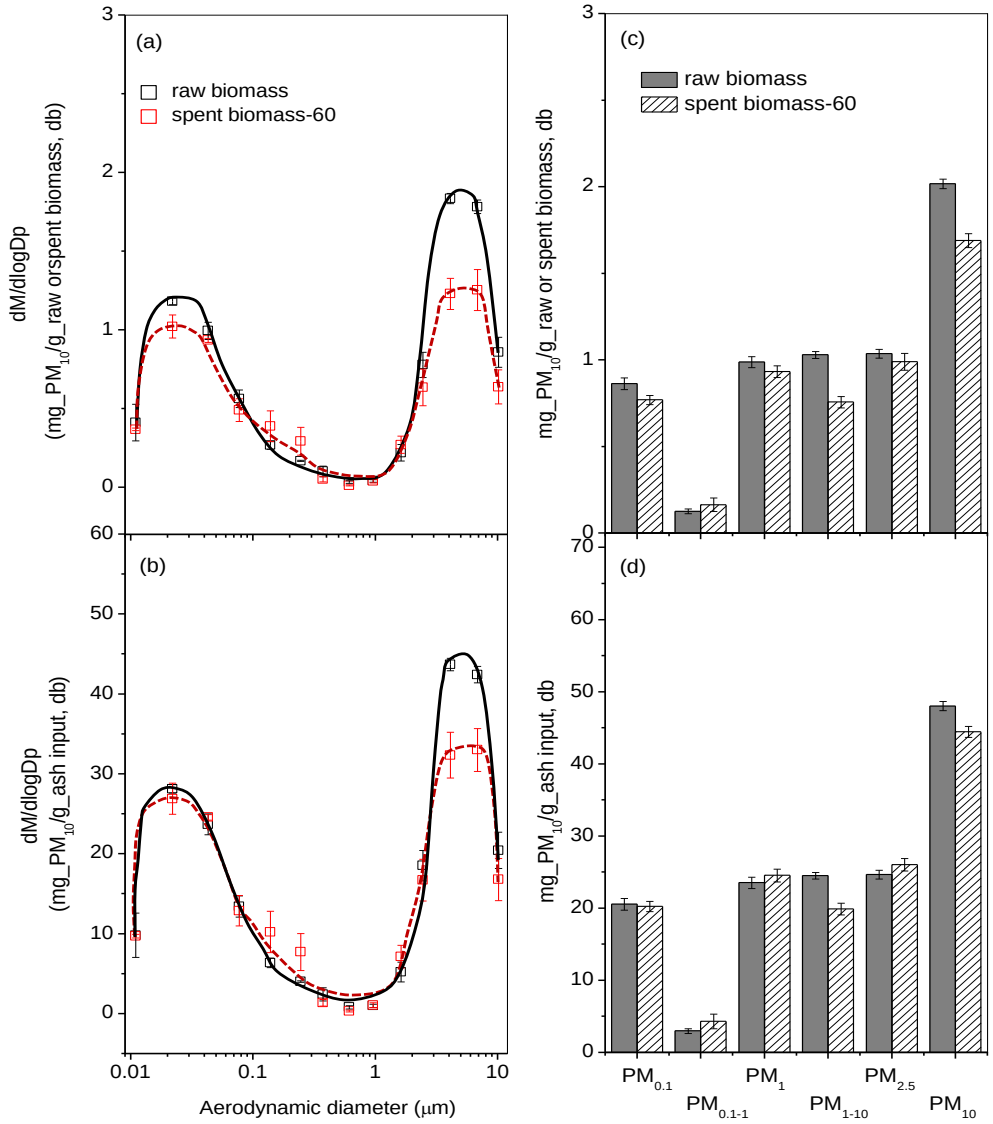

Figure 6- 2: (a and c) Mass-based PSDs of PM_{10} and (b and d) yields of $PM_{0.1}$, $PM_{0.1–1}$, PM_1, $PM_{1–10}$, $PM_{2.5}$, and PM_{10} from the combustion of the raw and torrefied biomass. Panels (a) and (b) are normalized to unit mass of the raw or spent biomass input into the furnace on a dry basis. Panels (c) and (d) are normalized to equivalent mass of ash input into the furnace. PMxx and PMyy−zz mean PM with aerodynamic diameters of <xx and yy−zz μm, respectively.

As shown in Figure 6-2(b), the yields of particulate matters with aerodynamic diameters of <0.1 μm ($PM_{0.1}$), <1 μm (PM_1), and <2.5 μm ($PM_{2.5}$) from the combustion of spent leaf-60 are slightly lower than that of raw leaf. The yield of $PM_{0.1\text{-}1}$ produced from spent leaf is slightly higher than that of raw leaf. However, the yield of PM_{1-10} (PM with an aerodynamic diameter of 1−10 μm) produced from spent leaf-60 is substantially lower compared to the raw leaf combustion. Therefore, PM10 produced from the spent leaf-60 is considerably lower compared to that from the raw leaf. It is reasonable to speculate that the reduction of PM10 yield in spent leaf may be due to the lower content of AAEM species and Cl as well as ash in the spent leaf-60.

To eliminate the impacts of the dissimilarity of ash contents on PM_{10} emission, the PSDs and yields of PM are normalized to the unit mass (dry basis) of ash input into the DTF, which are illustrated in panels c and d of Figure 6-2. The yields of $PM_{0.1\text{-}1}$, PM_1 and $PM_{2.5}$ in the raw leaf are slightly lower than that of the spent leaf, while there is no difference between the yield of $PM_{0.1}$ from the raw leaf and the spent leaf-60. However, the ash-based yield of $PM_{1\text{-}10}$ from spent leaf-60 is significantly lower than that of the raw leaf. As a result, the yield of PM_{10} from the spent leaf is, therefore, lower than that of the raw leaf as this yield is greatly contributed by the yield of $PM_{1\text{-}10}$. The lower yield of PM10 from the spent leaf than that from the raw leaf indicates that steam distillation not only reduces the AAEM contents in the raw leaf but also lowers the yield of PM_{10}.

6.4 The Transformation of Key PM_{10}-Forming Elements

To further understand the differences in the emission behaviour of PM_{10} from the raw and spent leaf, investigation of the transformation of key PM_{10}-forming elements, including Na, K, Cl, S, P (as water-soluble PO_4^{3-}), Mg, and Ca and their distribution in PM_{10} are conducted.

Figure 6-3 shows the mass based PSDs of Na, K, Cl, S, P, Mg, and Ca, the yields of while are presented at Figure 6-4. The PSDs of Na, K, Cl and SO_4^{2-} exhibit a unimodal distribution with a peak diameter of 0.043-0.22 μm. Those of Ca and Mg also show a

unimodal particles distribution but the peak is concentrated at 4.087-6.852 μm. On the contrary, the PSDs of PO_4^{3-} exhibit a bimodal distribution, with a fine mode at 0.077-0.246 μm and a coarse mode at 4.087-6.852 μm.

During biomass combustion, Na, K and Cl are easily volatilised and released [176, 257] and then they undergo gas-phase reactions, homogenous nucleation or heterogeneous condensation reactions on the surface of fine particles[158, 258-260]. Similarly, $SO4^{2-}$ in fine particles are formed through either homogenous gas-phase reactions and/or heterogeneous reactions of S components with the surface of existing fine particles [261-265]. Therefore, as clearly shown at Figure 6-4, PM_1 are dominated by Na, K, Cl and SO_4^{2-}. It is also interesting to note that the yields of Na and Cl in the fine particles from the spent leaf-60 are higher than that from the raw leaf.

The bimodal distributions of PSDs of PO_4^{3-} peak at a fine mode of ~0.077-0.246 μm and coarse mode of ~4.087-6.852 μm. It can be clearly seen from Figure 6-3 that the distribution of the water soluble PO_4^{3-} in fine particles is lower than in coarse particle. Approximately 29-32% of PO_4^{3-} is distributed in PM_1, while the remaining is distributed in PM_{1-10}. The presence of water soluble PO_4^{3-} in PM_1 is in accordance with previous research on biomass combustion[266]. This could be attributed to the gas-phase reaction during combustion. Whereas, the presence of PO_4^{3-} in PM^{1-10} could be related to the char fragmentation during biomass combustion[176].

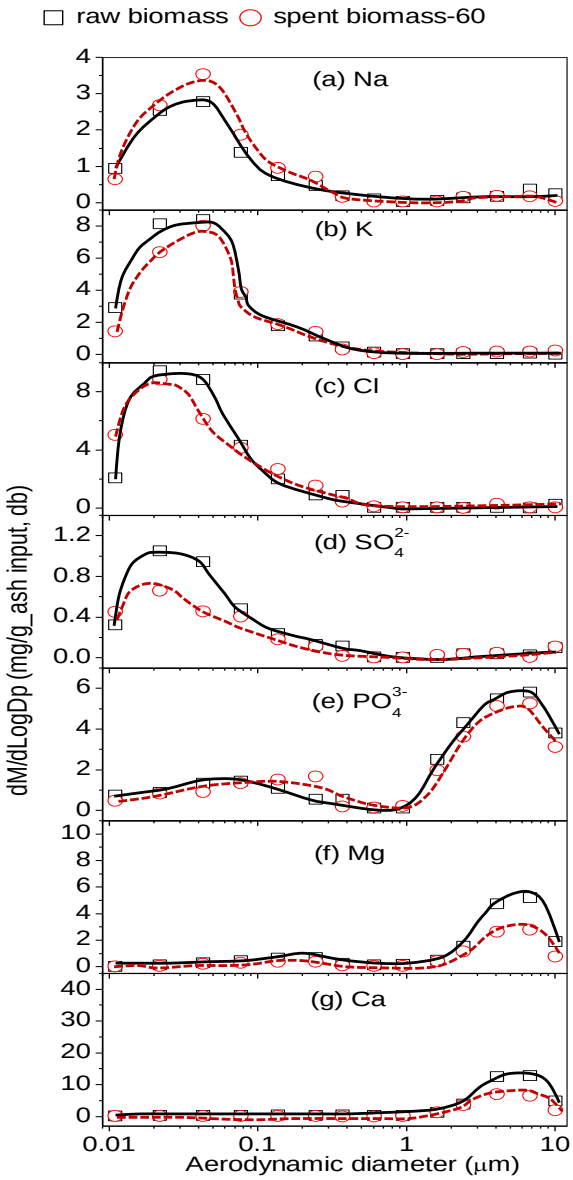

Figure 6- 3: Elemental mass size distributions of (a) Na, (b) K, (c) Cl, (d) SO_4^{2-}, (e) PO_4^{3-}, (f) Mg, and (g) Ca in PM_{10} from the combustion of the raw and spent biomass. Data are normalized to equivalent mass of ash input into the furnace, calculated from the dry mass of combustion feedstock input into the furnace and its ash content (wt %, dry basis).

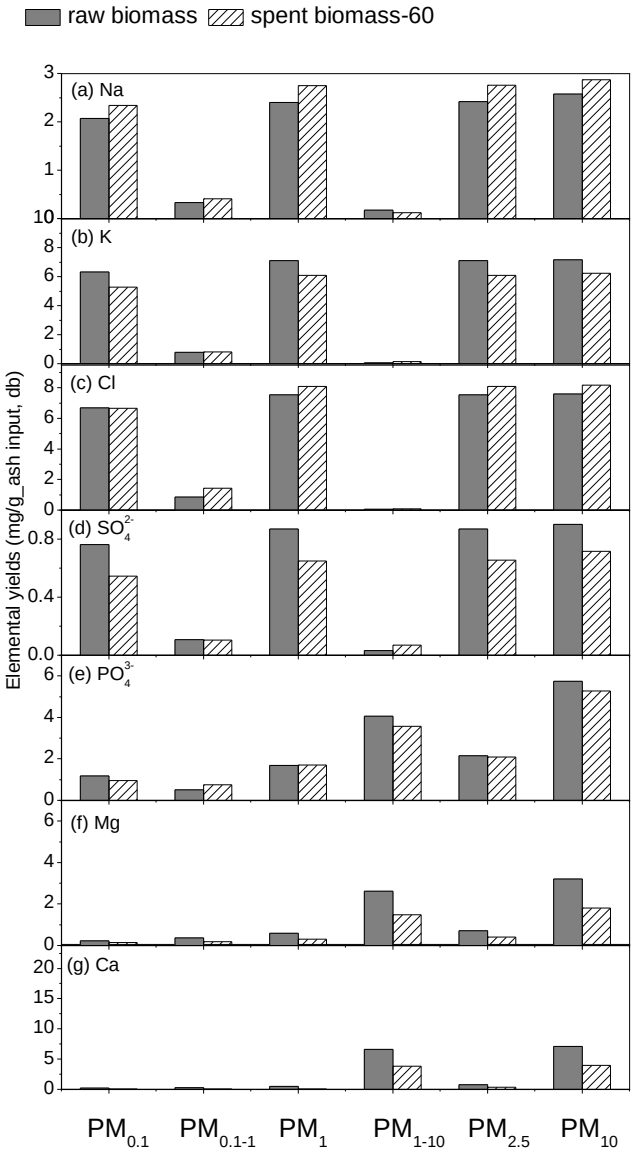

Figure 6- 4: Yields of (a) Na, (b) K, (c) Cl, (d) SO_4^{2-}, (e) PO_4^{3-}, (f) Mg, and (g) Ca in $PM_{0.1}$, $PM_{0.1-1}$, PM_1, PM_{1-10}, $PM_{2.5}$, and PM_{10} from the combustion of the raw and spent biomass. The yields are normalized to equivalent mass of ash input into the furnace, calculated from the dry mass of combustion feedstock input into the furnace and its ash content (wt %, dry basis).

Figure 6-3 shows the PSDs of Ca and Mg which peak at coarse mode of ~4.087-6.852 μm and ~6.852 μm, respectively. Thus, most of Ca (~82%) and Mg (~93-97%) are distributed in PM_{1-10}. The major occurrence of Ca and Mg in PM_{1-10} could be attributed to at least two possible mechanisms. The first mechanism is the catalysed sintering process[267]. The example for this process is the sintering of calcium oxides (CaO) from the decomposition of calcium carbonat ($CaCO_3$) in CO_2 atmosphere above 897ºC. The result of the sintering is large Ca-rich minerals. The second mechanism is the interactions between Ca or Mg with Al and Si minerals which leads to the formation of silicates and/or aluminosilicates. As discussed in section 6.2, there are high proportions of Ca and Mg in the form of water insoluble inorganics. The water insoluble components could present either as silicates or aluminosilicates which have low melting points. During the combustion, low melting point component could promote the char fragmentation resulting the formation of PM_{1-10}.

With regard to the distributions of Ca and Mg in PM_{10}, it should be noted the occurrence of both Ca and Mg in fine particle (PM_1) is not negligible. The distribution of fine particles Ca and Mg could be attributed to the presence of more volatile Ca and Mg and their subsequent oxides which will interact in the surface of fine particles and be released as PM_1. The formation of PM_1 containing Ca and Mg could be described via the following mechanisms: (1) formation of volatile Ca and Mg oxides during char combustion , (2) devolatilisation of Ca and Mg and their oxides, and (3) reduction of CaO and MgO in the char followed by vaporisation, oxidation and nucleation[268, 269].

Overall, from Figures 6-3 and 6-4, the combustion of spent leaf-60 leads to a lower yield of PM_{10} than the raw leaf due to the removal of some AAEM species and Cl during steam distillation.

6.5 Conclusions

This chapter discusses the characteristics of spent leaves from steam distillation process and the behaviour of PM_{10} during the combustion of the raw and spent leaves using a laboratory-scale DTF. The major conclusions are as follows:

1. Steam distillation has lowered the contents of AAEM (Na, K, Mg, and Ca) and Cl in its spent leaf. The retention of AAEM species are approximately 77-89% while that of Cl is ~68%. In both the raw and spent leaves, majorities of Na, K and K are water-soluble. However, the water solubility of Mg is less than 50% and that of Ca is <5%.

2. Both in feedstock-based yield and ash-based yield, the PSDs of PM_{10} from the raw and spent leaves exhibit a bimodal distribution ,with a fine mode (peak diameter: ~ 0.02 μm) and a coarse mode (peak diameter: ~4.09 μm), respectively. The combustion of the raw leaf results in a higher yield of PM_{10}, in comparison with that from the spent leaf-60.

3. The PSDs of Na, K, Cl and S show a single mode at ~0.043-0.22 μm. The yields of Na, K, Cl and SO_4^{2-} in PM_1 from both the raw leaf and the spent leaf-60 are ~93-95%, ~98-99%, ~99%, and ~90-96%, respectively.

4. The PSD of water soluble PO_4^{3-} exhibits a bimodal distribution, with a fine mode at ~0.077-0.246 μm and a coarse mode at ~4.087-6.852 μm. Overall, ~29-32% of PO_4^{3-} is distributed in PM_1 whereas the remaining is distributed in PM_{1-10}.

CHAPTER 7 EMISSION OF INORGANIC PM10 FROM THE COMBUSTION OF TORREFIED BIOMASS UNDER PULVERIZED-FUEL CONDITIONS

7.1 Introduction

As discussed in section 2.2 of chapter 2, mallee biomass is an important second-generation bioenergy feedstock in Australia because it can be produced at a low cost and a large scale and with low environmental burdens[1, 216]. Direct combustion of raw biomass as a fuel in stationary applications is however challenging because it is bulky and of high moisture content and has poor grindability[78, 270]. These shortcomings of raw biomass can be eliminated to a large extent via torrefaction that heats it at temperatures below 300 °C in the absence of air. Compared to raw biomass, torrefied biomass has higher energy density, reduced hydrophilicity and improved grindability[82, 271]. These advanced features make torrefied biomass particularly suitable for power generation via direct combustion and/or co-combustion with coal in pulverized-fuel boilers.

Combustion of solid fuels (e.g., biomass) in stationary applications leads to substantial emissions of fine inorganic particulate matter (PM) with an aerodynamic diameter <10 μm (PM_{10})[158, 161, 255], which adversely impacts both environment and human health[181]. While PM_{10} emission from raw biomass combustion has been extensively studied[158, 161, 209, 272], little work has thus far been conducted on that from torrefied biomass combustion under pulverized-fuel conditions[273]. In particular, how torrefaction affects the PM_{10} emission from torrefied biomass combustion remains unclear due to the lack of comparison study on both torrefied biomass and its corresponding raw biomass. Torrefaction process not only removes some chlorine (Cl) in raw biomass but also alters the occurrence forms of other key PM_{10}-forming elements

(e.g., Na, K, Mg and Ca)[203]. Therefore, the emission of PM_{10} from torrefied biomass combustion may be considerably different with that from raw biomass.

Consequently, this chapter aims to carry out a systematic investigation into the emission behaviour of inorganic PM_{10} from torrefied biomass combustion under pulverized-fuel conditions. A mallee leaves was torrefied at 220, 250 and 280 °C to prepare several torrefied biomass samples. The raw and torrefied biomass samples were then combusted at 1400 °C in air using a laboratory-scale drop-tube furnace (DTF). The produced inorganic PM_{10} was then collected and characterised to investigate its emission behaviour.

7.2 Yields and Properties of the Torrefied Biomass

The yields of residue solid (i.e., torrefied biomass) from the torrefaction of the raw biomass at 220, 250, and 280 °C are ~83, ~69, and ~63 wt%, respectively. The weight loss during biomass torrefaction is primarily due to the thermal decomposition of hemicellulose and lignin compounds of short chains[271] and to a lesser extent, the release of eucalyptus essential oil as discussed in Section 4-2. Table 7-1 shows basic fuel properties of the raw and torrefied biomass. Compared to those of the raw biomass, the contents of ash, fixed carbon and C in the torrefied biomass increase by ~31−55%, ~6−31% and ~9−21%, respectively, accompanied with reductions in the contents of volatile matter, H and O by ~2−8%, ~8−13% and ~12−31%, respectively. As a result, the lower heating values (LHV) of the torrefied biomass are ~4−12% higher than that of the raw biomass. Table 1 also indicates that, torrefaction leads to considerable increases in the contents of AAEM species but a substantial decrease in that of Cl in the torrefied biomass, in comparison with those of the raw biomass. The discrepancies in these fuel properties of the raw and torrefied biomass are intensified with increasing torrefaction temperature.

Table 7- 1: Properties of the raw and torrefied biomass

Samples	Raw biomass	Torrefied biomass produced at various temperatures (°C)		
		220	250	280
moisture (wt%, air-dried basis)	5.0	2.8	2.3	2.0
proximate analysis (wt%, dry basis)				
ash	4.2	5.5	6.3	6.5
volatile matter	77.8	75.5	70.8	69.9
fixed carbon	18.0	19.0	22.9	23.6
ultimate analysis (wt%, dry and ash-free basis)				
C	56.0	61.2	65.6	67.8
H	7.1	6.3	6.2	6.5
N	1.33	1.25	1.46	1.30
S	0.13	0.02	0.02	0.01
Cl	0.24	0.13	0.12	0.09
O (by difference)	35.2	31.1	26.6	24.3
LHV[a] (MJ/kg, air-dried basis)	19.6	20.4	21.4	22.0
contents of inorganic species (wt%, dry basis)				
Na	0.581	0.694	0.825	0.867
K	0.323	0.386	0.453	0.484
Mg	0.165	0.200	0.236	0.251
Ca	0.761	0.756	0.802	0.834
Si	0.060	0.075	0.099	0.107
Al	0.032	0.036	0.053	0.061
Fe	0.017	0.027	0.025	0.030
P	0.117	0.143	0.146	0.158

[a] Lower heating value, calculated on the basis of proximate and ultimate analysis via two steps. One is the estimation of higher heating value (HHV) based on the equation developed by Sheng et al.[241]. The other is to calculate LHV via equation: LHV=HHV–0.0245M–0.212H–0.0008O, where M, H, and O are the contents of moisture, hydrogen and oxygen, respectively.

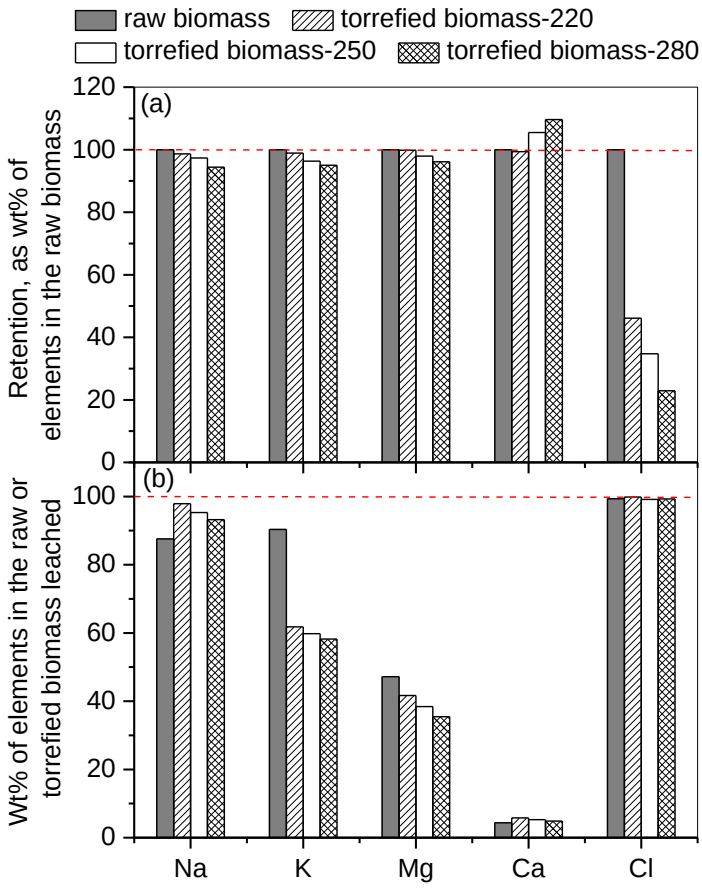

Figure 7-1: Retentions of Na, K, Mg, Ca and Cl in the torrefied biomass produced at 220, 250 and 280 °C (a) and water-leachable fractions of these elements in the raw and torrefied biomass (b).

Figure 7-1 presents the retention of AAEM species and Cl in the torrefied biomass. As expected, ~100% of AAEM species are retained in the torrefied biomass because of the relatively low temperatures (220−280 °C) employed. In contrast, the Cl release increases from ~54% at 220 °C to ~77% at 280 °C. Such substantial Cl release at low temperatures can be explained by at least two mechanisms. One is the release of methyl chloride (CH_3Cl)[188, 189]. The other is the interactions between chloride and biomass organic structure (e.g., cellulose), leading to the release of gaseous hydrogen chloride (HCl)[249]. The data show that biomass torrefaction clearly offers another advantage –

potentially mitigating Cl-related issues such as ash deposition[59], corrosion[274] and fine PM emissions[242]. Figure 7-1b further illustrates the mass fraction of AAEM species and Cl in the raw and torrefied biomass leached by water under batch condition. The majorities (~88−100%) of Na, K and Cl in the raw biomass can be leached out via water whereas the quantity of water-leachable Mg and Ca is relatively low, consistent with our previous study on mallee biomass leaching[205]. Most importantly, torrefaction leads to a considerable reduction in water-leachable fractions of K and Mg in the torrefied biomass, compared to those in the raw leaves. A similar phenomenon was also reported previously[203]. Apart from water-soluble inorganic species, water leaching under batch conditions also removes part of water-insoluble (but acid-soluble) inorganic species due to the acidic nature of the leachate[205]. However, the considerable discrepancies in the quantity of water-leachable K and Mg in the raw and torrefied biomass clearly indicate the changes in the occurrence forms of these elements during torrefaction. Such changes can be attributed to the transformations of the chemical forms of some AAEM species (exist as carboxylates[275]) during torrefaction[202]. As a result, the AAEM species that are originally associated with these functional groups may form new bonds in the torrefied biomass. Overall, torrefaction not only removes considerable amount of Cl but also alters the occurrence forms of AAEM species (particularly K and Mg) in the raw biomass, indicating possible discrepancies in the emission of inorganic PM_{10} from the combustion of the raw and torrefied biomass.

7.3 Particle Size Distributions (PSDs) and Yields of PM_{10} and Key Inorganic Elements in PM_{10}

Figures 7-2a and 7-2b present the PSDs and yields of the inorganic PM_{10} produced from the combustion of the raw and torrefied biomass samples, respectively, normalized to unit mass (dry basis) of the feedstock input into the DTF. Clearly, the PSDs of PM_{10} all follow a bimodal distribution: a fine mode at ~0.02 μm and a coarse mode at ~4.09 μm. As a result, ~21−49% and ~51−79% of PM_{10} end up in PM_1 and PM_{1-10}, respectively.

The yields of PM with aerodynamic diameters of <0.1 μm ($PM_{0.1}$), 0.1−1 μm ($PM_{0.1-1}$), <1 μm (PM_1) and <2.5 μm ($PM_{2.5}$) from the combustion of the raw and torrefied biomass are similar. On the contrary, the torrefied biomass combustion results in substantial increase in the yields of PM_{1-10} (i.e., PM with an aerodynamic diameter of 1−10 μm) and PM_{10}, in comparison with those from the raw biomass combustion. Increasing torrefaction temperature from 220 to 280 °C intensifies this trend. Such discrepancies in the emission behaviour of PM_{10} from the raw and torrefied biomass can be attributed to two reasons. One is the dissimilarity in the ash contents, as shown in Table 7-1. The other is that the ability of ash-forming elements in producing PM_{10} may be different. To eliminate the former's impacts on PM_{10} emission, the PSDs and yields of PM_{10} are normalized to the unit mass (dry basis) of ash input into the DTF (see Figures 6-2c and 6-2d). Indeed, the PM_{10}-forming ability of inorganic species in the raw and torrefied biomass is considerably different. While the ash-based yield of $PM_{0.1-1}$ remains unchanged, the combustion of the torrefied biomass leads to a considerable reduction in that of $PM_{0.1}$ (and thereby PM_1), compared to that of the raw biomass. Such reduction is generally intensified with increasing torrefaction temperature. A similar trend is also observed for $PM_{2.5.}$ Oppositely, the ash-based yields of PM_{1-10} and thereby PM_{10} from the torrefied biomass are substantially higher than those from the raw biomass, consistent with that observed for its counterpart on the basis of combustion feedstock. This implies that torrefaction has led to the alteration of fuel structure and thereby the changed PM_{1-10}-forming ability of the inorganic species in the torrefied biomass.

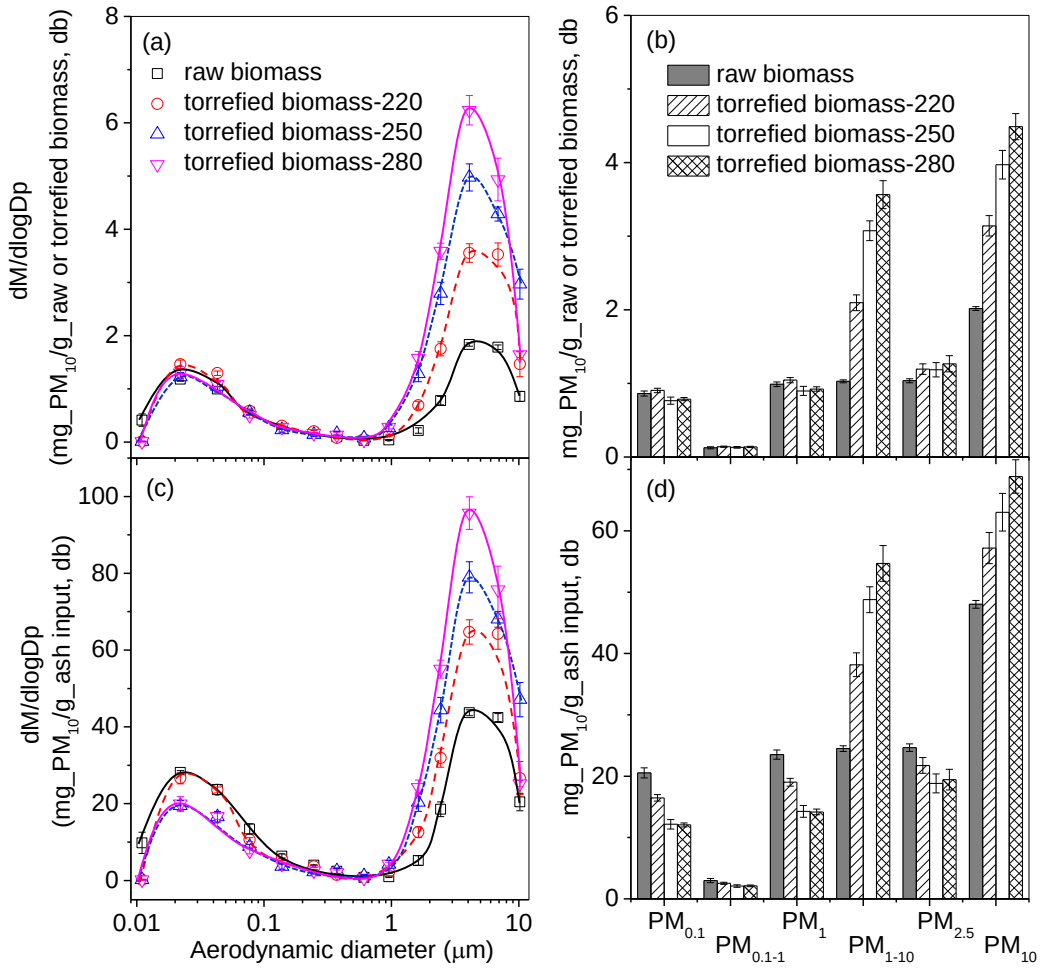

Figure 7-2: Mass-based particle size distributions of PM_{10} (a and c) and yields of $PM_{0.1}$, $PM_{0.1\text{-}1}$, PM_{1}, $PM_{1\text{-}10}$, $PM_{2.5}$ and PM_{10} (b and d) from the combustion of the raw and torrefied biomass. Panels a-b are normalized to unit mass of the raw or torrefied biomass input into the furnace, on a dry basis. Panels c-d are normalized to equivalent mass of ash input into the furnace. PM_{xx} and $PM_{yy\text{-}zz}$ mean particulate matter (PM) with aerodynamic diameters of <xx and yy-zz μm, respectively.

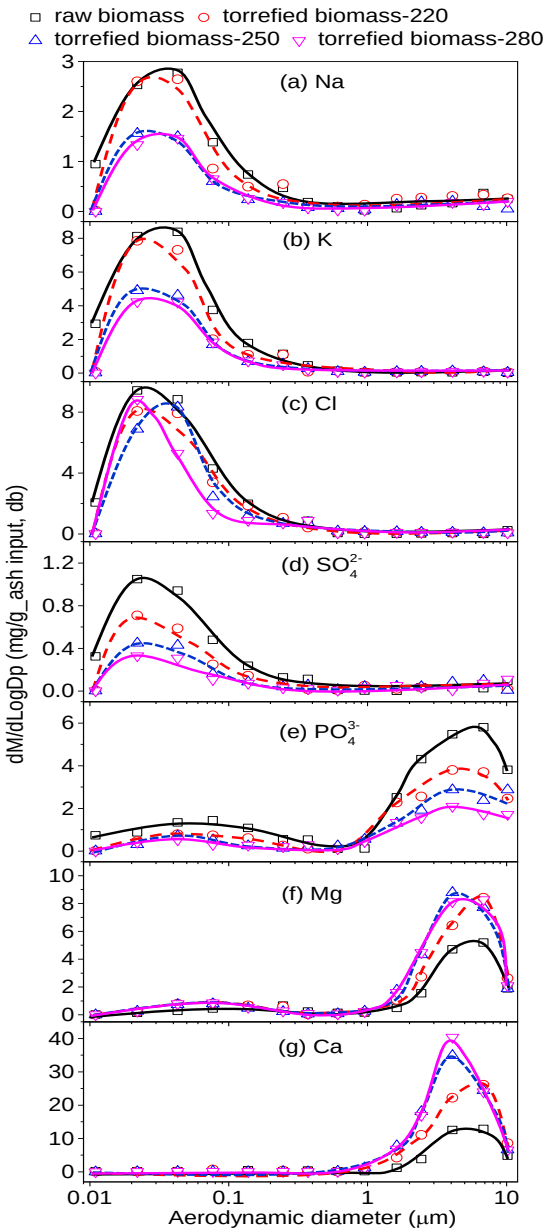

Figure 7-3: Elemental mass size distributions of (a) Na, (b) K, (c) Cl, (d) SO_4^{2-}, (e) PO_4^{3-}, (f) Mg and (g) Ca in (PM_{10}) from the combustion of the raw and torrefied biomass. Data are normalized to equivalent mass of ash input into the furnace, calculated from the dry mass of combustion feedstock input into the furnace and its ash content (wt%, db).

To further understand the differences in the emission behaviour of PM_{10} from the raw and torrefied biomass, efforts were then taken to investigate the transformation of key PM_{10}-forming elements, including Na, K, Cl, S, P (as water-soluble PO_4^{3-}), Mg and Ca, and their distribution in the PM_{10}. The mass-based PSDs of these elements and their yields in $PM_{10,}$ on the basis of equivalent ash input into the DTF, are illustrated in Figures 7-3 and 7-4, respectively, which lead to four important observations.

First, the PSDs of volatile elements, including Na, K, Cl and S, all demonstrate a unimodal distribution, with a mode diameter of ~0.02−0.04 μm (see Figures 7-3a - 3d). It is well-established that these volatile elements are easily released during both devolatilisation[176] and char combustion[257], followed by a series of gas phase reactions, homogeneous nucleation and/or heterogeneous condensation/reaction of the Na-, K-, Cl- and S-containing vapours on the surface of existing fine particles[176, 258]. As a result, ~87−93% of Na, ~97−99% of K and Cl, and ~82−97% of S in PM_{10} are distributed in PM_1 (see Figures 7-4a-4d).

Second, water-soluble PO_4^{3-} exhibits a bimodal distribution: a fine mode at ~0.04−0.08 μm and a coarse mode at ~4.09−6.85 μm (see Figure 3e). Consequently, ~21−29% of total water-soluble PO_4^{3-} in PM_{10} is distributed in PM_1 whereas the remaining ends up in $PM_{1\text{-}10}$ (see Figure 7-4e). Water-soluble PO_4^{3-} in PM is of particular importance because it is responsible for undesired eutrophication problems once the PM terminates in water[276]. The presence of water soluble PO_4^{3-} in PM_1, which was also reported in a previous study on biomass combustion[266], clearly indicates that some P in the raw and torrefied biomass has gone through gaseous phase during combustion. On the other hand, water-soluble PO_4^{3-} in $PM_{1\text{-}10}$ is attributed to the partial dissolution of magnesium phosphate [$Mg_3(PO_4)_2$] and calcium phosphate [$Ca_3(PO_4)_2$]. This can be deduced as follows. According to the solubility of the two phosphates at room temperature, up to ~0.02 mg PO_4^{3-} [in form of $Mg_3(PO_4)_2$] and ~0.12 mg PO_4^{3-} [in form of $Ca_3(PO_4)_2$] can be dissolved in 10 ml water. During PM leaching, a maximum of ~0.05 mg PO_4^{3-} is dissolved in 10 ml water, which is in the range of ~0.02−0.12. In addition, as illustrated

in Figure 7a, water-insoluble P in PM1-10 is up to ~7.8 times greater than that in form of PO_4^{3-} dissolved in water. This suggests the co-existence of both $Mg_3(PO_4)_2$ and $Ca_3(PO_4)_2$ in PM_{1-10} and their partial dissolution during water leaching.

Third, refractory Mg and Ca behave similarly and are concentrated in PM_{1-10} during the combustion of the raw and torrefied biomass. As shown in Figures 7-3f - 3g and 7-4f - 4g, both Mg and Ca show a major peak at ~4.09−6.85 μm, leading to their preferable partition in PM_{1-10} (i.e., ~82−88% and ~93−99% of total Mg and Ca in PM_{10} end up in PM_{1-10}, respectively). At least two mechanisms are responsible for the dominant distribution of Mg and Ca in PM_{1-10}. One is the so-called catalysed sintering process[267]. For example, under CO_2 atmosphere, meta-stable calcium carbonate ($CaCO_3$) will be repeatedly formed and decomposed at temperatures above 897 °C, leading to the sintering of pure calcium oxide (CaO) particles and thereby the formation of large Ca-rich particles after char is burnt out[267].

The other mechanism is the interactions between Mg (or Ca) and minerals containing Si and Al[199] leading to the formation of silicates and/or aluminosilicates and their subsequent coalescence on the surface of the burning char particle. The coalescence of these products may also result in the retention of Mg- and Ca-phosphates nearby in PM_{1-10}. Indeed, as illustrated in Figure 5b-5c, both water-soluble and water-insoluble Mg and Ca are present in PM_{1-10}. The water-soluble fractions may include the oxides of Mg and Ca and their partially-dissolved phosphates. The water-insoluble fractions, together with Al and Si (see Figures 5d-5e) as well as water-insoluble P (see Figure 5a) observed in PM_{1-10}, indicate the presence of silicates and/or aluminosilicates as well as undissolved phosphates.

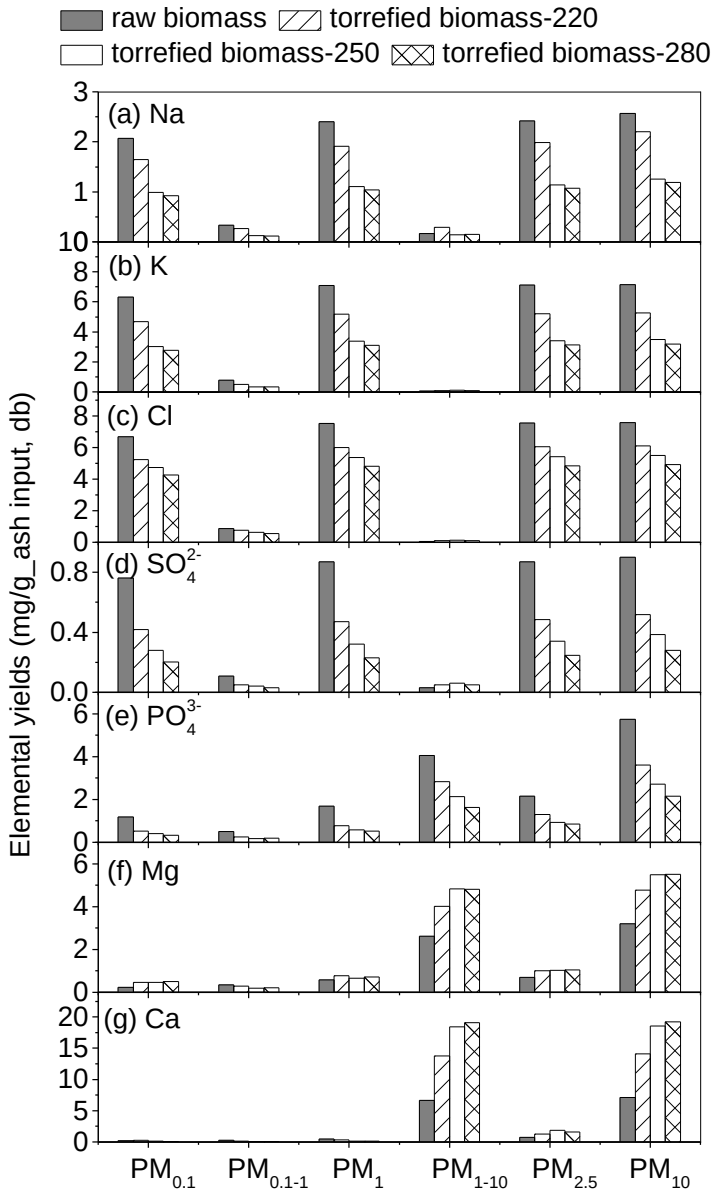

Figure 7-4: Yields of (a) Na, (b) K, (c) Cl, (d) SO_4^{2-}, (e) PO_4^{3-}, (f) Mg and (g) Ca in $PM_{0.1}$, $PM_{0.1-1}$, PM_1, PM_{1-10}, $PM_{2.5}$ and PM_{10} from the combustion of the raw and torrefied biomass. The yields are normalized to equivalent mass of ash input into the furnace, calculated from the dry mass of combustion feedstock input into the furnace and its ash content (wt%, db).

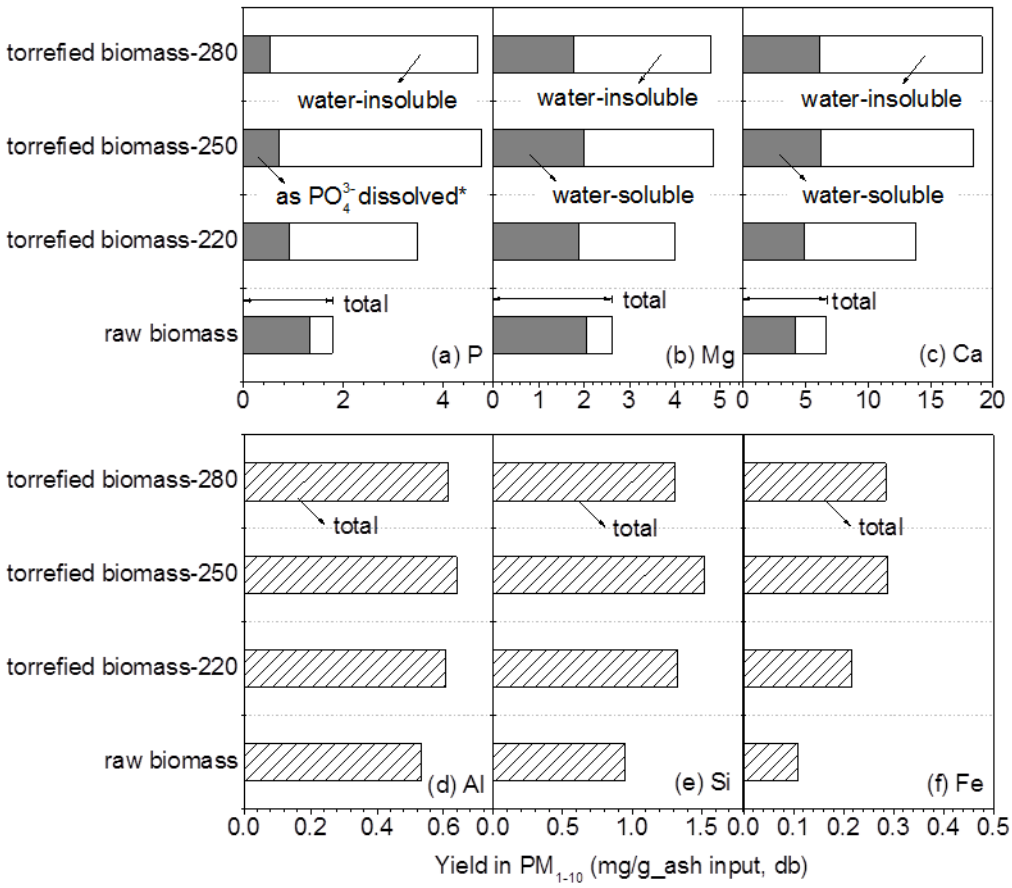

Figure 7-5: Ash-based yields of (a) P, (b) Mg, (c) Ca, (d) Al, (e) Si and (f) Fe in PM_{1-10} from the combustion of the raw and torrefied biomass. *The gray bars in panel a represent P in form of PO_4^{3-} dissolved in water.

For both mechanisms, the partition of Mg and Ca in PM_{1-10} is substantially influenced by the proximity among ash-forming species in the parent fuels. A higher ash content in the fuel indicates higher proximity so that the catalysed sintering process and/or the interactions with other Si- and Al-containing minerals are more severe and consequently more Mg and Ca being retained in PM_{1-10}. For instance, our recent work[277] demonstrated that, during the combustion of a Victorian brown coal, ~73% and ~85% of total Mg and Ca in PM_{10} are distributed in PM_{1-10}, respectively, which are considerably lower than those observed in this study, predominantly due to the substantially lower ash

content (~0.9 wt%, dry basis) of the Victorian brown coal[277] in comparison to those of the raw and torrefied biomass (see Table 7-1).

Fourth and last, the quantities of Mg and Ca distributed in PM_1 are small but observable. As illustrated in Figures 7-4f - 4g, Mg in PM_1 accounts for ~12−18% of that in PM_{10} and, similarly, ~1−7% of total Ca in PM_{10} is present in PM_1. The partition of the two elements in PM_1 can be explained via three known mechanisms: (i) the release of fine-disbursed fume oxides of Mg and Ca during char combustion[277]; (ii) the release of Mg and Ca during devolatilisation and their subsequent oxidation[242]; and (iii) in-char reduction of MgO (or CaO) followed by vaporisation, oxidation and homogeneous nucleation[268].

7.4 Further Discussion and Practical Implications

Considering the data presented in the last two Sections, possible mechanisms responsible for the discrepancies in the ash-based yields of $PM_{0.1}$ and PM_{1-10} from the combustion of the raw and torrefied biomass samples (see Figure 7-2d) can be deduced. For $PM_{0.1}$, it is dominantly composed of Na, K, Cl, and to a lesser extent, P and S (see Figures 7-3a - 3e and 7-4a - 4e). A close examination suggests that the molar ratios of (Na+K)/(Cl+2S+3P) in the $PM_{0.1}$ is ~0.8−1.1 (close to 1.0), confirming the dominance of alkali (Na and K) chlorides and the presence of their phosphates and sulfates. Further efforts were then taken to correlate the contents of Na, K and Cl in the raw and torrefied biomass samples and the yields of $PM_{0.1}$ from their combustion, with the results presented in Figure 7-6. Clearly, the yields of $PM_{0.1}$ are largely independent of the contents of Na and K whereas a fairly linear relationship is observed for the correlation between $PM_{0.1}$ yields and Cl content in the parent fuels. In fact, the presence of Cl results in the formation of alkali chlorides that are stable under combustion conditions[59]. The formed alkali chlorides will further experience homogeneous nucleation and/or heterogeneous condensation/reaction on the surface of existing fine particles[176, 269, 278] and thereby effectively contribute to $PM_{0.1}$ emission. In the

absence of Cl, at least part of the Na and K vapours are expected to inevitably react with the inner wall of the reaction tube during combustion, leading to the reduction of their yields in $PM_{0.1}$. Therefore, compared to those from the raw biomass combustion, the reduction in the yields of $PM_{0.1}$ as well as Na, K and Cl in $PM_{0.1}$ from the torrefied biomass combustion is mainly due to the considerable release of Cl (up to ~77%) in the raw biomass during torrefaction, despite of the ~100% retentions of Na and K (see Figure 7-1).

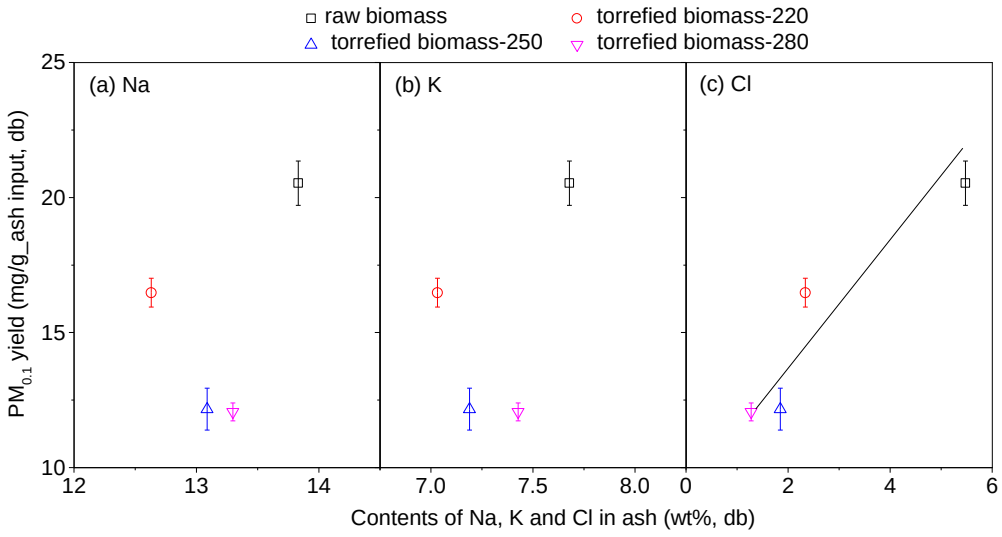

Figure 7-6: Correlation between the contents of (a) Na, (b) K and (c) Cl in the raw and torrefied biomass and the yields of $PM_{0.1}$ from their combustion.

As shown in Figures 7-2d, 7-4f - 4g and 7-5a-5c, the ash-based yields of PM_{1-10} as well as Mg, Ca and P in PM_{1-10} from the torrefied biomass are much higher than those from the raw biomass. Such trend is continuously intensified with increasing torrefaction temperature from 220 to 280 °C. The yields of Si, Al and Fe in PM_{1-10} generally follow a similar trend but are considerably lower than those of Mg, Ca and P (see Figure 5). It is well-established that inherent inorganic species coalescence and char fragmentation

are two principle mechanisms governing PM_{1-10} emission during solid fuel (e.g., coal and/or biomass) combustion[176, 269, 278]. The former suppresses whereas the latter promotes PM_{1-10} emission. In comparison with those from the raw biomass combustion, the increased ash-based yields of both PM_{1-10} and its key forming elements (Mg, Ca and P) from the torrefied biomass combustion are most likely due to the intensified char fragmentation as shown in our recent study on biochar combustion[176]. In addition, as presented in Figure 7-5, the increase in the yields of Mg and Ca in PM_{1-10} is mainly due to the increase in their water-insoluble fractions, most likely in the forms of silicates and/or aluminosilicates that are of low melting points, as well as undissolved phosphates. This further suggests that char fragmentation was enhanced during the combustion of the torrefied biomass, otherwise such water-insoluble Mg and Ca would have further experienced coalescence to form particles larger than 10 μm after the char is burnt out.

From a practical viewpoint, it is important to assess the yields of inorganic PM_{10} per unit of useful energy (i.e., LHV) input into the furnace. Such energy-based data are presented in Figure 7-7, benchmarking against those from two other typical solid fuels used in Australia (a Victorian brown coal and a Collie sub-bituminous coal), under the same combustion conditions. The effect of torrefaction on the energy-based PM emission is dependent on both the size of the PM and torrefaction temperature. For example, while the yields of $PM_{0.1-1}$ and $PM_{2.5}$ remain unchanged, there are significant differences in the yields of $PM_{0.1}$, PM_1, PM_{1-10} and PM_{10} from the combustion of the raw and torrefied biomass samples. The yields of $PM_{0.1}$ (and thereby PM_1) from the torrefied biomass−220 are similar to those from the raw biomass but are ~21−23% higher than those from the torrefied biomass prepared at 250 and 280 °C. The results suggest that to achieve a considerable reduction in the emissions of $PM_{0.1}$ and PM_1, a minimum torrefaction temperature of 250 °C would be required. Such reduction is a result of the trade-off between the increase in the LHV and ash content and the decrease in the Cl content of the torrefied biomass, in comparison with those of the raw biomass. In contrast, the combustion of the torrefied biomass leads to an increase in the yields of

PM_{1-10} by a factor of ~1−2 and such an increase is continuously enhanced with increasing torrefaction temperature. This is not surprised given the increase in their ash-loading levels (i.e., g of ash per MJ of LHV embedded in the fuels) and the possibly intensified char fragmentation during the combustion of the torrefied biomass. Indeed, a close relationship is observed between the ash loading levels of the parent fuels and the energy-based yields of PM_{1-10} from their combustion, as illustrated in Figure 7-8. The results also suggest that while torrefaction improves fuel properties of the torrefied biomass, the combustion of the torrefied biomass produces higher energy-based PM_{1-10} yield than that of the raw biomass.

Benchmarking the energy-based PM yields (see Figure 7-7) from the raw and torrefied biomass with those from the Victorian brown coal and the Collie coal leads to several important findings. First, the yields of $PM_{0.1}$ from the raw and torrefied biomass are considerably higher than those from the two coals because of the higher contents of Na, K and, in particular, Cl in the biomass samples (see Table 7-1). Second, the yield of $PM_{0.1-1}$ from the Victorian brown coal is the highest, in comparison with that from other fuels. The ash loading level of the Victorian brown coal is ~0.4 g_ash/MJ_LHV[277], substantially lower than those from the raw and torrefied biomass (see Figure 6-8). Therefore, the highest yield of $PM_{0.1-1}$ from the Victorian brown coal is most likely because the abundant of organically-bound Mg, Ca and Fe in the coal[277]. As a result, the yields of PM_1 from the raw and torrefied biomass are comparable with that from the Victorian brown coal but considerably higher than that from the Collie coal. Third, compared to that of other fuels, the combustion of the Collie coal produces the highest yield of PM_{1-10}. The ash loading level of the collie coal is ~2.1 g_ash/MJ_LHV[208], considerably lower than that of the torrefied biomass. Thus, the highest yield of PM_{1-10} from the collie coal can be attributed to the abundant fine included mineral particles smaller than 10 μm in the coal[208]. Fourth, the combustion of the raw and torrefied biomass as well as the Collie coal yields similar amount of $PM_{2.5}$, which are markedly lower than that from the Victorian brown coal. Fifth and last, the yields of PM_{10} from

the torrefied biomass are ~36−51% lower than that from the Collie coal. The torrefied biomass shows better performance than the Collie coal in terms of reducing PM_{10} emission.

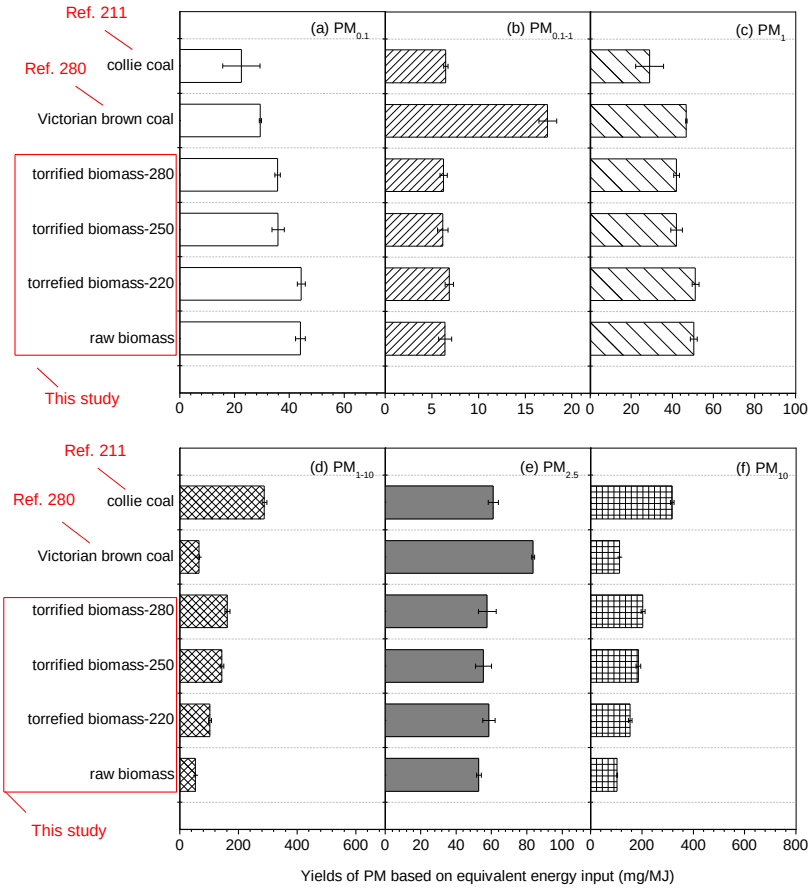

Figure 7-7: Yields of (a) $PM_{0.1}$, (b) $PM_{0.1-1}$, (c) PM_1, (d) PM_{1-10}, (e) $PM_{2.5}$ and (f) PM_{10} from the combustion of the raw and torrefied biomass, benchmarking against those from the combustion of a Victorian brown coal and a Collie coal. Data are normalized to unit lower heating value (LHV) input into the furnace.

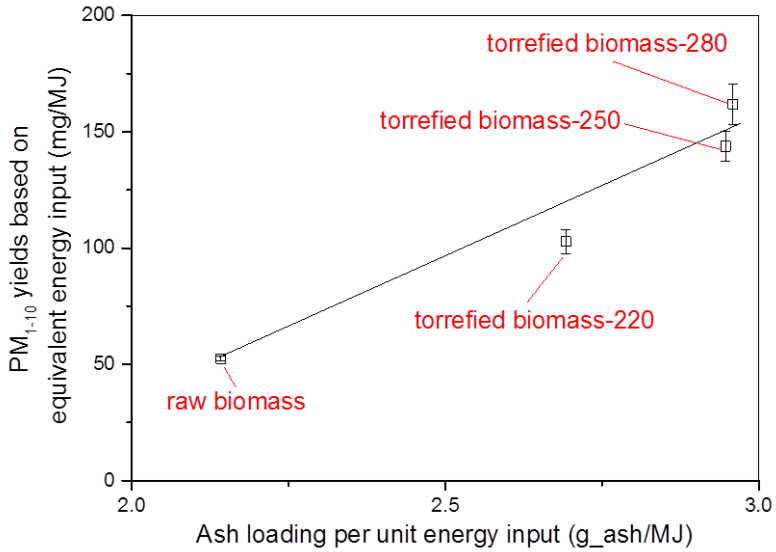

Figure 7-8: Correlation between ash loading levels of the raw and torrefied biomass and the energy-based yields of PM_{1-10} from their combustion

7.5 Conclusions

The torrefaction at 220−280 °C removes ~54−77% of Cl in the raw biomass and changes the occurrence forms of the AAEM species in the torrefied biomass. As a result, these ash-forming species in the raw and torrefied biomass demonstrate different ability in producing inorganic PM_{10} during combustion. Specifically, the ash-based yields of $PM_{0.1}$ as well as Na, K and Cl in $PM_{0.1}$ from the torrefied biomass combustion are considerably lower than those from the raw biomass. This can be attributed to the release/loss of Cl in the raw biomass during torrefaction. On the other hand, compared to that of the raw biomass, the combustion of the torrefied biomass leads to substantial increases in the ash-based yields of PM_{1-10} as well as Mg and Ca in PM_{1-10}, most likely due to intensified char fragmentation. Practically, in comparison with the raw biomass, the torrefied biomass combustion results in little changes in the energy-based yields of $PM_{2.5}$ but considerable increases in those of PM_{10}.

CHAPTER 8 CONCLUSIONS AND RECOMMENDATIONS

8.1 Introduction

The main findings of the present study are summarised in this chapter. This study has gained fundamental knowledge on extraction of essential oil behaviour and its effects on properties of spent biomass as a fuel. This research also has obtained important knowledge on formation of particulate matter during combustion of treated biomass including spent biomass and its chars produced via pyrolysis, and torrefied biomass. 1,8-cineole component can be completely extracted from mallee leaves using steam distillation technique which can be an innovative strategy to improve efficiency of conventional steam distillation. A novel understanding on mallee leaves pre-treatment via torrefaction and pyrolysis of spent leaves has also been an achievement in this research. It offers an opportunity to address a strategy in the wide adoption of the efficient and effective biomass utilisation for power generation. This research has also obtained crucial knowledge on nutrients recycle in solid fuels by water leaching which may contribute on optimising nutrients sources in soil for plants growth and more importantly can minimize problems related to ash deposits in biomass power generation. Fundamental insights on the emission of inorganic PM during the combustion spent and torrefied biomass has also been revealed in this study. Some recommendations are also provided for future study in this area.

8.2 Conclusions

8.2.1 Steam Distillation of Mallee Leaves: Extraction of 1,8-Cineole and Changes in Fuel Properties of Spent Biomass

- The extraction of 1,8-cineole from the mallee leaf is fast within the first 15 min, becomes slow afterward and is almost completed after steam distillation for 60 min.

- The fast step is likely regulated by the rate of latent heat for the evaporation of 1,8-cineole and thereby follows zero-order kinetics under the experimental conditions.

- The slow step appears to be governed by the internal diffusion of residual 1,8-cineole in the leaf, following first-order kinetics.

- Steam distillation has little effect on the proximate and ultimate analyses as well as mass energy density of the spent leaf.

- Steam distillation removes a considerable amount of total organic carbon from leaves and leads to substantial reductions in the concentrations of Mg, Ca, and Cl in the spent leaf.

- Water leaching of AAEM species and Cl in the raw leaves and the spent leaf−60 follows first-order kinetics whereas the leaching profile of C exhibits two different first-order rates.

- The leaching equilibrium values and the leaching rates of AAEM species in the spent leaf−60 are considerably lower than those of the raw leaf.

- Cl in both the raw leaf and the spent leaf−60 is completely water-soluble, the leaching rate of which in the spent leaf−60 is considerably higher than that of the raw leaves.

- The fast leaching step of C in the spent leaf−60 is identical to that of C in the raw leaves whereas the leaching rate of C in the slow step for the spent leaves−60 is higher.

- The overall removals of Mg, Ca, and C after steam distillation for 60 min followed by water leaching are considerably higher than those of water leaching only, indicating the changes in the occurrence forms of Mg, Ca, and the organic structure in the leaves during steam distillation.

8.2.2 Pyrolysis of Spent Biomass from Mallee Leaves Steam Distillation: Biochar Properties and Recycling of Inherent Inorganic Nutrients

- Under identical pyrolysis conditions, whereas the effects of the feedstock on the yields, proximate analysis, and elemental analysis of the biochars are negligible.
- The contents of Na, K, Mg, Ca and Cl in the biochars from the raw leaves are generally higher than those in the biochars from the spent leaves.
- The feedstock has little effects on the retentions of these inorganic species except for Ca in all the biochars and Cl in the fast pyrolysis biochars.
- The quantities of water-leachable Na, K, and Cl in the biochars from the mallee leaves are considerably higher than those in the biochars from the spent leaves whereas those of Mg in the slow pyrolysis biochars follow an opposite trend.
- Regardless of the feedstock, increasing pyrolysis temperature from 400 to 500 or 600 °C leads to considerable decreases in the overall recycling rates of Na and Mg in all the biochars as well as those of K and C in the fast pyrolysis biochars.
- The fast pyrolysis of the spent leaves−60 at 500 °C seems to be suitable to simultaneously produce 1,8-cineole, bio-oil, and biochar.
- The biochar has favourable properties for returning its inherent inorganic nutrients to soil.

8.2.3 Inorganic PM_{10} Emission from The Combustion of Spent Leaf after Steam distillation.

- Steam distillation has lowered the contents of AAEM (Na, K, Mg, and Ca) and Cl in its spent leaf. The retention of AAEM species is approximately 77-89% while that of Cl is ~68%. In both the raw and spent leaves, majorities of Na, K and K are water-soluble. However, the water solubility of Mg is less than 50% and that of Ca is <5%.

- Both in feedstock-based yield and ash-based yield, the PSDs of PM_{10} from the raw and spent leaves exhibit a bimodal distribution ,with a fine mode (peak diameter: ~ 0.02 μm) and a coarse mode (peak diameter: ~4.09 μm), respectively. The combustion of the raw leaf results in a higher yield of PM_{10}, in comparison with that from the spent leaf-60.

- The PSDs of Na, K, Cl and S show a single mode at ~0.043-0.22 μm. The yields of Na, K, Cl and SO_4^{2-} in PM_1 from both the raw leaf and the spent leaf-60 are ~93-95%, ~98-99%, ~99%, and ~90-96%, respectively.

- The PSD of water soluble PO_4^{3-} exhibits a bimodal distribution, with a fine mode at ~0.077-0.246 μm and a coarse mode at ~4.087-6.852 μm. Overall, ~29-32% of PO_4^{3-} is distributed in PM_1 whereas the remaining is distributed in PM_{1-10}.

8.2.4 Emission of Inorganic PM_{10} from the Combustion of Torrefied Biomass under Pulverized-Fuel Conditions

- The torrefaction at 220−280 °C removes ~54−77% of Cl in the raw biomass and changes the occurrence forms of the AAEM species in the torrefied biomass.

- The ash-forming species in the raw and torrefied biomass demonstrate different ability in producing inorganic PM10 during combustion. Specifically, the ash-based yields of $PM_{0.1}$ as well as Na, K and Cl in $PM_{0.1}$ from the torrefied biomass combustion are considerably lower than those from the raw biomass. This can be attributed to the release/loss of Cl in the raw biomass during torrefaction.

- Compared to that of the raw biomass, the combustion of the torrefied biomass leads to substantial increases in the ash-based yields of PM_{1-10} as well as Mg and Ca in PM_{1-10}, most likely due to intensified char fragmentation.

- In comparison with the raw biomass, the torrefied biomass combustion results in little changes in the energy-based yields of $PM_{2.5}$ but considerable increases in those of PM_{10}.

8.3 Recommendations

Based on the experiment results obtained in this PhD study, several recommendations that require further investigation are outlined as below:

- The effects of steam flow rate on essential oil extraction and spent leaf properties are required since this variable has an important role in the extraction characteristic during steam distillation. In this research, the steam flow was only maintained at maximum 1.3 kg/min/m^2 due to the limitation of the experimental system. It is recommended to carry out several experiments at various steam flows to identify the optimum condition.

- The effect of steam distillation on spent leaves' grindability is also another interesting aspect in this research area because steam distillation disrupts oil gland which may improve the grindability of the spent leaves in comparison to the raw leaves.

- The grindability of char produced from spent leaves pyrolysis at low temperature is also an important aspect in biomass pre-treatment in comparison to those prepared from raw leaves and spent leaves.

- The study of reactivity of chars produce from spent leaves and torrefied biomas is also another important future research in order to provide insight into the influence of char chemical make-up on rates of oxidation.

REFERENCES

1. Wu, H., et al., *Production of Mallee Biomass in Western Australia: Energy Balance Analysis†.* Energy & Fuels, 2007. **22**(1): p. 190-198.
2. Bartle, J., et al., *Acacia species as large-scale crop plants in the Western Australian wheatbelt.* ConserV. Sci. West., 2002. **2**: p. 96-108.
3. Yu, Y., et al., *Mallee Biomass as a Key Bioenergy Source in Western Australia: Importance of Biomass Supply Chain.* Energy & Fuels, 2009. **23**(6): p. 3290-3299.
4. Boland, D.J., J.J. Brophy, and A.P.N. House, *Eucalyptus leaf oils: use, chemistry, distillation and marketing.* Journal of Chromatography A, 1992. **598**(2): p. 316.
5. E Soh, M. and S. G W, *The Application of Cineole as a grease solvent.* Flavour Frag. J., 2002. **17**: p. 278-286.
6. F Leit, B.A., et al., *Production of p-cymene and hydrogen froma bio-renewable feedstock_1,8-cineole (eucalyptus oil).* Green Chem. , 2010: p. 70-76.
7. Wu, H., et al., *Effect of Hydrodistillation on 1,8-Cineole Extraction from Mallee Leaf and the Fuel Properties of Spent Biomass.* Industrial & Engineering Chemistry Research, 2011.
8. Wannapeera, J., B. Fungtammasan, and N. Worasuwannarak, *Effects of temperature and holding time during torrefaction on the pyrolysis behaviors of woody biomass.* Journal of analytical and applied pyrolysis, 2011. **92**(1): p. 99-105.
9. Arias, B., et al., *Influence of torrefaction on the grindability and reactivity of woody biomass.* Fuel Processing Technology, 2008. **89**(2): p. 169-175.
10. Bridgeman, T.G., et al., *An investigation of the grindability of two torrefied energy crops.* Fuel, 2010. **89**(12): p. 3911-3918.
11. L I N D, E., et al., *Volatilization of the Heavy Metals during Circulating Fluidized Bed Combustion of Forest Residue.* Environ. Sci. Technol., 1999. **33**: p. 496-502.
12. Maynard, A.D. and R.L. Maynard, *A derived association between ambient aerosol surface area and excess mortality using historic time series data.* Atmospheric Environment, 2002. **36**(36–37): p. 5561-5567.
13. Harper, R.J. and R.J. Gilkes, *Aeolian influences on the soils and landforms of the southern Yilgarn Craton of semi-arid, southwestern Australia.* Geomorphology, 2004. **59**(1–4): p. 215-235.
14. Peck, A.J. and T. Hatton, *Salinity and the discharge of salts from catchments in Australia.* Journal of Hydrology, 2003. **272**(1–4): p. 191-202.
15. Lambers, H., *Introduction, Dryland Salinity: A Key Environmental Issue in Southern Australia.* Plant and Soil, 2003. **257**(2): p. 5-7.
16. Hatton, T.J., J. Ruprecht, and R.J. George, *Preclearing hydrology of the Western Australia wheatbelt: Target for the future.* Plant and Soil, 2003. **257**(2): p. 341-356.
17. Liew, J.J., *Carbon sequestration of Eucalyptus polybractea and D2 as an indicator of below ground biomass.*, in *School of Environmental Systems Engineering*. 2009, The University of Western Australia: Perth.

18. McMahon, L., B. George, and R. Hean. *Eucalyptus polybractea*. 2010; Available from: https://www.google.com.au/search?sourceid=navclient&ie=UTF-8&rlz=1T4ADFA_enAU477AU477&q=plantation+of+Eucalyptus+polybractea+in+western+australia.
19. Clarke, C.J., et al., *Dryland salinity in south-western Australia: its origins, remedies, and future research directions.* Soil Research, 2002. **40**(1): p. 93-113.
20. Bartle, J., et al., *Scale of biomass production from new woody crops for salinity control in dryland agriculture in Australia.* Int. J. Global Energy, 2007. **27**: p. 115–137.
21. Sochacki, S.J., R.J. Harper, and K.R.J. Smettem, *Estimation of woody biomass production from a short-rotation bio-energy system in semi-arid Australia.* Biomass and Bioenergy, 2007. **31**(9): p. 608-616.
22. Harper, R.J., et al., *Bioenergy Feedstock Potential from Short-Rotation Woody Crops in a Dryland Environment†.* Energy & Fuels, 2009. **24**(1): p. 225-231.
23. *http://www.oilmallee.org.au/images/uploads/photo_gallery/image10.jpg (accessed on September 14, 2014)*.
24. Finkbeiner, M., *Carbon footprinting—opportunities and threats.* The International Journal of Life Cycle Assessment, 2009. **14**(2): p. 91-94.
25. Cherubini, F., et al., *Energy- and greenhouse gas-based LCA of biofuel and bioenergy systems: Key issues, ranges and recommendations.* Resources, Conservation and Recycling, 2009. **53**(8): p. 434-447.
26. Yu, Y. and H. Wu, *Bioslurry as a Fuel. 2. Life-Cycle Energy and Carbon Footprints of Bioslurry Fuels from Mallee Biomass in Western Australia.* Energy & Fuels, 2010. **24**(10): p. 5660-5668.
27. Johnson, E., *Goodbye to carbon neutral: Getting biomass footprints right.* Environmental Impact Assessment Review, 2009. **29**(3): p. 165-168.
28. Houghton, R.A. and J.L. Hackler, *Emissions of carbon from forestry and land-use change in tropical Asia.* Global Change Biology, 1999. **5**(4): p. 481-492.
29. Saikku, L., S. Soimakallio, and K. Pingoud, *Attributing land-use change carbon emissions to exported biomass.* Environmental Impact Assessment Review, 2012. **37**(0): p. 47-54.
30. Searchinger, T., et al., *Use of U.S. Croplands for Biofuels Increases Greenhouse Gases Through Emissions from Land-Use Change.* Science, 2008. **319**(5867): p. 1238-1240.
31. Eggleston, S., et al., *IPCC Guidelines for National Greenhouse Gas Inventories; Intergovernmental Panel on Climate Change (IPCC).* Agriculture, Forestry, and Other Land Use, 2006. **4**.
32. McKendry, P., *Energy production from biomass (part 1): overview of biomass.* Bioresource Technology, 2002. **83**(1): p. 37-46.
33. Duku, M.H., S. Gu, and E.B. Hagan, *A comprehensive review of biomass resources and biofuels potential in Ghana.* Renewable and Sustainable Energy Reviews, 2011. **15**: p. 404–415.
34. He, M., et al., *Yield and properties of bio-oil from the pyrolysis of mallee leaves in a fluidised-bed reactor.* Fuel, 2012. **102**(0): p. 506-513.
35. Barton, A., *The Oil Mallee Project, A Multifaceted Industrial Ecology Case Study.* Journal of Industrial Ecology, 2000. **3**: p. 161-176.

36. Singh, H.P., et al., *Characterization and Antioxidant Activity of Essential Oils from Fresh and Decaying Leaves of Eucalyptus tereticornis.* Journal of Agricultural and Food Chemistry, 2009. **57**(15): p. 6962-6966.
37. Batish, D.R., et al., *Eucalyptus essential oil as a natural pesticide.* Forest Ecology and Management, 2008. **256**(12): p. 2166-2174.
38. Elaissi, A., et al., *Antibacterial activity and chemical composition of 20 Eucalyptus species' essential oils.* Food Chemistry, 2011. **129**(4): p. 1427-1434.
39. Ben Jemâa, J.M., et al., *Seasonal variations in chemical composition and fumigant activity of five Eucalyptus essential oils against three moth pests of stored dates in Tunisia.* Journal of Stored Products Research, 2012. **48**(0): p. 61-67.
40. Gilles, M., et al., *Chemical composition and antimicrobial properties of essential oils of three Australian Eucalyptus species.* Food Chemistry, 2010. **119**(2): p. 731-737.
41. Abbott, P.S. *Commercial eucalyptus oil production*. in *The Eucalyptus Oil Production Seminar*. 1989. Gnowangerup: Miscellaneous Publication
42. Wildy, D.T., J.S. Pate, and J.R. Bartle, *Variations in composition and yield of leaf oils from alley-farmed oil mallees (Eucalyptus spp.) at a range of contrasting sites in the Western Australian wheatbelt.* Forest Ecology and Management, 2000. **134**(1–3): p. 205-217.
43. Barton, A. *Commercial possibilities for high-cineole Western Australian eucalyptus oil* in *The Eucalyptus Oil Production Seminar*. 1989. Gnowangerup: Miscellaneous Publication
44. Goodger, J.Q.D., C.A. Connelly, and I.E. Woodrow, *Examination of the consistency of plant traits driving oil yield and quality in short-rotation coppice cultivation of Eucalyptus polybractea.* Forest Ecology and Management, 2007. **250**(3): p. 196-205.
45. Lassak, E.V. *The Australian eucalyptus oil industry : past and present* in *The Eucalyptus Oil Production Seminar* 1989. Gnowangerup: Miscellaneous Publication.
46. Hernandez, E., *Essential Oils | Distillation*, in *Encyclopedia of Separation Science*, D.W. Editor-in-Chief: Ian, Editor. 2000, Academic Press: Oxford. p. 2739-2744.
47. Bachir, R.G. and M. Benali, *Antibacterial activity of the essential oils from the leaves of Eucalyptus globulus against Escherichia coli and Staphylococcus aureus.* Asian Pacific Journal of Tropical Biomedicine, 2012. **2**(9): p. 739-742.
48. Giamakis, A., et al., *Eucalyptus camaldulensis: volatiles from immature flowers and high production of 1,8-cineole and β-pinene by in vitro cultures.* Phytochemistry, 2001. **58**(2): p. 351-355.
49. Kumar, G., A.K. Panda, and R.K. Singh, *Optimization of process for the production of bio-oil from eucalyptus wood.* Journal of Fuel Chemistry and Technology, 2010. **38**(2): p. 162-167.
50. Romdhane, M. and C. Tizaoui, *The kinetic modelling of a steam distillation unit for the extraction of aniseed (\+i\ Pimpinella anisum \-i\) essential oil.* Journal of chemical technology and biotechnology, 2005. **80**(7): p. 759.
51. Teranishi, R., et al., *Comparison of batchwise and continuous steam distillation-solvent extraction recovery of volatiles from oleoresin capsicum, African type (Capsicum frutescens).* Journal of Agricultural and Food Chemistry, 1980. **28**(1): p. 156-157.
52. Moncada, J., J.A. Tamayo, and C.A. Cardona, *Techno-economic and environmental assessment of essential oil extraction from Citronella (Cymbopogon winteriana) and*

Lemongrass (Cymbopogon citrus): A Colombian case to evaluate different extraction technologies. Industrial Crops and Products, 2014. **54**(0): p. 175-184.

53. Masango, P., *Cleaner production of essential oils by steam distillation.* Journal of Cleaner Production, 2005. **13**: p. 833-839.
54. Boutekedjiret, C., et al., *Extraction of rosemary essential oil by steam distillation and hydrodistillation.* Flavour and Fragnance Journal, 2003. **18**: p. 481–484.
55. Önal, E.P., B.B. Uzun, and A.E. Pütün, *Steam pyrolysis of an industrial waste for bio-oil production.* Fuel Processing Technology, 2011. **92**: p. 879-885.
56. Miller, S.F. and B.G. Miller, *The occurrence of inorganic elements in various biofuels and its effect on ash chemistry and behavior and use in combustion products.* Fuel Processing Technology, 2007. **88**(11–12): p. 1155-1164.
57. Wu, H., et al., *Removal and Recycling of Inherent Inorganic Nutrient Species in Mallee Biomass and Derived Biochars by Water Leaching.* Industrial & Engineering Chemistry Research, 2011. **50**(21): p. 12143-12151.
58. Raveendran, K., A. Ganesh, and K.C. Khilar, *Influence of mineral matter on biomass pyrolysis characteristics.* Fuel, 1995. **74**: p. 1812-1822.
59. Baxter, L.L., et al., *The behavior of inorganic material in biomass-fired power boilers: field and laboratory experiences.* Fuel Processing Technology, 1998. **54**(1–3): p. 47-78.
60. Marschner, H., *Mineral Nutrition of Higher Plants*. 2nd ed. 2002: Academic Press.
61. van Lith, S.C., et al., *Release to the Gas Phase of Inorganic Elements during Wood Combustion. Part 2: Influence of Fuel Composition.* Energy & Fuels, 2008. **22**: p. 1598–1609.
62. Zevenhoven-Onderwater, M., *Ash-forming Matter in Biomass Fuels*, in *Department of Chemical Engineering*. 2002, Abo Akademi University: Abo/Turku, Finland.
63. Broadley, M., et al., *Chapter 8 - Beneficial Elements*, in *Marschner's Mineral Nutrition of Higher Plants (Third Edition)*, P. Marschner, Editor. 2012, Academic Press: San Diego. p. 249-269.
64. Dayton, D.C., R.J. French, and T.A. Milne, *Direct Observation of Alkali Vapor Release during Biomass Combustion and Gasification. 1. Application of Molecular Beam/Mass Spectrometry to Switchgrass Combustion.* Energy & Fuels, 1995. **9**(5): p. 855-865.
65. Knudsen, J.N., P.A. Jensen, and K. Dam-Johansen, *Transformation and Release to the Gas Phase of Cl, K, and S during Combustion of Annual Biomass.* Energy & Fuels, 2004. **18**(5): p. 1385-1399.
66. Baxter, L.L. *Pollutant emissions and deposit formation during combustion of biomass fuels*. in *Third Contractors Meeting 'Alkali Deposits Found in Biomass Power Plants'*. November 30 (1993). Livermore, California.
67. Jenkins, B.M., R.R. Bakker, and J.B. Wei, *On the properties of washed straw.* Biomass and Bioenergy, 1996. **10**(4): p. 177-200.
68. Dayton, D.C., et al., *Release of Inorganic Constituents from Leached Biomass during Thermal Conversion.* Energy & Fuels, 1999. **13**(4): p. 860-870.
69. Shah, K.V., et al., *Correlating the effects of ash elements and their association in the fuel matrix with the ash release during pulverized fuel combustion.* Fuel Processing Technology, 2010. **91**(5): p. 531-545.

70. Hawkesford, M., et al., *Chapter 6 - Functions of Macronutrients*, in *Marschner's Mineral Nutrition of Higher Plants (Third Edition)*, P. Marschner, Editor. 2012, Academic Press: San Diego. p. 135-189.
71. Franceshi, V.R. and H.T.J. Horner, *Calcium Oxalate Crystals in Plants.* The Botanical Review, 1980. **46**: p. 361-427.
72. Bryers, R.W., *Fireside slagging, fouling, and high-temperature corrosion of heat-transfer surface due to impurities in steam-raising fuels.* Progress in Energy and Combustion Science, 1996. **22**(1): p. 29-120.
73. Jenkins, B.M., et al. *Composition of ash deposits in biomass fueled boilers: results of full-scale experiments and laboratory simulations*. in *American Society of Agriculture Engineers*. June 19–22 1994. Kansas City.
74. Tumuluru, J.S., et al., *A review on biomass torrefaction process and product properties for energy applications.* INdustrial Biotechnology, 2011. **7**: p. 384-401.
75. Demirbas, A., *Combustion characteristics of different biomass fuels.* Progress in Energy and Combustion Science, 2004. **30**(2): p. 219-230.
76. EverGreen Renewable, L. *Biomass Torrefaction as a Preprocessing Step for Thermal Conversion; Reducing costs in the biomass supply chain Available at: http://evergreenrenewable.com/welcome_files/Biomass%20torrefaction.pdf*. 2009.
77. Olsen, G., et al., *DeVeloping multiple purpose species for large scale reVegetation, search project final report (nht project 973849); Department of Conservation and Land Management: Perth, Western Australia.* 2004.
78. Abdullah, H. and H. Wu, *Biochar as a Fuel: 1. Properties and Grindability of Biochars Produced from the Pyrolysis of Mallee Wood under Slow-Heating Conditions.* Energy & Fuels, 2009. **23**(8): p. 4174-4181.
79. Pipatmanomai, S., *Overview and Experiences of Biomass Fluidized Bed Gasification in Thailand.* Journal of Sustainable Energy & Environment Special Issue, 2011: p. 29-33.
80. Nussbaumer, T., *Combustion and Co-combustion of Biomass: Fundamentals, Technologies, and Primary Measures for Emission Reduction†.* Energy & Fuels, 2003. **17**(6): p. 1510-1521.
81. Prins, M.J., K.J. Ptasinski, and F.J.J.G. Janssen, *Torrefaction of wood: Part 1. Weight loss kinetics.* Journal of analytical and applied pyrolysis, 2006. **77**(1): p. 28-34.
82. Khazraie Shoulaifar, T., et al., *Impact of Torrefaction on the Chemical Structure of Birch Wood.* Energy & Fuels, 2014. **28**(6): p. 3863-3872.
83. Saleh, S.B., et al., *Influence of Biomass Chemical Properties on Torrefaction Characteristics.* Energy & Fuels, 2013. **27**(12): p. 7541-7548.
84. Ciolkosz, D. and R. Wallace, *A review of torrefaction for bioenergy feedstock production.* Biofuels, Bioproducts and Biorefining, 2011. **5**(3): p. 317-329.
85. Lipinsky, E.S., J.R. Arcate, and T.B. Reed, *Enhanced Wood Fuels via Torrefaction.* Fuel Chemistry Division Preprints, 2002. **47(1)**: p. 408.
86. Nimlos, M.N., et al., *Biomass Torrefaction Studies with a Molecular Beam Mass Spectrometer.* Prepr. Pap.-Am. Chem. Soc., Div. Fuel Chem., 2003. **48(2)**: p. 590.
87. Felfli, F.F., et al., *Wood briquette torrefaction.* Energy for Sustainable Development, 2005. **9**(3): p. 19-22.

88. O¨zc¸imen, D. and F. Karaosmanog˘lu, *Production and characterization of bio-oil and biochar from rapeseed cake.* Renewable Energy, 2004. **29**: p. 779–787.
89. Ghetti, P., L. Ricca, and L. Angelini, *Thermal analysis of biomass and corresponding pyrolysis products.* Fuel, 1996. **75**: p. 565-573.
90. Czernik, S. and A.V. Bridgwater, *Overview of Applications of Biomass Fast Pyrolysis Oil.* Energy & Fuels, 2004. **18**(2): p. 590-598.
91. Evans, R.J. and T.A. Milne, *Molecular characterization of the pyrolysis of biomass.* Energy & Fuels, 1987. **1**(2): p. 123-137.
92. Scott, D.S., J. Plskorz, and D. Radleln, *Liquid Products from the Continuous Flash Pyrolysis of Biomass.* Ind. Eng. Chem. ProcessDes. Dev., 1985. **24**: p. 581-588.
93. Agblevor, F.A., S. Besler, and A.E. Wiselogel, *Fast Pyrolysis of Stored Biomass Feedstocks.* Energy & Fuels, 1995. **9**(4): p. 635-640.
94. Radlein, D., *Fast pyrolysis of natural polysaccharides as a potential industrial process.* Journal of analytical and applied pyrolysis, 1991. **19**(C): p. 41-63.
95. Shafizadeh, F., *Introduction to Pyrolysis of Biomass - Review.* Journal of Analytical and Applied Pyrolysis, 1982. **3**: p. 283-305.
96. Qu, T., et al., *Experimental Study of Biomass Pyrolysis Based on Three Major Components: Hemicellulose, Cellulose, and Lignin.* Industrial & Engineering Chemistry Research, 2011. **50**(18): p. 10424-10433.
97. Yang, H., et al., *In-Depth Investigation of Biomass Pyrolysis Based on Three Major Components: Hemicellulose, Cellulose and Lignin.* Energy & Fuels, 2005. **20**(1): p. 388-393.
98. Lv, D., et al., *Effect of cellulose, lignin, alkali and alkaline earth metallic species on biomass pyrolysis and gasification.* Fuel Processing Technology, 2010. **91**: p. 903–909.
99. Abnisa, F., et al., *Utilization possibilities of palm shell as a source of biomass energy in Malaysia by producing bio-oil in pyrolysis process.* Biomass and Bioenergy, 2011. **xxx**: p. 1-10.
100. Samolada, M.C., T. Stoicos, and I.A. Vasalos, *An Investigation of the Factors Controlling the Pyrolysis Product Yield of Greek Wood Biomass in a Fluidized Bed.* Journal of Analytical and Applied Pyrolysis, 1990. **18**: p. 127-141.
101. Shafizadeh, F., et al., *Production of Levoglucosan and Glucose from Pyrolysis of Cellulosic Materials.* Journal of Applied Polymer Science, 1979. **23**: p. 3525-3539.
102. Funazukurl, T., *Correlation of Volatile Products from Fast Cellulose Pyrolysis.* Ind. Eng. Chem. Process Des. Dev., 1986. **25**: p. 172-181.
103. Figueiredo, J.L., et al., *Pyrolysis of holm-oak wood: influence of temperature and particle size.* FUEL, 1989. **68**: p. 1012-1016.
104. Pu¨tu¨n, A.e.E., E. Apaydın, and E. Pu¨tu¨n, *Rice straw as a bio-oil source via pyrolysis and steam pyrolysis.* Energy, 2004. **29**: p. 2171–2180.
105. Onay, O. and O.M. Kockar, *Technical note: Slow, fast and flash pyrolysis of rapeseed.* Renewable Energy, 2003. **28**: p. 2417–2433.
106. Guerrero, M., et al., *Pyrolysis of eucalyptus at different heating rates: studies of char characterization and oxidative reactivity.* J. Anal. Appl. Pyrolysis, 2005. **74**: p. 307–314.

107. Onay, O., *Influence of pyrolysis temperature and heating rate on the production of bio-oil and char from safflower seed by pyrolysis, using a well-swept fixed-bed reactor.* Fuel Processing Technology, 2007. **88**(5): p. 523-531.
108. Demiral, I. and E.A. Ayan, *Pyrolysis of grape bagasse: Effect of pyrolysis conditions on the product yields and characterization of the liquid product.* Bioresource Technology, 2011. **102**: p. 3946-3951.
109. Liu, Q., et al., *Interactions of biomass components during pyrolysis: A TG-FTIR study.* Journal of analytical and applied pyrolysis, 2011. **90**: p. 212-218.
110. Wang, G., et al., *Pretreatment of biomass by torrefaction.* Chinese Science Bulletin, 2011. **56**(14): p. 1442-1448.
111. Bahng, M.-K., et al., *Current technologies for analysis of biomass thermochemical processing: A review*. Analytica Chimica Acta, 2009. **651**: p. 117–138.
112. Tsai, W.T., M.K. Lee, and Y.M. Chang, *Fast pyrolysis of rice straw, sugarcane bagasse and coconut shell in an induction-heating reactor.* J. Anal. Appl. Pyrolysis, 2006. **76**: p. 230–237.
113. Bridgwater, A.V. and G.V.C. Peacocke, *Fast pyrolysis processes for biomass.* Renewable and Sustainable Energy Reviews, 2000. **4**: p. 1-73.
114. Keown, D.M., et al., *Volatilisation of alkali and alkaline earth metallic species during the pyrolysis of biomass: differences between sugar cane bagasse and cane trash.* Bioresource Technology, 2005. **96**: p. 1570–1577.
115. Matsuoka, K., et al., *Transformation of alkali and alkaline earth metals in low rank coal during gasification.* Fuel, 2008. **87**: p. 885–893.
116. Quyn, D.M., et al., *Volatilisation and catalytic effects of alkali and alkaline earth metallic species during the pyrolysis and gasification of Victorian brown coal. Part II. Effects of chemical form and valence.* Fuel, 2002. **81**: p. 151-158.
117. Quyn, D.M., H. Wu, and C.-Z. Li, *Volatilisation and catalytic effects of alkali and alkaline earth metallic species during the pyrolysis and gasification of Victorian brown coal. Part I. Volatilisation of Na and Cl from a set of NaCl-loaded samples.* Fuel, 2002. **81**: p. 143-149.
118. Wu, H., D.M. Quyn, and C.-Z. Li, *Volatilisation and catalytic affects of alkali and alkaline earth metallic species during the pyrolysis and gasification of Victorian brown coal. Part III. The importance of the interaction between volatiles and char at high temperature.* Fuel, 2002. **81**: p. 1033-1039.
119. Raveendran, K., A. Ganesh, and K.C. Khilar, *Pyrolysis characteristics of biomass and biomass components.* Fuel, 1996. **75**: p. 987-998.
120. Hosokai, S., et al., *Spontaneous Generation of Tar Decomposition Promoter in a Biomass Steam Reformer.* Chemical Engineering Research and Design, 2005. **83(A9)**: p. 1093–1102.
121. Fahmi, R., et al., *The effect of alkali metals on combustion and pyrolysis of Lolium and Festuca grasses, switchgrass and willow.* Fuel, 2007. **86**: p. 1560–1569.
122. Wang, Y., et al., *Comparisons of Biochar Properties from Wood Material and Crop Residues at Different Temperatures and Residence Times.* Energy & Fuels, 2013. **27**(10): p. 5890-5899.

123. Zhang, J. and C. You, *Water Holding Capacity and Absorption Properties of Wood Chars.* Energy & Fuels, 2013. **27**(5): p. 2643-2648.
124. Asai, H., et al., *Biochar amendment techniques for upland rice production in Northern Laos: 1. Soil physical properties, leaf SPAD and grain yield.* Field Crops Research, 2009. **111**(1–2): p. 81-84.
125. Laird, D.A., et al., *Review of the pyrolysis platform for coproducing bio-oil and biochar.* Biofuels, Bioproducts and Biorefining, 2009. **3**(5): p. 547-562.
126. Mullen, C.A., et al., *Bio-oil and bio-char production from corn cobs and stover by fast pyrolysis.* Biomass and Bioenergy, 2010. **34**(1): p. 67-74.
127. Roberts, K.G., et al., *Life Cycle Assessment of Biochar Systems: Estimating the Energetic, Economic, and Climate Change Potential.* Environmental Science & Technology, 2009. **44**(2): p. 827-833.
128. Glaser, B., J. Lehmann, and W. Zech, *Ameliorating physical and chemical properties of highly weathered soils in the tropics with charcoal – a review.* Biology and Fertility of Soils, 2002. **35**(4): p. 219-230.
129. Lehmann, J., *A handful of carbon.* Nature, 2007. **447**(7141): p. 143-144.
130. McHenry, M.P., *Agricultural bio-char production, renewable energy generation and farm carbon sequestration in Western Australia: Certainty, uncertainty and risk.* Agriculture, Ecosystems & Environment, 2009. **129**(1–3): p. 1-7.
131. Lehmann, J. and S. Joseph, *Biochar for environmental management: science and technology*. 2009, Earthscan: London.
132. Berglund, L.M., T.H. DeLuca, and O. Zackrisson, *Activated carbon amendments to soil alters nitrification rates in Scots pine forests.* Soil Biology and Biochemistry, 2004. **36**(12): p. 2067-2073.
133. Lehmann, J., J. Gaunt, and M. Rondon, *Bio-char Sequestration in Terrestrial Ecosystems – A Review.* Mitigation and Adaptation Strategies for Global Change, 2006. **11**(2): p. 395-419.
134. Zhang, A., et al., *Effect of biochar amendment on maize yield and greenhouse gas emissions from a soil organic carbon poor calcareous loamy soil from Central China Plain.* Plant and Soil, 2012. **351**(1-2): p. 263-275.
135. Wang, J., et al., *Effects of biochar amendment in two soils on greenhouse gas emissions and crop production.* Plant and Soil, 2012. **360**(1-2): p. 287-298.
136. Lehmann, J., *Bio-energy in the black.* Frontiers in Ecology and the Environment, 2007. **5**(7): p. 381-387.
137. Lehmann, J., et al., *Nutrient availability and leaching in an archaeological Anthrosol and a Ferralsol of the Central Amazon basin: fertilizer, manure and charcoal amendments.* Plant and Soil, 2003. **249**(2): p. 343-357.
138. Gaunt, J.L. and J. Lehmann, *Energy Balance and Emissions Associated with Biochar Sequestration and Pyrolysis Bioenergy Production.* Environmental Science & Technology, 2008. **42**(11): p. 4152-4158.
139. Liang, B., et al., *Black Carbon Increases Cation Exchange Capacity in Soils.* Soil Sci. Soc. Am. J., 2006. **70**(5): p. 1719-1730.
140. James, G., et al., *Evaluating phenanthrene sorption on various wood chars.* Water Research, 2005. **39**(4): p. 549-558.

141. Dugan, E., et al. *Bio-char from sawdust, maize stover and charcoal: Impact on water holding capacities (WHC) of three soils from Ghana*. in *The 19th World Congress of Soil Science, Soil Solutions for a Changing World*. 2010. Brisbane, Australia.
142. Karhu, K., et al., *Biochar addition to agricultural soil increased CH4 uptake and water holding capacity – Results from a short-term pilot field study.* Agriculture, Ecosystems & Environment, 2011. **140**(1–2): p. 309-313.
143. Laird, D.A., *The Charcoal Vision: A Win–Win–Win Scenario for Simultaneously Producing Bioenergy, Permanently Sequestering Carbon, while Improving Soil and Water Quality All rights reserved. No part of this periodical may be reproduced or transmitted in any form or by any means, electronic or mechanical, including photocopying, recording, or any information storage and retrieval system, without permission in writing from the publisher.* Agron. J., 2008. **100**(1): p. 178-181.
144. Gaskin, J.W., et al., *Effect of Low‐Temperature Pyrolysis Conditions on Biochar for Agricultural Use.* American Society of Agricultural and Biological Engineers, 2008. **51(6)**: p. 2061-2069.
145. Chan, K.Y., et al., *Using poultry litter biochars as soil amendments.* Soil Research, 2008. **46**(5): p. 437-444.
146. Chan, K.Y., et al., *Agronomic values of greenwaste biochar as a soil amendment.* Soil Research, 2007. **45**(8): p. 629-634.
147. Steiner, C., et al., *Long term effects of manure, charcoal and mineral fertilization on crop production and fertility on a highly weathered Central Amazonian upland soil.* Plant and Soil, 2007. **291**(1-2): p. 275-290.
148. Jensen, P.A., B. Sander, and K. Dam-Johansen, *Removal of K and Cl by leaching of straw char.* Biomass and Bioenergy, 2001. **20**(6): p. 447-457.
149. Jenkins, B.M., et al., *Combustion properties of biomass.* Fuel Processing Technology, 1998. **54**(1–3): p. 17-46.
150. Westberg, H.M., M. Byström, and B. Leckner, *Distribution of Potassium, Chlorine, and Sulfur between Solid and Vapor Phases during Combustion of Wood Chips and Coal.* Energy & Fuels, 2002. **17**(1): p. 18-28.
151. Turnbull, J.H., *Use of biomass in electric power generation: the california experience.* Biomass and Bioenergy, 1993. **4**(2): p. 75-84.
152. Nielsen, H.P., F.J. Frandsen, and K. Dam-Johansen, *Lab-Scale Investigations of High-Temperature Corrosion Phenomena in Straw-Fired Boilers.* Energy & Fuels, 1999. **13**(6): p. 1114-1121.
153. Nielsen, H.P., et al., *The implications of chlorine-associated corrosion on the operation of biomass-fired boilers.* Progress in Energy and Combustion Science, 2000. **26**(3): p. 283-298.
154. Tillman, D.A., D. Duong, and M. Bruce, *Chlorine in Solid Fuels Fired in Pulverized Fuel Boilers s Sources, Forms, Reactions, and Consequences: a Literature Review.* Energy & Fuels 2009. **23**: p. 3379–3391.
155. Miles, T.R., et al., *Boiler deposits from firing biomass fuels.* Biomass and Bioenergy, 1996. **10**(2–3): p. 125-138.
156. Tortosa Masiá, A.A., et al., *Characterising ash of biomass and waste.* Fuel Processing Technology, 2007. **88**(11–12): p. 1071-1081.

157. Christensen, K.A., M. Stenholm, and H. Livbjerg, *The combustion of straw: —submicron aerosol particles and gas pollutants.* Journal of Aerosol Science, 1995. **26, Supplement 1**(0): p. S173-S174.
158. Johansson, L.S., et al., *Particle emissions from biomass combustion in small combustors.* Biomass and Bioenergy, 2003. **25**(4): p. 435-446.
159. Seames, W.S., *An initial study of the fine fragmentation fly ash particle mode generated during pulverized coal combustion.* Fuel Processing Technology, 2003. **81**(2): p. 109-125.
160. Strand, M., et al., *Laboratory and Field Test of a Sampling Method for Characterization of Combustion Aerosols at High Temperatures.* Aerosol Science and Technology, 2004. **38**(8): p. 757-765.
161. Boman, C., et al., *Characterization of Inorganic Particulate Matter from Residential Combustion of Pelletized Biomass Fuels.* Energy & Fuels, 2004. **18**(2): p. 338-348.
162. Johansson, L.S., et al., *Emission characteristics of modern and old-type residential boilers fired with wood logs and wood pellets.* Atmospheric Environment, 2004. **38**(25): p. 4183-4195.
163. Khan, A.A., et al., *Biomass combustion in fluidized bed boilers: Potential problems and remedies.* Fuel Processing Technology, 2009. **90**(1): p. 21-50.
164. McElroy, M.W., et al., *Size Distribution of Fine Particles from Coal Combustion.* Science, 1982. **215**(4528): p. 13-19.
165. Valmari, T., et al., *Fly ash formation and deposition during fluidized bed combustion of willow.* Journal of Aerosol Science, 1998. **29**(4): p. 445-459.
166. Heyder, J., et al., *Deposition of particles in the human respiratory tract in the size range 0.005–15 μm.* Journal of Aerosol Science, 1986. **17**(5): p. 811-825.
167. Amdur, M.O. and M. Corn, *The Irritant Potency of Zinc Ammonium Sulfate Of Different Particle Sizes.* American Industrial Hygiene Association Journal, 1963. **24**(4): p. 326-333.
168. Brunekreef, B. and S.T. Holgate, *Air pollution and health.* The Lancet, 2002. **360**(9341): p. 1233-1242.
169. Pope, C.A., et al., *Particulate Air Pollution as a Predictor of Mortality in a Prospective Study of U.S. Adults.* American Journal of Respiratory and Critical Care Medicine, 1995. **151**(3_pt_1): p. 669-674.
170. Pope, I.C., et al., *LUng cancer, cardiopulmonary mortality, and long-term exposure to fine particulate air pollution.* JAMA, 2002. **287**(9): p. 1132-1141.
171. Neas, L.M., *Fine particulate matter and cardiovascular disease.* Fuel Processing Technology, 2000. **65–66**(0): p. 55-67.
172. Polichetti, G., et al., *Effects of particulate matter (PM10, PM2.5 and PM1) on the cardiovascular system.* Toxicology, 2009. **261**(1–2): p. 1-8.
173. Obernberger, I., T. Brunner, and G. Bärnthaler, *Chemical properties of solid biofuels—significance and impact.* Biomass and Bioenergy, 2006. **30**(11): p. 973-982.
174. Obernberger, I., et al., *Concentrations of inorganic elements in biomass fuels and recovery in the different ash fractions.* Biomass and Bioenergy, 1997. **12**(3): p. 211-224.
175. Gao, X. and H. Wu, *Aerodynamic Properties of Biochar Particles: Effect of Grinding and Implications.* Environmental Science & Technology Letters, 2013. **1**(1): p. 60-64.

176. Gao, X. and H. Wu, *Biochar as a Fuel: 4. Emission Behavior and Characteristics of PM1 and PM10 from the Combustion of Pulverized Biochar in a Drop-Tube Furnace.* Energy & Fuels, 2011. **25**(6): p. 2702-2710.
177. Wiinikka, H. and R. Gebart, *The Influence of Air Distribution Rate on Particle Emissions in Fixxed Bed Combustion of Biomass.* Combustion Science and Technology, 2005. **177**(9): p. 1747-1766.
178. Wiinikka, H. and R. Gebart, *Experimental investigations of the influence from different operating conditions on the particle emissions from a small-scale pellets combustor.* Biomass and Bioenergy, 2004. **27**(6): p. 645-652.
179. Latva-Somppi, J., et al., *Ash formation during fluidized-bed incineration of paper mill waste sludge.* Journal of Aerosol Science, 1998. **29**(4): p. 461-480.
180. Skrifvars, B.-J., et al., *Ash behaviour in a pulverized wood fired boiler—a case study.* Fuel, 2004. **83**(10): p. 1371-1379.
181. Lind, T., et al., *Volatilization of the Heavy Metals during Circulating Fluidized Bed Combustion of Forest Residue.* Environ. Sci. Technol., 1999. **33**(3): p. 496-502.
182. Oleschko, H., et al., *Influence of coal composition on the release of Na-, K-, Cl-, and S-species during the combustion of brown coal.* Fuel, 2007. **86**(15): p. 2275-2282.
183. Bridgeman, T.G., et al., *Torrefaction of reed canary grass, wheat straw and willow to enhance solid fuel qualities and combustion properties.* Fuel, 2008. **87**(6): p. 844-856.
184. Jensen, P.A., et al., *Experimental Investigation of the Transformation and Release to Gas Phase of Potassium and Chlorine during Straw Pyrolysis.* Energy & Fuels 2000. **14**: p. 1280-1285.
185. Shoulaifar, K.T., et al., *Ash-Forming Matter in Torrefied Birch Wood: Changes in Chemical Association.* Energy & Fuels, 2013. **27**(10): p. 5684-5690.
186. Johansen, J.M., et al., *Release of K, Cl, and S during Pyrolysis and Combustion of High-Chlorine Biomass.* Energy & Fuels, 2011. **25**(11): p. 4961-4971.
187. Zintl, F., B. Stromberg, and E. Bjorkman. *Release of Chlorine from Biomass at Gasification Conditions.* in *The 10th European Conference on Biomass for Energy and Industry*. 1998. Wurzburg, Germany.
188. Saleh, S.B., et al., *Release of Chlorine and Sulfur during Biomass Torrefaction and Pyrolysis.* Energy & Fuels, 2014. **28**(6): p. 3738-3746.
189. Hamilton, J.T.G., et al., *Chloride Methylation by Plant Pectin: An Efficient Environmentally Significant Process.* Science, 2003. **301**(5630): p. 206-209.
190. van Lith, S.C., et al., *Release to the Gas Phase of Inorganic Elements during Wood Combustion. Part 1: Development and Evaluation of Quantification Methods.* Energy & Fuels, 2006. **20**(3): p. 964-978.
191. Yan, W., et al., *Mass and Energy Balances of Wet Torrefaction of Lignocellulosic Biomass†.* Energy & Fuels, 2010. **24**(9): p. 4738-4742.
192. Knudsen, J.N., et al., *Sulfur Transformations during Thermal Conversion of Herbaceous Biomass.* Energy & Fuels, 2004. **18**(3): p. 810-819.
193. Khalil, R.A., M. Seljeskog, and J.E. Hustad, *Sulfur Abatement in Pyrolysis of Straw Pellets.* Energy & Fuels, 2008. **22**(4): p. 2789-2795.
194. Olsson, J.G., et al., *Alkali Metal Emission during Pyrolysis of Biomass.* Energy & Fuels, 1997. **11**(4): p. 779-784.

195. Davidsson, K.O., B.J. Stojkova, and J.B.C. Pettersson, *Alkali Emission from Birchwood Particles during Rapid Pyrolysis.* Energy & Fuels, 2002. **16**(5): p. 1033-1039.
196. Davidsson, K.O., et al., *The effects of fuel washing techniques on alkali release from biomass.* Fuel, 2002. **81**(2): p. 137-142.
197. Davidsson, K.O., J.B.C. Pettersson, and R. Nilsson, *Fertiliser influence on alkali release during straw pyrolysis.* Fuel, 2002. **81**(3): p. 259-262.
198. Knudsen, J.N., *Volatilization of Inorganic Matter during Combustion of Annual Biomass*. 2004, Technical University of Denmark: Lyngby, Denmark.
199. Wornat, M.J., et al., *Structural and compositional transformations of biomass chars during combustion.* Combustion and Flame, 1995. **100**(1–2): p. 131-143.
200. Wigmans, T., H. Haringa, and J.A. Moulijn, *Nature, activity and stability of active sites during alkali metal carbonate-catalysed gasification reactions of coal char.* Fuel, 1983. **62**(2): p. 185-189.
201. Dayton, D. and T. Milne, *Laboratory Measurements of Alkali Metal Containing Vapors Released during Biomass Combustion*, in *Applications of Advanced Technology to Ash-Related Problems in Boilers*, L. Baxter and R. DeSollar, Editors. 1996, Springer US. p. 161-185.
202. Khazraie Shoulaifar, T., et al., *Measuring the concentration of carboxylic acid groups in torrefied spruce wood.* Bioresource Technology, 2012. **123**(0): p. 338-343.
203. Khazraie Shoulaifar, T., et al., *Ash-Forming Matter in Torrefied Birch Wood: Changes in Chemical Association.* Energy Fuels, 2013. **27**(10): p. 5684-5690.
204. Keown, D.M., J.-i. Hayashi, and C.-Z. Li, *Effects of volatile–char interactions on the volatilisation of alkali and alkaline earth metallic species during the pyrolysis of biomass.* Fuel, 2008. **87**(7): p. 1187-1194.
205. Liaw, S.B. and H. Wu, *Leaching characteristics of organic and inorganic matter from biomass by water: differences between batch and semi-continuous operations.* Ind. Eng. Chem. Res., 2013. **52**(11): p. 4280-4289.
206. Rahim, M.U., et al., *Release of Chlorine during Mallee Bark Pyrolysis.* Energy Fuels, 2012. **27**(1): p. 310-317.
207. Williams, A., M. Pourkashanian, and J.M. Jones, *Combustion of pulverised coal and biomass.* Progress in Energy and Combustion Science, 2001. **27**(6): p. 587-610.
208. Gao, X., et al., *Roles of Inherent Fine Included Mineral Particles in the Emission of PM10 during Pulverized Coal Combustion.* Energy & Fuels, 2012. **26**(11): p. 6783-6791.
209. Gao, X. and H. Wu, *Effect of Sampling Temperature on the Properties of Inorganic Particulate Matter Collected from Biomass Combustion in a Drop-Tube Furnace.* Energy & Fuels, 2010. **24**(8): p. 4571-4580.
210. Nuamah, A., et al., *5.05 - Biomass Co-Firing*, in *Comprehensive Renewable Energy*, A. Sayigh, Editor. 2012, Elsevier: Oxford. p. 55-73.
211. Rahim, M.U., X. Gao, and H. Wu, *A method for the quantification of chlorine in low-rank solid fuels.* Energy Fuels, 2013. **27**(11): p. 6992-6999.
212. Hecker, W.C., et al., *Effects of burnout on char oxidation kinetics.* Symposium (International) on Combustion, 1992. **24**(1): p. 1225-1231.
213. Ngu, L.-n., H. Wu, and D.-k. Zhang, *Characterization of Ash Cenospheres in Fly Ash from Australian Power Stations.* Energy & Fuels, 2007. **21**(6): p. 3437-3445.

214. Kopyscinski, J., T.J. Schildhauer, and S.M.A. Biollaz, *Production of synthetic natural gas (SNG) from coal and dry biomass – A technology review from 1950 to 2009.* Fuel, 2010. **89**(8): p. 1763-1783.
215. Vassilev, S.V., et al., *An overview of the chemical composition of biomass.* Fuel, 2010. **89**(5): p. 913-933.
216. Bartle, J.R. and A. Abadi, *Toward Sustainable Production of Second Generation Bioenergy Feedstocks†.* Energy & Fuels, 2010. **24**(1): p. 2-9.
217. Mulligan, C.J., L. Strezov, and V. Strezov, *Thermal Decomposition of Wheat Straw and Mallee Residue Under Pyrolysis Conditions†.* Energy & Fuels, 2009. **24**(1): p. 46-52.
218. Wu, H., Y. Yu, and K. Yip, *Bioslurry as a Fuel. 1. Viability of a Bioslurry-Based Bioenergy Supply Chain for Mallee Biomass in Western Australia.* Energy & Fuels, 2010. **24**(10): p. 5652-5659.
219. Hayashi, J.-i., et al., *Low-Temperature Gasification of Biomass and Lignite: Consideration of Key Thermochemical Phenomena, Rearrangement of Reactions, and Reactor Configuration.* Energy & Fuels, 2014. **28**(1): p. 4-21.
220. Chen, W.-Y., et al., *Photochemical and acoustic interactions of biochar with CO2 and H2O: Applications in power generation and CO2 capture.* AIChE Journal, 2014. **60**(3): p. 1054-1065.
221. Fushimi, C., et al., *Elucidation of the interaction among cellulose, xylan, and lignin in steam gasification of woody biomass.* AIChE Journal, 2009. **55**(2): p. 529-537.
222. Edris, A.E., *Pharmaceutical and therapeutic Potentials of essential oils and their individual volatile constituents: a review.* Phytotherapy Research, 2007. **21**(4): p. 308-323.
223. Su, V., et al., *Plasmodium falciparum growth is arrested by monoterpenes from eucalyptus oil.* Flavour and Fragrance Journal, 2008. **23**(5): p. 315-318.
224. Gomes, A., L. Serrano, and F. Farelo, *Solid-liquid equilibria in 1,8-cineole/terpenic hydrocarbon systems.* Journal of Chemical & Engineering Data, 1988. **33**(2): p. 194-196.
225. Ammon, D.G., et al., *Rapid and Accurate Determination of Terpenes in the Leaves of Eucalyptus Species.* ANALYST, 1985. **110**: p. 921-924.
226. Hili, P., C.S. Evans, and R.G. Veness, *Antimicrobial action of Essential Oil: the effect of dimethylsulfoxide on the actifity of cinnamon oil.* Applied Microbiology, 1996: p. 269-275.
227. Milthorpe, P.L., et al., *Optimum planting densities for the production of eucalyptus oil from blue mallee (Eucalyptus polybractea) and oil mallee (E. kochii).* Industrial Crops and Products, 1998. **8**: p. 219–227.
228. Cooper, D., G. Olsen, and J. Bartle, *Capture of agricultural surplus water determines the productivity and scale of new low-rainfall woody crop industries.* Aust J of Exp Agr, 2005. **45**(11): p. 1369-1388.
229. Kumar, K.S., *Extraction of Essential Oil Using Steam Distillation.* Thesis-National Institute of Technology Rourkela, 2010.
230. Peng, F., et al., *Comparison of different extraction methods: steam distillation, simultaneous distillation and extraction and headspace co-distillation, used for the analysis of the volatile components in aged flue-cured tobacco leaves.* Journal of Chromatography A, 2004. **1040**(1): p. 1-17.

231. Li, H. and J.L. Madden, *Analysis of leaf oils from a Eucalyptus species trial.* Biochemical Systematics and Ecology, 1995. **23**(2): p. 167-177.
232. Yatagai, M. and T. Takahashi, *Essential oils and successive extractives of Eucalyptus leaves.* Biomass, 1984. **4**(4): p. 305-310.
233. Li, H., J.L. Madden, and B.M. Potts, *Variation in volatile leaf oils of the Tasmanian Eucalyptus species—1. Subgenus Monocalyptus.* Biochemical Systematics and Ecology, 1995. **23**(3): p. 299-318.
234. Li, H., J.L. Madden, and N.W. Davies, *Variation in leaf oils of Eucalyptus nitens and E. denticulata.* Biochemical Systematics and Ecology, 1994. **22**(6): p. 631-640.
235. Li, H., J.L. Madden, and B.M. Potts, *Variation in volatile leaf oils of the Tasmanian Eucalyptus species II. Subgenus Symphyomyrtus.* Biochemical Systematics and Ecology, 1996. **24**(6): p. 547-569.
236. Pirali-Kheirabadi, K., M. Razzaghi-Abyaneh, and A. Halajian, *Acaricidal effect of Pelargonium roseum and Eucalyptus globulus essential oils against adult stage of Rhipicephalus (Boophilus) annulatus in vitro.* Veterinary Parasitology, 2009. **162**(3–4): p. 346-349.
237. Johns, M.R., J.E. Johns, and V. Rudolph, *Steam distillation of tea tree (Melaleuca alternifolia) oil.* J. Sci. Food Agric., 1992. **58**(1): p. 49-53.
238. Hall, K., *4.14 - Future Perspective on Hydrogen and Fuel Cells*, in *Comprehensive Renewable Energy*, A. Sayigh, Editor. 2012, Elsevier: Oxford. p. 351-360.
239. Farhat, A., et al., *Eco-friendly and cleaner process for isolation of essential oil using microwave energy: experimental and theoretical study.* J Chromatogr A, 2009. **1216**(26): p. 5077-85.
240. Xavier, V.B., et al., *Mathematical modeling for extraction of essential oil from Baccharis spp. by steam distillation.* Industrial Crops and Products, 2011. **33**(3): p. 599-604.
241. Sheng, C. and J.L.T. Azevedo, *Estimating the higher heating value of biomass fuels from basic analysis data.* Biomass and Bioenergy, 2005. **28**(5): p. 499-507.
242. Gao, X. and H. Wu, *Combustion of Volatiles Produced in Situ from the Fast Pyrolysis of Woody Biomass: Direct Evidence on Its Substantial Contribution to Submicrometer Particle (PM1) Emission.* Energy & Fuels, 2011. **25**(9): p. 4172-4181.
243. Zevenhoven, M., et al., *Characterization of Ash-Forming Matter in Various Solid Fuels by Selective Leaching and Its Implications for Fluidized-Bed Combustion.* Energy Fuels, 2012. **26**(10): p. 6366-6386.
244. Bridgwater, A.V., D. Meier, and D. Radlein, *An overview of fast pyrolysis of biomass.* Organic Geochemistry, 1999. **30**(12): p. 1479-1493.
245. Bourke, J., et al., *Do All Carbonized Charcoals Have the Same Chemical Structure? 2. A Model of the Chemical Structure of Carbonized Charcoal†.* Industrial & Engineering Chemistry Research, 2007. **46**(18): p. 5954-5967.
246. Kong, Z., et al., *Leaching characteristics of inherent inorganic nutrients in biochars from the slow and fast pyrolysis of mallee biomass.* Fuel, 2014. **128**(0): p. 433-441.
247. Kim, K.H., et al., *Influence of pyrolysis temperature on physicochemical properties of biochar obtained from the fast pyrolysis of pitch pine (Pinus rigida).* Bioresour. Technol., 2012. **118**(0): p. 158-162.

248. Okuno, T., et al., *Primary Release of Alkali and Alkaline Earth Metallic Species during the Pyrolysis of Pulverized Biomass.* Energy & Fuels, 2005. **19**(5): p. 2164-2171.
249. Rahim, M.U., X. Gao, and H. Wu, *Release of Chlorine from the Slow Pyrolysis of NaCl-loaded Cellulose at Low Temperatures.* Proc. Combust. Inst., 2014: p. http://dx.doi.org/10.1016/j.proci.2014.07.020.
250. Knudsen, J.N., et al., *Secondary Capture of Chlorine and Sulfur during Thermal Conversion of Biomass.* Energy & Fuels, 2005. **19**(2): p. 606-617.
251. Cantrell, K.B., et al., *Impact of pyrolysis temperature and manure source on physicochemical characteristics of biochar.* Bioresour. Technol., 2012. **107**(0): p. 419-428.
252. Uchimiya, M., T. Ohno, and Z. He, *Pyrolysis temperature-dependent release of dissolved organic carbon from plant, manure, and biorefinery wastes.* J. Anal. Appl. Pyrolysis, 2013. **104**(0): p. 84-94.
253. Spokas, K.A., et al., *Qualitative analysis of volatile organic compounds on biochar.* Chemosphere, 2011. **85**(5): p. 869-882.
254. Brown, T.R., M.M. Wright, and R.C. Brown, *Estimating profitability of two biochar production scenarios: slow pyrolysis vs fast pyrolysis.* Biofuels Bioprod. Biorefining, 2011. **5**(1): p. 54-68.
255. Jiménez, S. and J. Ballester, *Effect of co-firing on the properties of submicron aerosols from biomass combustion.* Proceedings of the Combustion Institute, 2005. **30**(2): p. 2965-2972.
256. *http://www.eucalyptusoil.com/australian-oil-production/production-today/environmental-benefits (accessed on August 05, 2014).*
257. Nielsen, H.P., et al., *Deposition of potassium salts on heat transfer surfaces in straw-fired boilers: a pilot-scale study.* Fuel, 2000. **79**(2): p. 131-139.
258. Lind, T., et al., *ASH formation mechanisms during combustion of wood in circulating fluidized beds.* Proc. Combust. Inst., 2000. **28**(2): p. 2287-2295.
259. Christensen, A.K., *The formation of submicron particles from the combustion of straw. PhD Dissertation*. 1995, Technical University of Denmark, Lyngby, Denmark.
260. Pagels, J., et al., *Characteristics of aerosol particles formed during grate combustion of moist forest residue.* Journal of Aerosol Science, 2003. **34**(8): p. 1043-1059.
261. Hanby, V.L., *Sodium Sulphate Formation and Deposition in Marine Gas Turbine.* J. Eng. Power, 1974. **96**: p. 129-133.
262. Fielder, W.L., C.A. Stearns, and F.J. Kohl, *Reactions of NaCl with Gaseous SO 3, SO 2, and O 2.* J. Electrochem. Soc., 1984. **131**: p. 2414-2417.
263. Steinberg, M. and K. Schofield, *The chemistry of sodium with sulfur in flames.* Progress in Energy and Combustion Science, 1990. **16**(4): p. 311-317.
264. Steinberg, M. and K. Schofield, *The controlling chemistry in flame generated surface deposition of Na2SO4 and the effects of chlorine.* Symposium (International) on Combustion, 1996. **26**(2): p. 1835-1843.
265. Srinivasachar, S., et al., *A kinetic description of vapor phase alkali transformations in combustion systems.* Progress in Energy and Combustion Science, 1990. **16**(4): p. 303-309.

266. Jiménez, S. and J. Ballester, *Influence of operating conditions and the role of sulfur in the formation of aerosols from biomass combustion.* Combust. Flame, 2005. **140**(4): p. 346-358.
267. Chenevert, B.C., J.C. Kramlich, and K.M. Nichols, *Ash characteristics of high alkali sawdust and sanderdust biomass fuels.* Symp. (Int.) Combust., 1998. **27**(2): p. 1719-1725.
268. Neville, M., et al., *Vaporization and condensation of mineral matter during pulverized coal combustion.* Symp. (Int.) Combust., 1981. **18**(1): p. 1267-1274.
269. Helble, J.J. and A.F. Sarofim, *Influence of char fragmentation on ash particle size distributions.* Combust. Flame, 1989. **76**(2): p. 183-196.
270. Abdullah, H., K.A. Mediaswanti, and H. Wu, *Biochar as a Fuel: 2. Significant Differences in Fuel Quality and Ash Properties of Biochars from Various Biomass Components of Mallee Trees.* Energy Fuels, 2010. **24**(3): p. 1972-1979.
271. Phanphanich, M. and S. Mani, *Impact of torrefaction on the grindability and fuel characteristics of forest biomass.* Bioresource Technology, 2011. **102**(2): p. 1246-1253.
272. Lind, T., et al., *Effect of Chlorine and Sulfur on Fine Particle Formation in Pilot-Scale CFBC of Biomass.* Energy Fuels, 2006. **20**(Copyright (C) 2012 American Chemical Society (ACS). All Rights Reserved.): p. 61-68.
273. Ruscio, A., F. Kazanc, and Y.A. Levendis, *Characterization of Particulate Matter Emitted from Combustion of Various Biomasses in O2/N2 and O2/CO2 Environments.* Energy & Fuels, 2014. **28**(1): p. 685-696.
274. Harb, J.N. and E.E. Smith, *Fireside corrosion in pc-fired boilers.* Prog. Energy Combust. Sci., 1990. **16**(3): p. 169-190.
275. DeGroot, W.F. and F. Shafizadeh, *The influence of exchangeable cations on the carbonization of biomass.* J. Anal. Appl. Pyrolysis, 1984. **6**(3): p. 217-232.
276. Tyrrell, T., *The relative influences of nitrogen and phosphorus on oceanic primary production.* Nature, 1999. **400**(6744): p. 525-531.
277. Gao, X., et al., *Significant contribution of organically-bound Mg, Ca, and Fe to inorganic PM10 emission during the combustion of pulverized Victorian brown coal.* Fuel, 2014. **117, Part A**(0): p. 825-832.
278. Baxter, L.L. and R.E. Mitchell, *The release of iron during the combustion of Illinois No. 6 coal.* Combustion and Flame, 1992. **88**(1): p. 1-14.

APPENDIX COPYRIGHT PERMISSION STATEMENTS

A. Chapter 4, reprinted with permission from (Syamsuddin Yani, Xiangpeng Gao, Peter Grayling and Hongwei Wu. Steam Distillation of Mallee Leaf: Extraction of 1,8-cineole and Changes in the Fuel Properties of Spent Biomass, Fuel 2014, 133, 341–349). Copyright (2014) Elsevier

ELSEVIER LICENSE
TERMS AND CONDITIONS

Mar 13, 2016

This is a License Agreement between Syamsuddin Yani ("You") and Elsevier ("Elsevier") provided by Copyright Clearance Center ("CCC"). The license consists of your order details, the terms and conditions provided by Elsevier, and the payment terms and conditions.

All payments must be made in full to CCC. For payment instructions, please see information listed at the bottom of this form.

Supplier	Elsevier Limited The Boulevard,Langford Lane Kidlington,Oxford,OX5 1GB,UK
Registered Company Number	1982084
Customer name	Syamsuddin Yani
Customer address	Bumi Tirta gardenia H/17 Makassar, South Sulawesi 90231
License number	3827310735338
License date	Mar 13, 2016
Licensed content publisher	Elsevier
Licensed content publication	Fuel
Licensed content title	Steam distillation of mallee leaf: Extraction of 1,8-cineole and changes in the fuel properties of spent biomass
Licensed content author	Syamsuddin Yani,Xiangpeng Gao,Peter Grayling,Hongwei Wu
Licensed content date	1 October 2014

Licensed content volume number	133
Licensed content issue number	n/a
Number of pages	9
Start Page	341
End Page	349
Type of Use	reuse in a thesis/dissertation
Portion	full article
Format	both print and electronic
Are you the author of this Elsevier article?	Yes
Will you be translating?	No
Title of your thesis/dissertation	Distillation of Mallee Biomass for Eucalyptus Oil Extraction and Thermochemical Behaviour of the Spent Biomass
Expected completion date	Mar 2016
Estimated size (number of pages)	145
Elsevier VAT number	GB 494 6272 12
Permissions price	0.00 USD
VAT/Local Sales Tax	0.00 USD / 0.00 GBP
Total	0.00 USD

B. Chapter 5, reprinted with permission from (Xiangpeng Gao, Syamsuddin Yani and Hongwei Wu. Pyrolysis of Spent Biomass from Mallee leaf Steam Distillation: Biochar Properties and Recycling of Inherent Inorganic Nutrients, Energy & Fuels 2014, 28, 4642−4649). Copyright (2014) American Chemical Society

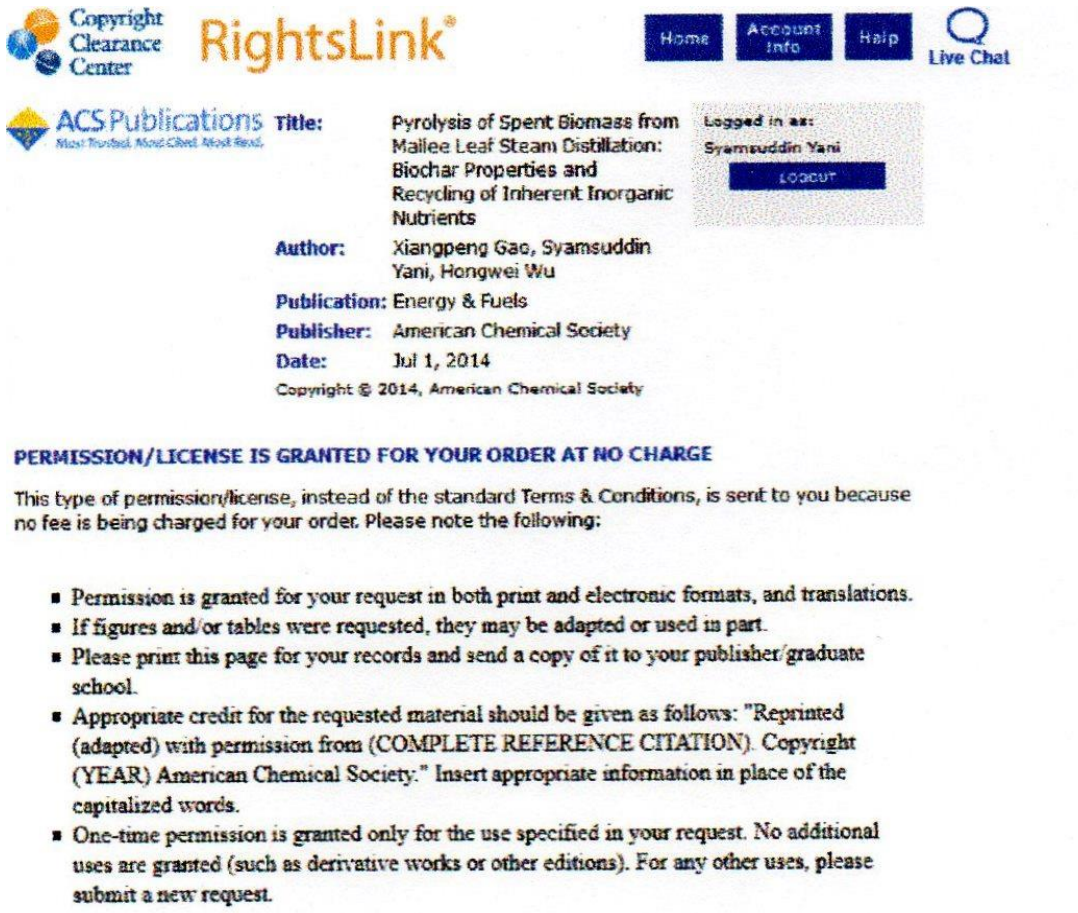

Copyright Clearance Center RightsLink®

Home | Account Info | Help | Live Chat

ACS Publications

Title: Pyrolysis of Spent Biomass from Mallee Leaf Steam Distillation: Biochar Properties and Recycling of Inherent Inorganic Nutrients

Logged in as: Syamsuddin Yani

LOGOUT

Author: Xiangpeng Gao, Syamsuddin Yani, Hongwei Wu

Publication: Energy & Fuels

Publisher: American Chemical Society

Date: Jul 1, 2014

Copyright © 2014, American Chemical Society

PERMISSION/LICENSE IS GRANTED FOR YOUR ORDER AT NO CHARGE

This type of permission/license, instead of the standard Terms & Conditions, is sent to you because no fee is being charged for your order. Please note the following:

- Permission is granted for your request in both print and electronic formats, and translations.
- If figures and/or tables were requested, they may be adapted or used in part.
- Please print this page for your records and send a copy of it to your publisher/graduate school.
- Appropriate credit for the requested material should be given as follows: "Reprinted (adapted) with permission from (COMPLETE REFERENCE CITATION). Copyright (YEAR) American Chemical Society." Insert appropriate information in place of the capitalized words.
- One-time permission is granted only for the use specified in your request. No additional uses are granted (such as derivative works or other editions). For any other uses, please submit a new request.

C. Chapter 6, reprinted with permission from (Xiangpeng Gao, Syamsuddin Yani and Hongwei Wu. Emission of Inorganic PM_{10} during the Combustion of Spent Biomass from Mallee Leaf Steam Distillation, Energy & Fuels 2015, 29, 5171-5175). Copyright (2015) American Chemical Society

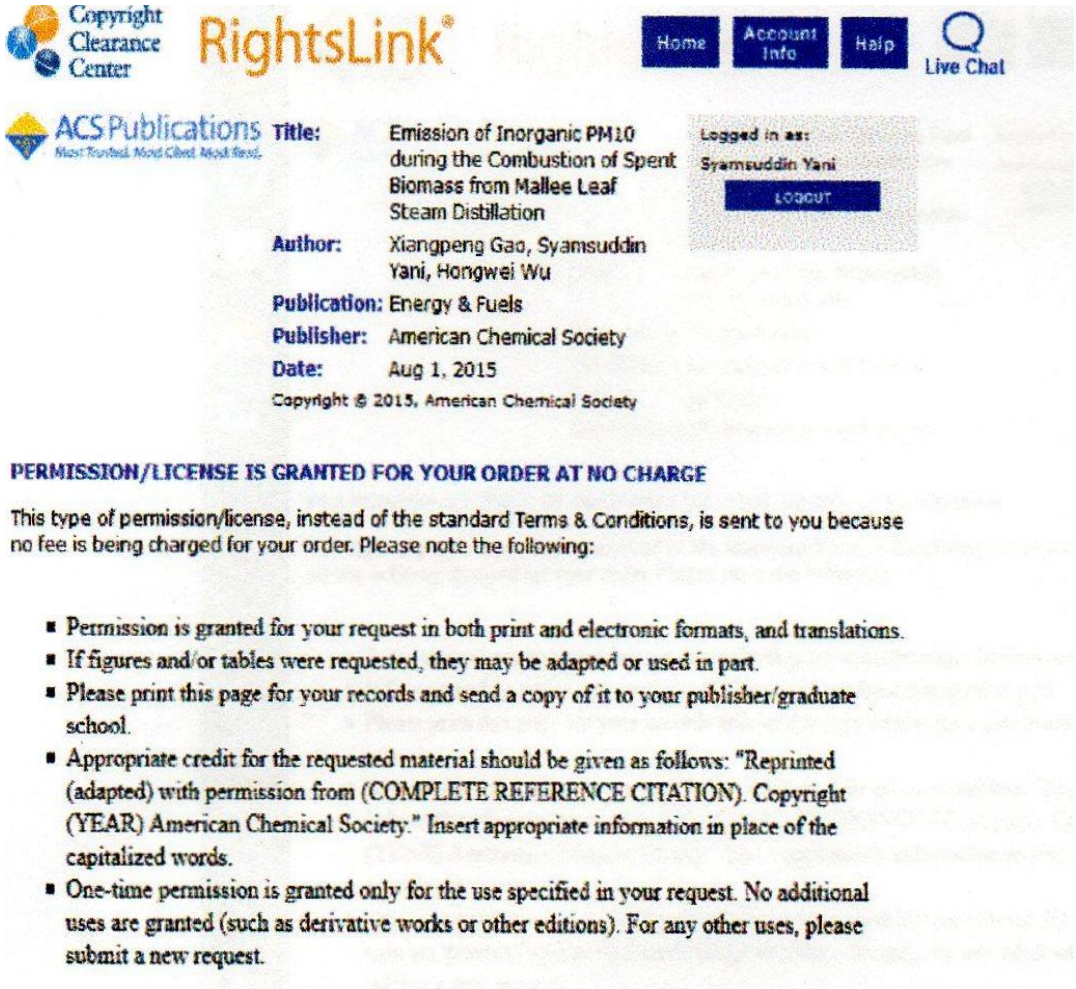

Copyright Clearance Center RightsLink®

Home | Account Info | Help | Live Chat

ACS Publications

Title: Emission of Inorganic PM10 during the Combustion of Spent Biomass from Mallee Leaf Steam Distillation

Author: Xiangpeng Gao, Syamsuddin Yani, Hongwei Wu

Publication: Energy & Fuels

Publisher: American Chemical Society

Date: Aug 1, 2015

Copyright © 2015, American Chemical Society

Logged in as: Syamsuddin Yani

LOGOUT

PERMISSION/LICENSE IS GRANTED FOR YOUR ORDER AT NO CHARGE

This type of permission/license, instead of the standard Terms & Conditions, is sent to you because no fee is being charged for your order. Please note the following:

- Permission is granted for your request in both print and electronic formats, and translations.
- If figures and/or tables were requested, they may be adapted or used in part.
- Please print this page for your records and send a copy of it to your publisher/graduate school.
- Appropriate credit for the requested material should be given as follows: "Reprinted (adapted) with permission from (COMPLETE REFERENCE CITATION). Copyright (YEAR) American Chemical Society." Insert appropriate information in place of the capitalized words.
- One-time permission is granted only for the use specified in your request. No additional uses are granted (such as derivative works or other editions). For any other uses, please submit a new request.

D. Chapter 7, reprinted with permission from (Syamsuddin Yani, Xiangpeng Gao and Hongwei Wu. Emission of Inorganic PM_{10} from The Combustion of Torrefied Biomass under Pulverized-Fuel Conditions, Energy & Fuels 2015, 29, 800-807). Copyright (2015) American Chemical Society

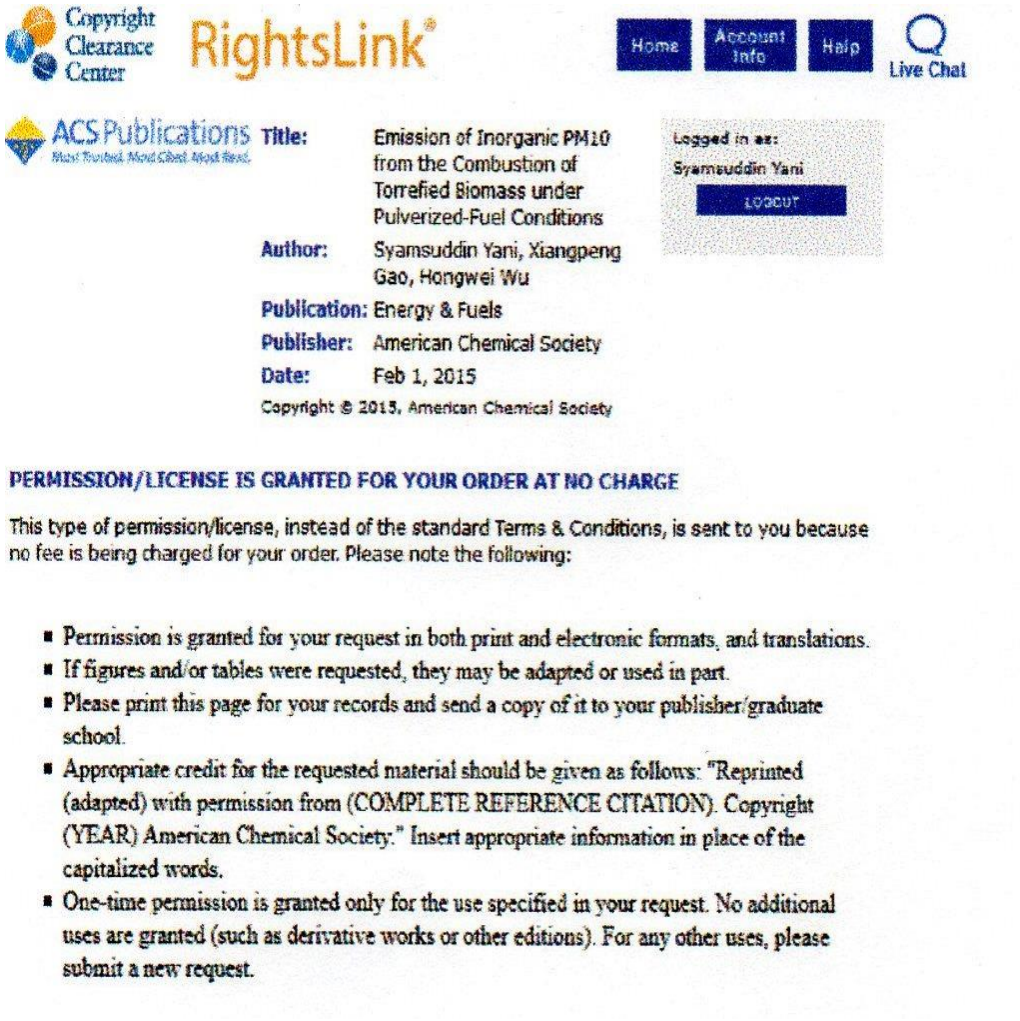

Copyright Clearance Center RightsLink®

Home | Account Info | Help | Live Chat

ACS Publications

Title: Emission of Inorganic PM10 from the Combustion of Torrefied Biomass under Pulverized-Fuel Conditions

Author: Syamsuddin Yani, Xiangpeng Gao, Hongwei Wu

Publication: Energy & Fuels

Publisher: American Chemical Society

Date: Feb 1, 2015

Copyright © 2015, American Chemical Society

Logged in as: Syamsuddin Yani

LOGOUT

PERMISSION/LICENSE IS GRANTED FOR YOUR ORDER AT NO CHARGE

This type of permission/license, instead of the standard Terms & Conditions, is sent to you because no fee is being charged for your order. Please note the following:

- Permission is granted for your request in both print and electronic formats, and translations.
- If figures and/or tables were requested, they may be adapted or used in part.
- Please print this page for your records and send a copy of it to your publisher/graduate school.
- Appropriate credit for the requested material should be given as follows: "Reprinted (adapted) with permission from (COMPLETE REFERENCE CITATION). Copyright (YEAR) American Chemical Society." Insert appropriate information in place of the capitalized words.
- One-time permission is granted only for the use specified in your request. No additional uses are granted (such as derivative works or other editions). For any other uses, please submit a new request.